Factors Affecting Pseudo Relative Permeability Curves

by

Saud Sultan Al-Otaibi

A Thesis Presented to the

FACULTY OF THE COLLEGE OF GRADUATE STUDIES

KING FAHD UNIVERSITY OF PETROLEUM & MINERALS

DHAHRAN, SAUDI ARABIA

In Partial Fulfillment of the
Requirements for the Degree of

MASTER OF SCIENCE

In

PETROLEUM ENGINEERING

June, 1992

Order Number 1354102

Factors affecting pseudo relative permeability curves

Al-Otaibi, Saud Sultan, M.S.

King Fahd University of Petroleum and Minerals (Saudi Arabia), 1992

U·M·I
300 N. Zeeb Rd.
Ann Arbor, MI 48106

FACTORS AFFECTING PSEUDO RELATIVE PERMEABILITY CURVES

BY

SAUD SULTAN AL-OTAIBI

A Thesis Presented to the

FACULTY OF THE COLLEGE OF GRADUATE STUDIES

KING FAHD UNIVERSITY OF PETROLEUM & MINERALS

DHAHRAN, SAUDI ARABIA

In Partial Fulfillment of the
Requirements for the Degree of

MASTER OF SCIENCE
In

PETROLEUM ENGINEERING

June 1992

KING FAHD UNIVERSITY OF PETROLEUM AND MINERALS
DHAHRAN, SAUDI ARABIA

COLLEGE OF GRADUATE STUDIES

This thesis, written by Mr. Saud Sultan Al-Otaibi under the direction of his Thesis Advisor and approved by his Thesis Committee, has been presented to and accepted by the Dean of the College of Graduate Studies, in partial fulfillment of the requirements for the degree of MASTER OF SCIENCE in Petroleum Engineering.

Thesis Committee:

A. A. Almajed
Dr. Abdulaziz A. Al-Majed
Thesis Advisor

M. A. Aggour
Dr. Mohamed A. Aggour
Member

H. Y. Al-Yousef
Dr. Hasan Y. Al-Yousef
Member

Dr. Khalid A. Al-Fossail
Department Chairman

Dr. Ala H. Al-Rabeh
Dean, College of Graduate Studies

Date: 14 July 1992

DEDICATION

I dedicate this work to my wife and children:Shiroog ,Sultan and Dhoha.

ACKNOWLEDGEMENT

Praise and gratitude be to the Almighty, the creator and sustainer of the Universe, and peace be upon his Prophet Muhammad.

My sincere appreciation and gratitude to Dr. Abdulaziz Al-Majed who, as my Thesis Committee Chairman, guided and helped me throughout my research. I would also like to express my sincere gratitude to Dr. Mohamed Aggour and Dr. Hasan Y. Al-Yousef for their valuable suggestions and instructions. I am also grateful to Saudi Aramco for permission to use the data and the computer facilities.

TABLE OF CONTENTS

LIST OF TABLES

LIST OF FIGURES

ملخص بحث

اسم الطالب : سعود سلطان العتيبي .

عنوان الدراسة : العوامل المؤثرة في منحنيات النفاذية النسبية الشبيهة .

التخصص : هندسة البترول .

التاريخ : ذوالحجة ١٤١٢هـ .

محاكاة المكامن للحقول الكبيرة مثل الموجودة في المملكة العربية السعودية يحتاج إلى عدد كبير من الخلايا المتشابكة . وتستخدم منحنيات النفاذية النسبيه الشبيهه لتخفيض الأبعاد في نماذج محاكاة المكامن وللأخذ في الإعتبار التغيرات في خواص الصخور داخل الخلايا . إن تعيين الخواص المؤثره على منحنيات النفاذيه النسبيه مهم جداً حتى يتسنى جمع خلايا النموذج في مجموعات مصنفه وبعد ذلك يستخرج منحنى نفاذيه نسبيه لكل مجموعه . إن الهدف من هذه الأطروحه هو تحديد تلك العوامل المؤثره في منحنيات النفاذيه النسبيه الشبيهه . لقد تم بحث الخواص المختلفه لصخور المكامن وموائعها وهذا البحث كذلك تعرض لإثبات صحة بعض هذه المنحنيات . ويمكن أن يستخلص من النتائج أن زاوية الإنحدار هي أكثر العوامل تأثيراً على منحنيات النفاذيه النسبيه الشبيهه . أما سُمك الطبقه وخواص الضغط والحجم والحراره فلها تأثير أقل ، في حين أن معدل الإنتاج ونسبة النفاذيه النسبيه العموديه إلى الأفقيه ليس لها تأثير يذكر في حدود المعدلات المدروسه . بينما النفاذيه المطلقه في الحالات التي فيها زاوية الإنحدار صغيره ليس لها تأثير ، فإنه عند الحالات التي فيها زاوية الإنحدار كبيره يجب أخذها في الإعتبار.

درجة الماجستير العلوم
جامعة الملك فهد للبترول والمعادن
الظهران ، المملكة العربية السعودية

THESIS ABSTRACT

Full Name of Student: Saud Sultan Al-Otaibi

Title of Study: FACTORS AFFECTING PSEUDO RELATIVE PERMEABILITY CURVES

Date of Degree: June 1992

To simulate very large field reservoirs like the ones existing in Saudi Arabia, a large number of grid cells is needed. Pseudo relative permeability curves are used to reduce the dimensionality of reservoir simulation models and to account for intra-cell rock properties variations. Identifying the parameters affecting pseudo relative permeability curves is very important so that the model cells can be grouped in different categories where the proper pseudo relative permeabilities are generated for each group. The objective of this thesis was to identify the factors affecting pseudo relative permeability curves. Different reservoir rock and fluid properties were studied. Validation of some curves are also shown. It was concluded that the most pronounced effect on pseudo relative permeability curves is caused by the reservoir dip angle. Layer thickness and PVT properties have also an effect. Production rate and vertical to horizontal permeability ratio have no significant effect on the parameter ranges studied. While absolute permeability for low dip angle cases has no effect, at high dip angle cases, absolute permeability effect should be taken into consideration.

MASTER OF SCIENCE DEGREE

KING FAHD UNIVERSITY OF PETROLEUM AND MINERALS
Dhahran, Saudi Arabia

Chapter 1

INTRODUCTION

Chapter 1

INTRODUCTION

With advancement of computers technology in both hardware and software, reservoir simulation is emerging as a powerful tool to study the displacement process in large complex reservoirs where it is most needed with sufficient realism. The results of such studies are used in reservoir management to take decisions regarding the reservoir development and future operations.

Simulating large and complex reservoirs with great details and high grid definitions can be very costly in both manpower and computer. They can be very lengthy and time consuming even with the presence of super-computers.

Reducing the number of reservoir simulation grids by using coarse grids ignores many reservoir description details and, consequently, the reservoir displacement process cannot be simulated properly.

Many studies have been made to try to reduce the dimensionality of the reservoir using methods which account for that missing dimensionality. To conduct simple reservoir simulation studies with a high confidence in the results, pseudo relative permeability curves have been used to simulate the reservoir displacement process using two-dimensional models instead of three-dimensional models.

In Saudi Arabia where complex and large size reservoirs exist, fine gridded reservoir simulations are very costly; and even coarse grid traditionally used to simulate these reservoirs are in the magnitude of tens or even hundreds of thousands of cells.

Pseudo relative permeability curves are not only needed to substitute three-dimensional models by two-dimensional models. They are also needed for the three-dimensional models because the reservoir geologic layers are usually reduced in the model layers to reduce the number of active model cells. Pseudo relative permeability curves are then used to account for the missing vertical layers definitions.

Modeling some reservoirs that are really complex and highly stratified like these found in Saudi Arabia can require dozens or even hundreds of sets of pseudo relative permeability functions.

The main purpose of this thesis is to study the effect of different fluids, rock and structure properties on pseudo relative permeability curves in a trial to reduce the number of pseudo relative permeability curves necessary for such reservoirs. A typical Saudi sandstone reservoir fluid and rock properties were used. Kyte and Berry method of calculating dynamic pseudo relative permeability functions was used because it is the most widely used in the industry at the present time.

Chapter 2

LITERATURE REVIEW

Chapter 2

LITERATURE REVIEW

In this chapter, the definition of absolute permeability is briefly discussed, then the relative permeability concept is reviewed and the methods of obtaining the relative permeability are mentioned as an introduction to the definition of pseudo relative permeability curves and their uses in petroleum industry especially in reservoir simulation modeling.

2.1 Absolute Permeability

Permeability is a property of the porous medium which is a measure of the conductivity of the medium, the ability to transmit fluids. It is defined and used as the constant of the proportionality of Darcy's law to describe the fluid flow of a homogeneous single phase fluid through the porous medium:

$$u = \frac{-K}{\mu} \frac{dP}{dL} \qquad (2.1)$$

where

u = the fluid velocity

K = absolute permeability or the constant of proportionality

μ = viscosity of the fluid

$\frac{dP}{dL}$ = pressure gradient along the flow direction

The constant of proportionality or the absolute permeability is solely dependent on the nature of formation and determined by the geometry of the rock pore system.

2.2 Relative Permeability Concept

In petroleum reservoirs more than one fluid exist. If fluids are immiscible and were flowed simultaneously through the porous medium, then each fluid has its own effective permeability. These effective permeabilities are mainly dependent on the saturations of each fluid.

For an oil-water system, it is conventional to plot both permeabilities as a function of the water saturation alone since the oil saturation, S_o, is related to the water saturation, S_w, by the simple relationship:

$$S_o = 1 - S_w \tag{2.2}$$

The relative permeability to a fluid is defined as the ratio of effective permeability at a given saturation of that fluid to a reference permeability. Different reference permeabilities are generally used in the industry which are:

a) Klinkenberg-corrected air permeability,

b) The effective permeability to non-wetting phase at residual wetting phase saturation, and

c) The absolute permeability to a fluid which does not react with the rock.

The base permeability most often used in defining relative permeability is absolute permeability. Typical relative permeability curves for a water-oil system are shown in Fig. 2.1. Considering the relative permeability curve for water, two points on this curve are known. When $S_w = S_{wc}$, the connate or irreducible water saturation, the water will not flow and $K_{rw} = 0$. Also, when $S_w = 1$ the rock is entirely saturated with water and the effective permeability to water is equal to the absolute permeability. Similarly, for the oil at S_{or}, the residual oil saturation, there will be no flow and relative permeability to oil at this point is equal to zero.

The basic shapes of relative-permeability curves for the principal rock types in a reservoir are usually defined by laboratory core tests on representative core samples. The most important factors affecting the relative permeability curves are wettability, fluid saturation, saturation history, pore geometry and fluid distribution. Relative permeability curves can be obtained theoretically especially for the less complex systems [1,2].

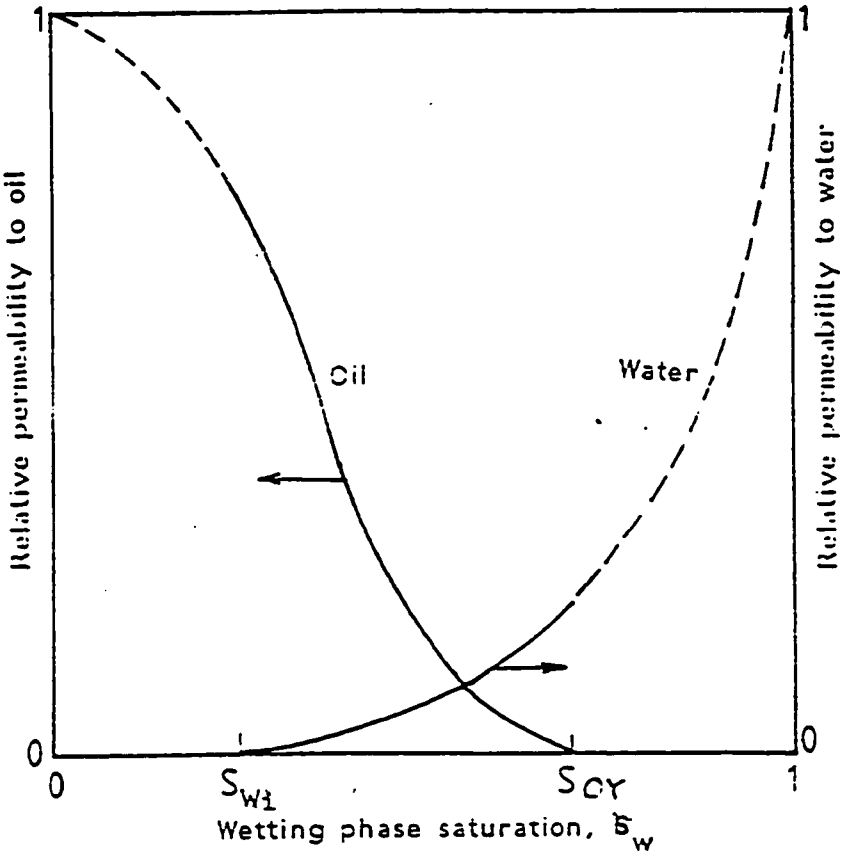

Fig.2.1: **Typical relative permeability curves for a pair of wetting and nonwetting fluids.**

Relative permeability is often one of the most difficult pieces of data to evaluate or obtain. The relations usually used in reservoir simulators can be obtained from one of the following three means depending on the availability of data:

1. Laboratory measurements using one of the two basic methods, steady-state method or unsteady-state displacement method. Details can be found in references [3] and [4].

2. Analytical and calculational methods which utilize the published fluid flow relationships obtained in laboratory studies on general type porous material or mathematical derivation of flow behavior based on experimentally obtained characteristics of reservoir rock. Model example of these methods can be found in reference [5].

3. Calculations from the field data where the relative permeability is determined from production data as a result of a statistical treatment of the entire reservoir, the procedure is treated in references [6] and [7].

2.3 Pseudo Relative Permeability Concept

The most reliable source of relative permeability data is from laboratory measurements performed on cores obtained from the reservoir of interest. For the measurements to be meaningful, considerable care

and effort must be taken to insure that in situ reservoir wettability is preserved during coring, surface handling, storage and measurement operations. Failure to preserve native wettability will cause the measured relative permeability values to be of little use for the reservoir study.

If a significant rock property variation is identified in a reservoir, it can be subdivided into different rock types. Since flow properties are a function of pore geometry, each lithological unit usually has a special relative permeability characteristics. Relative permeability data are not always available for each rock type, and there is a little reason to believe that a single, average relative permeability curve will be representative of the behavior of each layer or the whole reservoir. For this reason different approaches were proposed in reservoir simulation studies to better history match them [8,9].

Pseudo relative permeability curves are used instead of rock relative permeability curves in an effort to accommodate a third dimension in numerical simulators. A pseudo relative permeability curve is a weighted average of a rock or fluid properties, or combined rock-fluid properties. The average is done over a representative volume of the reservoir [19].

Rock relative permeability curves are usually used in the fine grid reservoir simulation studies. But due to the differences in flow mechanisms between a core plug and a large grid cell of full-field

model, laboratory derived relative permeability curves (rock curves) cannot be used to simulate accurately the flow of fluids between grid cells in a two-dimensional areal model or a three-dimensional model because it does not account for non-uniformities which occurs in the vertical plane of the formation. In addition, the use of the rock relative permeability curves can lead to significant differences between the actual field observed data and the model resulting sweep efficiencies, depending on the size, shape and geometry of the model cells.

To compensate for intra-cell variations in the rock properties and fluid saturations a refined grid can be used to minimize the effect of these variations. Representing these data in a model through small finite difference grid blocks can be expensive. At the same time, achieving adequate accuracies can be very costly even with the new super computers especially if the study is being performed for a large size multi-layer reservoir, a simplified comparison is shown in Fig. 2.2.

The use of pseudo relative permeability has been accepted in the industry as an approximate way to account for the effects of missing vertical stratification in the coarse grid reservoir models [22].

Pseudo relative permeability curves generation and implementation is an important part of many full-field models. Almost all areal models need pseudo relative permeability curves as well as many three-dimensional models depending on the thickness of the layers. The pseudo relative

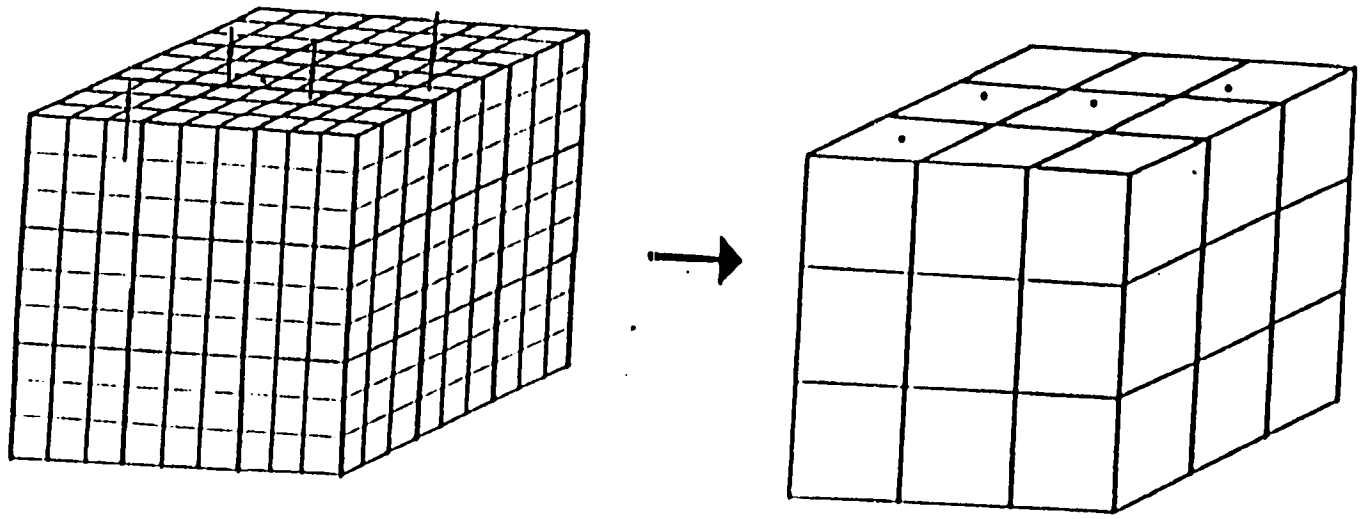

Fig.2.2: A schematic diagram showing two different models with a considerable reduction in number of cells if pseudo relative permeability curves are used.

permeability curves are needed in such studies to reduce the dimensionality of the model by reducing the number of model cells and using coarser grid sizes to save the engineers efforts and the computer CPU time.

The pseudo relative permeability curves were first introduced to the petroleum industry by Coats [10] in 1967. He developed an analytical method to calculate pseudo relative permeability curves based on the assumption of gravity-capillary equilibrium in the vertical direction or vertical equilibrium (VE). The vertical equilibrium concept assumes that, as depletion proceeds, gravity and capillary forces will be in equilibrium vertically in every grid block in the reservoir model. This condition where the potential of each phase is constant applies to reservoirs with good vertical permeability, large fluid density differences and low operating rates where the viscous-flow forces are small. Coats verified his method by calculations and experimental results.

When the vertical sweep is dominated by viscous forces instead of gravity forces, another method proposed by Hearn [11] can be used to calculate pseudo functions. These pseudo functions are based on a mathematical model and used to approximate the effect of vertical permeability variation in displacement projects such as water flooding where the reservoir is assumed to be stratified. The displacement process in each of the stratified layers is assumed to be piston-like

where residual oil is behind the front and connate water is ahead of the front.

In 1968, Martin [12] proposed a two dimensional simulator where the equations for three-phase, three-dimensional, compressible flow (including capillary) are reduced to a two-dimensional relation by partial integration. Using this method the effects of capillary and fluid segregation in the missing third dimension are represented. One principle restriction for using this method is that the reservoir thickness should be small compared to its areal extension. Martin also provided a firm theoretical foundation to Coats et al. [10] assumption of vertical equilibrium by developing the equations mathematically from basic flow equations. This method is more adequate to reservoirs with small thickness compared to the maximum distance across the reservoir as mentioned before and also the reservoir vertical permeability should be sufficient to allow the fluids to segregate.

Coats et al. [13] in 1971 proposed a method where a fully three-dimensional mathematical model that treats simultaneously both the areal and cross-sectional aspects of reservoir flow is employed to be used in the simulator. A quantitative criterion is provided for determining when vertical communication is good enough to permit use of the modified two-dimensional areal analysis.

Jacks et al. [14] proposed a procedure to generate dynamic pseudo relative permeability curves from cross-sectional models that represent

the reservoir to be studied. In this method, the vertical saturation distribution is developed through detailed simulation of the fluid displacement in a vertical cross-sectional model. This method makes no assumptions about the state of flow inside the reservoir and, in principle, are valid under all conditions including those of vertical equilibrium. By using this method, numerical dispersion of the full-field simulation model can be reduced significantly. Jacks et al. showed that using the dynamic pseudo relative permeability curves obtained using his method, a two dimensional model duplicates the results of a more rigorous three dimensional model results. He showed a three dimensional model, shown in Fig. 2.3, which has production wells drilled at the dashed line. A large aquifer underlies the oil zone but the water drive from the aquifer is limited because of a "tar barrier" that effectively reduces permeability in the shaded zone. The formation thickness and vertical stratification were considered uniform throughout the reservoir. Water injection Wells 1 and 2 were used to supplement the natural bottom water drive. An equivalent 2D areal model which had the same 17 x 7 grid and same well location was able to depict the two-phase fluid-flow equations in three dimensions when the pseudo relative peremability curves were used to accouunt for the vertical flow component in the 2D areal model. Results are shown in Fig. 2.4. The dynamic pseudo relative permeability curves generated from this model are rate sensitive. They are also strong functions of the initial saturation of the cell.

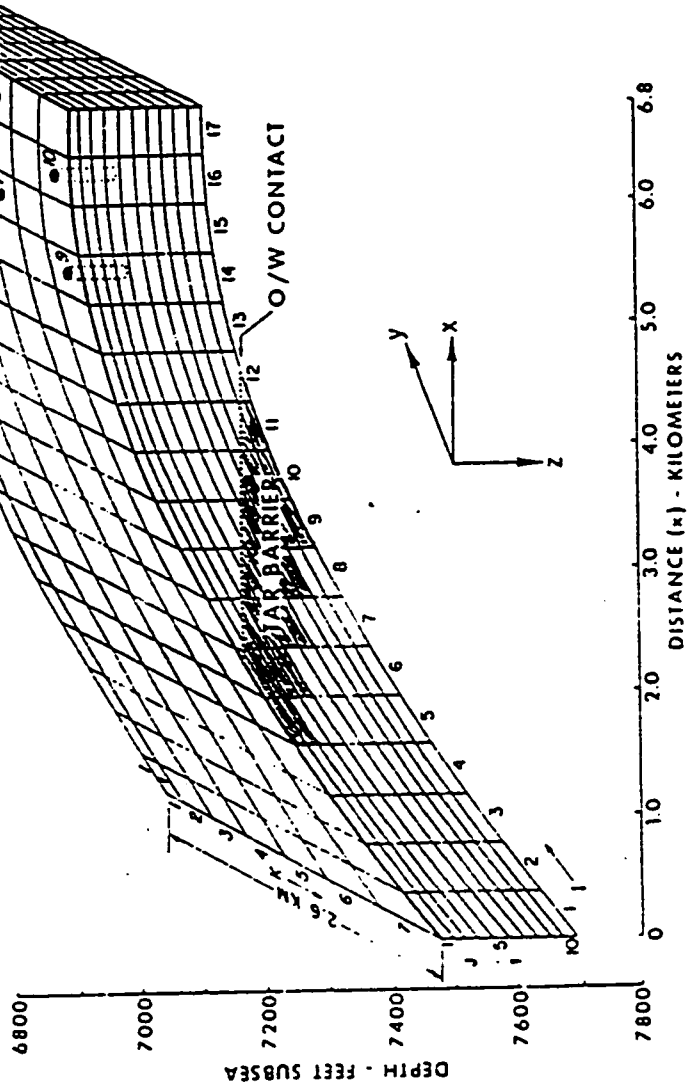

Fig.2.3: Three-Dimensional model of a typical pattern on flanks of a reservoir (After Ref. 14 and 30).

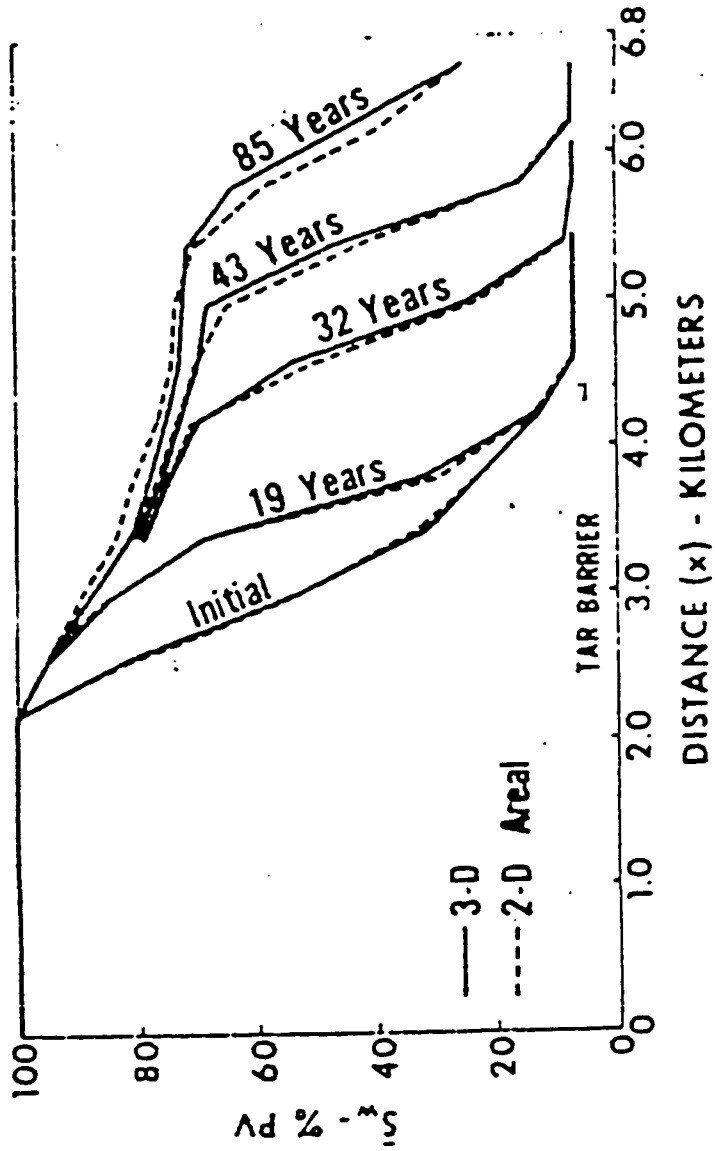

Fig. 2.4: Average water saturation distributions calculated using 3D and 2D areal models (After Ref. 14 and 30).

Kyte and Berry [15] have improved the Jacks et al. [14] procedure to allow the calculation of dynamic pseudo capillary pressure and to compensate for differences between grid sizes in the areal and cross-sectional models. In this method, pseudo relative permeability curves are also derived from cross-sectional runs. Pseudo relative permeabilities are calculated considering the interblock flow in the cross-section model by applying Darcy's law for multiphase flow. Using this method the numerical dispersion is reduced in the full-field size model to the magnitude of the numerical dispersion of the fine-grid cross-section. The application of the pseudo relative permeability curves developed is also illustrated in several examples in this paper. The dynamic pseudo relative permeabilities generated using this method are dependent on areal block length. For this reason, it is generally preferable to use square blocks of one size in the two-dimensional areal model. Otherwise different pseudo functions may be required for different model blocks simply because block dimensions change. They are also affected by the cell initial water saturation. More details about this method is described in the next chapter.

Killough and Foster [16] discussed the use of pseudo relative permeability curves in three-dimensional models. They observed almost identical results in their comparison of a three-layered model with vertical equilibrium pseudo relative permeability curves and pseudo capillary pressure which was used to match the results from a 22-layered model of a portion of the Empire Abo field reservoir.

Andrew et al. [17] developed a technique to account for the effect of subordinate phase production in cross-flow or non-wetting phase production after breakthrough in non-communicating layers. This adoption is an improvement to the original method of Hearn [11].

Starley [18] described a material-balance method for deriving interblock water/oil pseudo functions for application in coarsely gridded areal reservoir models. The pseudo functions are derived from fine-grid pattern models and account for various effects, including anisotropic formation properties, dominant displacement forces and correction for preferential directional flow. This method has several limitations and it is difficult to implement in a full-field model because of the fairly large number of functions and the "checkboard-like" assignment within patterns.

Pseudo relative permeability curves are also used in the model cells where individual wells are located to have a realistic well performance. Van Poolen et al. [21] proposed two methods to calculate the pseudo relative permeabilities at well locations. These methods are based on fully segregated flow, partial segregation and partial dispersion. Emanuel and Cook [23] expanded the concept of vertical cross-section, pseudo relative permeabilities to include vertical performance of individual wells. This method combines the effect of coning and well pseudo relative permeabilities for use in two dimensional areal models. Woods and Khurana [24] proposed a procedure for obtaining the pseudo

functions for the wells by the partial integration of flow equations to include water coning in three dimensional reservoir models. The pseudo functions are derived from results of simulation with a two dimensional coning model. The development is restricted to two-phase flow.

Thomas [19] examined various pseudo function concepts that have appeared in the technical literature. Emphasis was placed on gravity-segregated vertical equilibrium (VE) and dynamic pseudo concept that requires no assumption regarding the state of fluids in the reservoir. He concluded that pseudo relative permeabilities are directional and time-dependent functions.

Al-Yousef [25] developed a technique to improve the procedure to calculate the pseudo relative permeabilities from cross-sectional or three-dimensional models. The derivation was based on material balance and fluid flow equations. In this technique, the directional dependence of the pseudo relative permeabilities has been eliminated. Cross-sectional and three-dimensional examples demonstrating the use of the pseudo relative permeabilities were presented. The ability of pseudo relative permeabilities to account for gravity segregation and viscous and capillary cross-flow when used in two-dimensional areal models was also demonstrated.

In 1991, Stone [26] proposed a method for calculating two or three-phase pseudo functions from fine grid simulation in either two or three dimensions. It uses fractional flow formulation rather than Darcy's law

used by Kyte and Berry's method. These pseudo functions, when used in coarse grid simulation of the same reservoir, produce the accuracy of the original fine grid simulation. This method is valid for any production rate even when used to coalesce non-communicating grid layers.

To save time and effort for the future pseudo relative permeability studies for a typical Saudi sandstone reservoir, this sensitivity study was performed to identify the reservoir properties which have an impact on pseudo relative permeability curves. The minimum and maximum values of reservoir fluids, rock and structure properties were investigated. More details about the ranges of properties studied and their impact on pseudo relative permeability curves will be presented in Chapter 4.

The main objective of using pseudo relative permeability curves is to reduce the dimensionality of the reservoir model and, consequently reduce the number of the model cells which in turn saves a lot of manpower and computer CPU time. For very large reservoirs like Saudi Arabian sandstone reservoirs, even by using relatively large cell sizes, the typical total number of model cells is usually more than one hundred thousand cells. Consequently, high number of pseudo relative permeability curves are needed because of the properties variations in the reservoir. If the factors affecting pseudo relative permeability curves are identified, then a set of pseudo relative permeability curves

can be generated and the model cells can be grouped according to their similarities of a certain property and assigned the same curves. This type of work saves effort and time for the future pseudo relative permeability studies for these types of reservoirs.

Chapter 3

METHOD OF ANALYSIS

Chapter 3

METHOD OF ANALYSIS

For the conditions where the assumption of vertical equilibrium in the reservoir is not appropriate to describe the reservoir heterogeneity in the simulation study, one of the following two approaches should be used: 1) Include the missing third dimension in the reservoir model which will increase the number of the reservoir model cells making the study very costly for large reservoirs, or 2) apply the concept of dynamic pseudo relative permeability.

The dynamic pseudo relative permeability curves are derived from a detailed vertical cross-sections. These cross-sections should represent the reservoir under conditions to be expected in the areal or three-dimensional simulation model where these pseudo relative permeability curves are to be used. The pseudo relative permeability curves are then calculated from the cross-sectional model results. At each time-step, the pseudo relative permeabilities to water and oil for each block can be obtained if desired. The laboratory derived rock curves are used in these cross-sections among other reservoir representative parameters.

This section presents the method of analysis of the different pseudo relative permeability curves obtained from suitable cross-sectional models. First, a suitable cross-section for the property to be studied

is prepared and run. Then the pseudo relative permeability curves are generated and plotted. Each pseudo relative permeabilty curve is compared with the corresponding one to study the property under investigation. Finally, the validation of two cases were shown against a coarser two-dimensional model. A total of 32 different cross-section models were used in this study. Different reservoir fluids, rock and sturcture properties were investigated to study their effect on pseudo relative permeability curves on a typical Saudi Arabian sandstone reservoir. The following is a list of the parameters investigated:

1. PVT properties,
2. Ratio of vertical to horizontal permeabilities,
3. Layer thickness,
4. Production rate,
5. Reservoir dip angle, and
6. Absolute permeability.

3.1 General Cross-Section Model Description

A vertical fine-gridded cross-section consisting of 3000 cells (100 x 30) was used in studying the factors affecting pseudo relative permeability curves. The cross-section can be divided into three identical full-field layers. It is designed in this way to try to eliminate all the effects of the boundary conditions especially in the area where the pseudo relative permeability curves are generated and to have a

complete sweep of the area of interest to try to obtain the end points of studied pseudo relative permeability curves.

Figure 3.1 shows a schematic diagram of this cross-section. The cross-section total length in i-direction is 10 kilometers with original oil-water contact reaching up to half of the distance (5 kilometers). The fine-grid dimension in i-direction is 100 meters and the width (y-direction) was chosen to be 0.5 kilometers which is a reasonable full-field wide cell dimension. The dimension of the fine-grid cells are the same for all cases studied; however, the layer thickness was changed for the case where layer thickness effect is studied. Each one of the full-field layers (3 layers) contains 10 fine-gridded layers. The layer thickness is considered to be uniform throughout the reservoir.

The rock permeability curve used in all cross-sectional models is shown in Fig. 3.2.

Certain reservoir parameters used in the vertical fine-gridded cross-sectional models are kept constant for all comparison cases; these are porosity, connate water saturation, average horizontal permeability, rock and water compressibilities, average water density, and viscosity. Table 3.1. shows the values of these constant parameters. Average oil production rate per year used for all the cases is about 1.1% of original oil-in-place which is assumed to be the scaled rate for the historical performance of the reservoir.

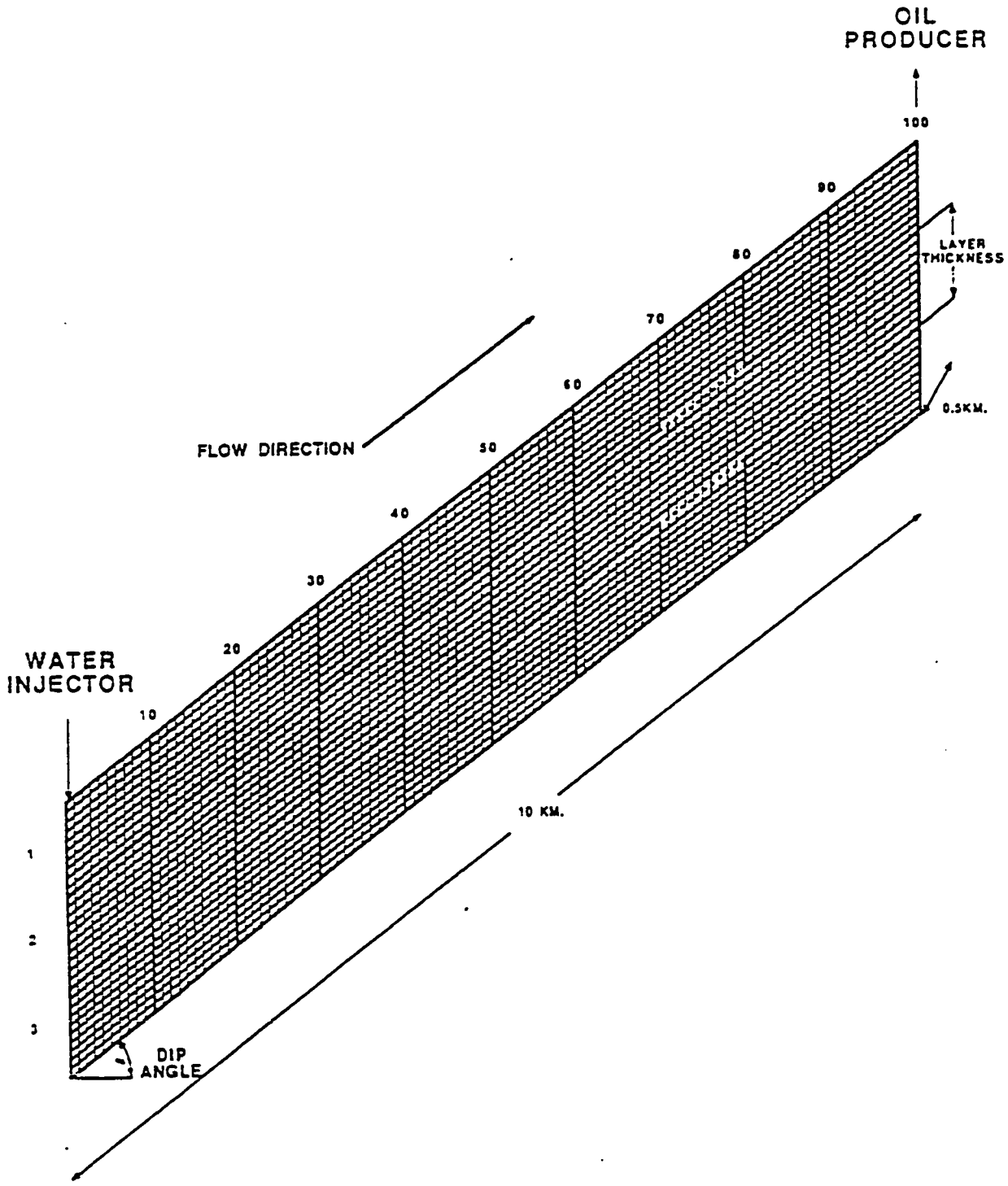

Fig.3.1: Schematic diagram of a cross-section used for developing pseudo relative permeability curves.

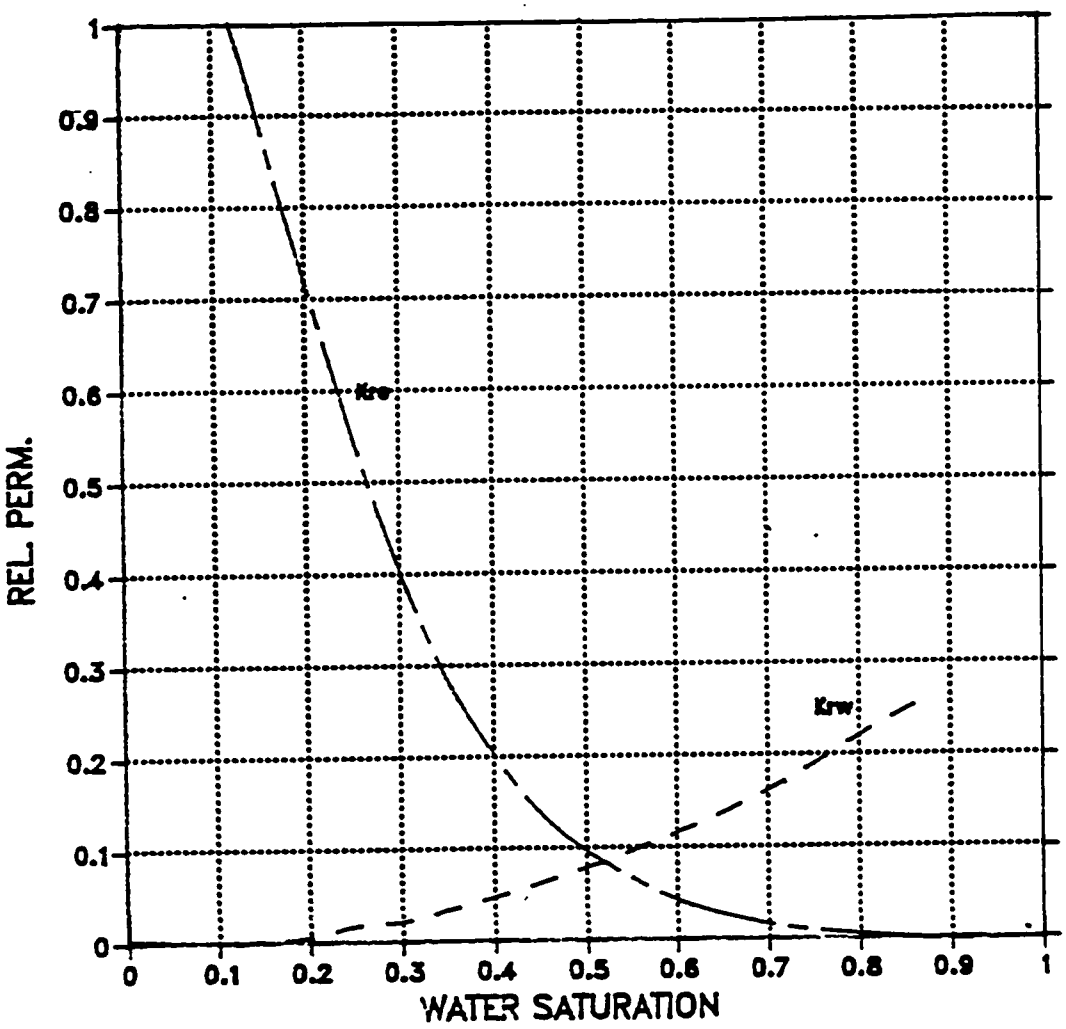

Fig.3.2: Rock relative permeability curve used in all fine-grid cross-section models to generate pseudo relative permeability curves.

Table 3.1: Reservoir Properties used in the Cross-Section (Fixed Parameters).

Location of Water-Oil Contact (Subsea)	5515 feet
Datum depth (Subsea)	5275 feet
Pressure at Datum Depth	2642 psi
Layer Width	1460 ft(0.5 km)
Porosity (Fraction)	0.28
Connate Water Saturation (Fraction)	0.12
Horizontal Permeability	5000 md
Rock Compressibility	$15.6 \times 10^{-1}\ psi^{-1}$
Water Compressibility	$2.28 \times 10^{-1}\ psi^{-1}$
Water Density	1.1143 gm/cc
Water Viscosity	0.645 cp
Water Formation Volume Factor	1.0 RB/STB
Oil Production Rate	1-1.2% OOIP/year
First Cell Depth (I=1) Angle 1° Thickness 110. (Subsea)	5489 ft
First Cell Depth (I=1) Angle 4° Thickness 110. (Subsea)	6414 ft
First Cell Depth (I=1) Angle 1° Thickness 50. (Subsea)	5102 ft
First Cell Depth (I=1) Angle 4° Thickness 50. (Subsea)	6574 ft

Because of the limitation of the maximum number of completions per well in the simulator used (15 completions per well), two producers were used both completed in column 100 (Fig. 3.1). One of them is completed in the fine-gridded layers 1 to 15 and the other producer is completed in the fine-gridded layers 16 to 30. Two injectors were used both completed in cell number 1 of the fine-gridded layers with the same completion strategy used for the producers for the same reason.

A commercial simulator was used in running the cross-sectional models using the supercomputer CRAY2. The average CPU time needed to run the 3000 cell model using 15 days time step for about 80 years averaged about 1695.0085 seconds per run using implicit pressure explicit saturation formulation (IMPES) solution technique.

In this study each coarse grid of the two-dimensional model is equal to five columns of the fine grid. Pseudo relative permeability curves generated from the fine gridded models were used in the equivalent two-dimensional coarse grid model and the water front movement across the fine grid model is compared with the two-dimensional coarse grid model as a function of time.

The procedure used to construct the pseudo relative permeability curves was as follows:

1. A suitable fine grid cross-section is built for the property to be studied.

2. The reservoir flow behavior for the minimum value of the property is simulated by the fine grid cross-sectional model as a function of time and the run is analyzed.

3. The parameters used in the pseudo relative permeability calculations are obtained.

4. Pseudo relative permeability curves are then calculated using Kyte and Berry method.

5. Steps 2 to 4 above are repeated for the maximum value of the property being studied and the results are then compared to see the impact of this property on the generated pseudo relative permeability.

To validate the use of the pseudo relative permeability curves, the results of a two-dimensional coarse grid model employing the pseudo relative permeability curves are compared to the results of a two-dimensional fine grid model employing the laboratory derived rock curves.

Figure 3.3 shows how a fine grid cross-sectional model is reduced to the corresponding coarse grid cross-sectional model.

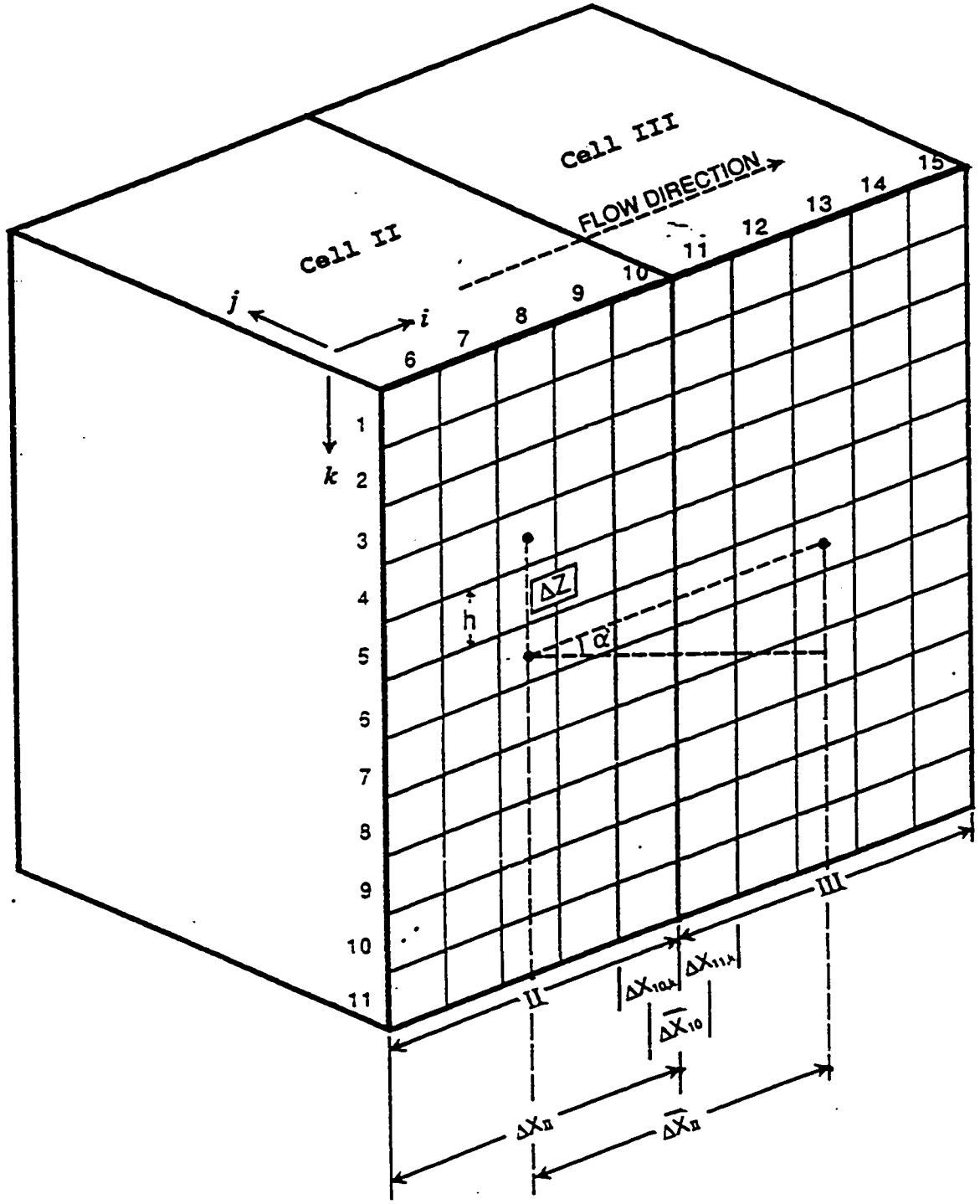

Fig.3.3: Schematic diagram showing two adjacent model cells where the pseudo relative permeability curve parameters are calculated.

3.2 Kyte and Berry Method

The following is the calculation procedure which is used in Kyte and Berry method:

1. The average water saturation S_w for cell number II in the coarse model is the pore-volume weighted average for all the small cross-sectional blocks presented in this block:

$$S_w = \frac{\sum_{i=6}^{10} \sum_{k=1}^{11} (h)_{i,k} (\varphi)_{i,k} (\Delta x)_{i,k} (Sw)_{i,k}}{\sum_{i=6}^{10} \sum_{k=1}^{11} (h)_{i,k} (\varphi)_{i,k} (\Delta x)_{i,k}} \qquad (3.1)$$

2. The total flow rate for water and oil across the boundary between the coarse blocks II and III are then calculated. These flow rates are the sum of the flow for each phase between individual cells stacked in columns 10 and 11.

$$q_o = \sum_{k=1}^{11} (q_o)_{10,k} \qquad (3.2)$$

and

$$q_w = \sum_{k=1}^{11} (q_w)_{10,k} \qquad (3.3)$$

3. To calculate the dynamic pseudo pressures for water and oil,

the phase pressure from each fine-grid cell is adjusted to the midpoint of the coarse model cell. For example for cell II, the middle column is column 8 and since the thickness is assumed uniform for all fine-grid cells the midpoint is located at cell (8, 6). Then for the oil phase;

$$P_{o_{II}} = \frac{\sum_{k=1}^{11} \left\{ \left[(P_o)_{8,k} + \frac{(\rho_o)_{8,k} (\Delta Z)_{8,k}}{144} \right] \left[K K_{ro} h \right]_{8,k} \right\}}{\sum_{k=1}^{11} (K K_{ro} h)_{8,k}} \tag{3.4}$$

Similarly for water;

$$P_{w_{II}} = \frac{\sum_{k=1}^{11} \left\{ \left[(P_w)_{8,k} + \frac{(\rho_w)_{8,k} (\Delta Z)_{8,k}}{144} \right] \left[K K_{rw} h \right]_{8,k} \right\}}{\sum_{k=1}^{11} (K K_{rw} h)_{8,k}} \tag{3.5}$$

The same procedure is used to calculate both oil and water dynamic pseudo pressures for the adjacent coarse model cell III ($P_{o_{III}}$ and $P_{w_{III}}$).

4. To calculate the dynamic pseudo relative permeability, the average coarse block permeability is first calculated, which is a harmonic average of the horizontal permeability of all vertical

stacks of blocks in the cross-section between midpoints of the upstream and the downstream coarse blocks II and III:

$$K_{II} = \frac{\overline{\Delta X}_{II}}{h_{II} \sum_{i=1}^{2} \frac{(\overline{\Delta X})_i}{(\overline{h}_i)\ (K_i)}} \qquad (3.6)$$

The average values of oil and water densities between the coarse model cells II and III are calculated first by phase volume-weighted averaging for both cells II, III, and then again phase volume-weighted averaging between the cells II and III. The same procedure is used to obtain average oil viscosity, while water viscosity is considered to be constant.

The dynamic pseudo relative permeabilities are then calculated using the following equations:

$$K_{ro} = \frac{888\ (\bar{q}_o)\ \bar{\mu}_{o_{II}}\ \Delta\overline{X}_{II}}{K_{II}\ h_{II} \left[P_{o_{II}} - P_{o_{III}} - \frac{\bar{\rho}_{o_{II}}\ \Delta\overline{X}_{II}\ Sin\alpha_{II}}{144} \right]} \qquad (3.7)$$

and similarly:

$$K_{rw} = \frac{888\ (\bar{q}_w)\ \bar{\mu}_{w_{II}}\ \Delta\bar{X}_{II}}{K_{II}\ h_{II}\left[P_{w_{II}} - P_{w_{III}} - \frac{\bar{\Gamma}_{w_{II}}\ \Delta\bar{X}_{II}\ Sin\alpha_{II}}{144}\right]} \qquad (3.8)$$

5. The dynamic pseudo capillary pressure can be obtained:

$$P_c = P_{o_{II}} - P_{w_{II}} \qquad (3.9)$$

Chapter 4

RESULTS AND DISCUSSIONS

Chapter 4

RESULTS AND DISCUSSIONS

Two different sets of data are used to study the effect of different rock, reservoir and fluid properties. The results are represented by plotting the calculated pseudo relative permeability curves for the two factors together to show the effect of the studied factors in the pseudo relative permeability generated from each cross-section. For example, to study the effect of thickness on pseudo relative permeability two thicknesses were chosen to be the maximum and minimum of the reservoir typical thickness; one is 110 feet and the other is 50 feet. The resultant pseudo relative permeability curves from the two thicknesses are plotted for all cross-sections keeping all other parameters constant except thickness. In the following discussions, the parameters used are specified and their effect of them is shown for all cases studied. Individual pseudo relative permeability curves for all cases are shown in the appendix.

4.1 Reservoir PVT Properties Effect

Two sets of PVT data are typically used for this reservoir. These two PVT data represent the reservoir depending on the depth of the reservoir. The two PVT data are shown in Tables 4.1 and 4.2. They are labeled here as PVT1 and PVT2 respectively. The PVT1 has a

Table 4.1: Oil PVT Properties (PVT #1)

Pressure (psia)	Bo (RB/STB)	Density (gm/cc)	Viscosity (cp)	Solution Gas (SCF/STB)
100.0	1.0715	2.5147	35.06	23.0
300.0	1.0903	0.9835	11.45	69.0
500.0	1.1090	0.8759	6.74	115.0
937.0(BPP)	1.1501	0.8136	3.45	215.0
1000.0	1.1490	0.8136	3.489	215.0
1200.0	1.1468	0.8136	3.560	215.0
1400.0	1.1446	0.8136	3.632	215.0
1600.0	1.1425	0.8136	3.703	215.0
1800.0	1.1403	0.8136	3.775	215.0
2000.0	1.1381	0.8136	3.846	215.0
2200.0	1.1360	0.8136	3.918	215.0
2400.0	1.1338	0.8136	3.989	215.0
2600.0	1.1316	0.8136	4.061	215.0
2800.0	1.1295	0.8136	4.132	215.0
3000.0	1.1273	0.8136	4.204	215.0
3200.0	1.1251	0.8136	4.276	215.0
3400.0	1.1230	0.8136	4.347	215.0
3600.0	1.1208	0.8136	4.419	215.0
3800.0	1.1186	0.8136	4.490	215.0
4000.0	1.1165	0.8136	4.562	215.0
4200.0	1.1143	0.8136	4.633	215.0
4400.0	1.1121	0.8136	4.705	215.0
4600.0	1.1100	0.8136	4.776	215.0
4800.0	1.1078	0.8136	4.848	215.0
5000.0	1.1056	0.8136	4.919	215.0
5200.0	1.1035	0.8136	4.991	215.0

Table 4.2: Oil PVT Properties (PVT #2)

Pressure (psia)	Bo (RB/STB)	Density (gm/cc)	Viscosity (cp)	Solution Gas (SCF/STB)
100.0	1.0715	2.5147	35.06	23.0
300.0	1.0903	0.9835	11.45	69.0
500.0	1.1090	0.8759	6.74	115.0
1000.0	1.1560	0.8094	3.21	229.0
1200.0	1.1747	0.7993	2.63	275.0
1389.0(BPP)	1.1925	0.7925	2.23	318.0
1400.0	1.1924	0.7925	2.236	318.0
1600.0	1.1901	0.7925	2.307	318.0
1800.0	1.1879	0.7925	2.379	318.0
2000.0	1.1856	0.7925	2.451	318.0
2200.0	1.1834	0.7925	2.522	318.0
2400.0	1.1811	0.7925	2.594	318.0
2600.0	1.1789	0.7925	2.665	215.0
2800.0	1.1766	0.7925	2.737	318.0
3000.0	1.1744	0.7925	2.808	318.0
3200.0	1.1721	0.7925	2.880	318.0
3400.0	1.1699	0.7925	2.951	318.0
3600.0	1.1676	0.7925	3.023	318.0
3800.0	1.1654	0.7925	3.094	318.0
4000.0	1.1632	0.7925	3.166	318.0
4200.0	1.1609	0.7925	3.237	318.0
4400.0	1.1587	0.7925	3.309	318.0
4600.0	1.1564	0.7925	3.380	318.0
4800.0	1.1542	0.7925	3.452	318.0
5000.0	1.1519	0.7925	3.523	318.0
5200.0	1.1497	0.7925	3.595	318.0

bubble point pressure of 937 psia and the PVT2 bubble point pressure is 1389 psia. The oil density values at bubble point pressures of PVT1 and PVT2 are 0.8136 gm/cc and 0.7925 gm/cc respectively. Each one of the two PVT data was used in all sets of cross-sections. The comparison of the resultant pseudo relative permeability curves are shown in Figs. 4.1 through 4.4. It can be noticed that PVT properties have an effect on pseudo relative permeability curves, this effect is minimal in the cross-sections where the thickness is large (110 feet) and the dip angle is low (1°). The maximum effect is noticed for the smaller thickness (50 feet) and the higher reservoir dip angle of (4°). The PVT properties have this effect because the lighter oil has different mobility ratio than the heavier oil, the smaller the mobility ratio the better the volumetric sweep and K_{ro} will be higher for the same water saturation value. This effect is also shown for the heavier oil but in a lower scale compared to the lighter oil.

4.2 Ratio of Vertical Permeability to Horizontal Permeability

A typical sandstone reservoir has discontinuous shale streaks in some areas of the reservoir depending on the sedimentation process of the reservoir. The existence of these shale streaks may have an influence on the fluid movement in the reservoir. The area where the shale streaks exist is called the stringer sands while the area where no shale is noticed is called the main sand.

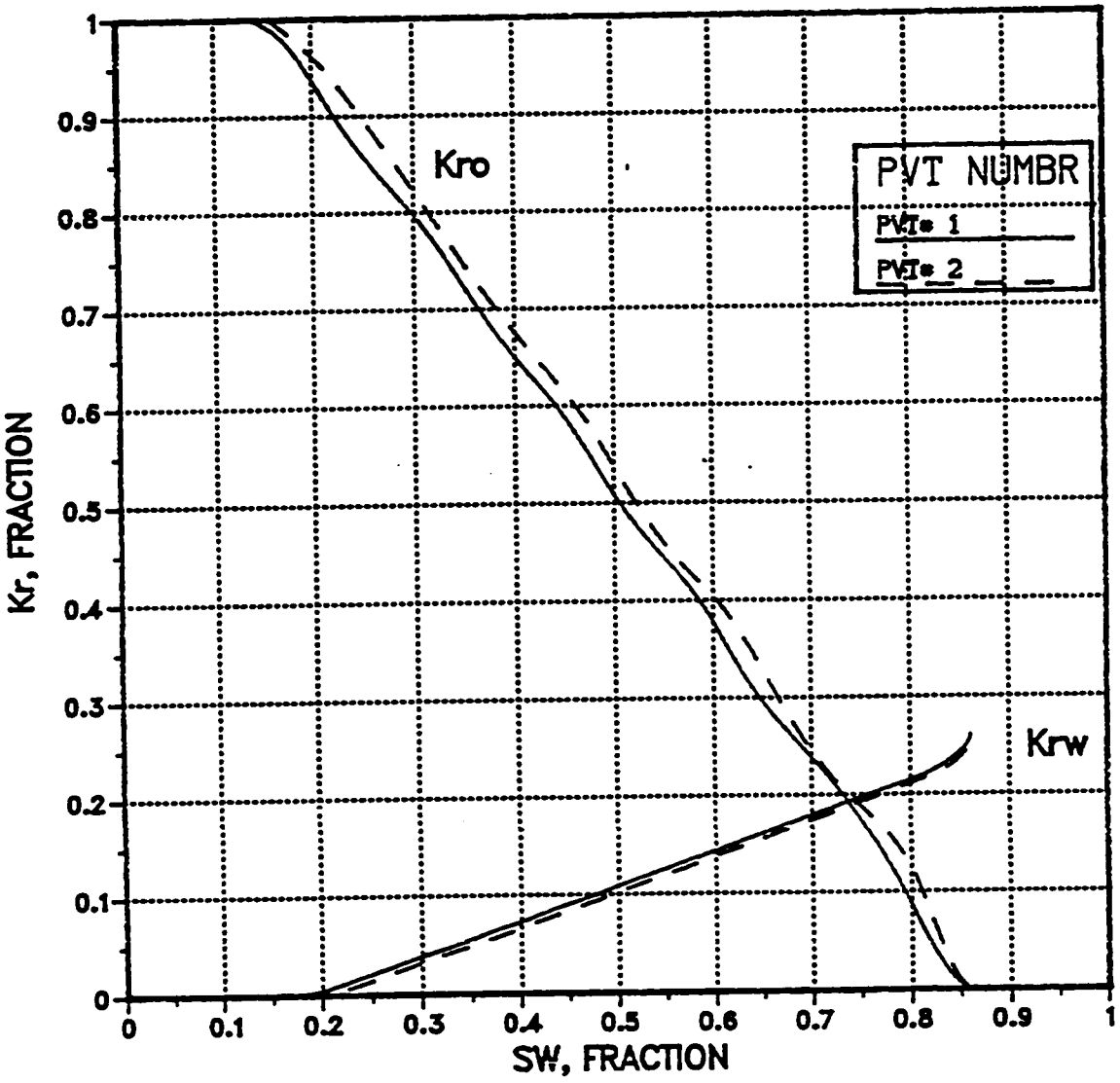

Fig.4.1: PVT data effect for the cross-section - thickness = 110', layers = 11-20, Kv/Kx = 0.7, cells = 71-80, angle 1.

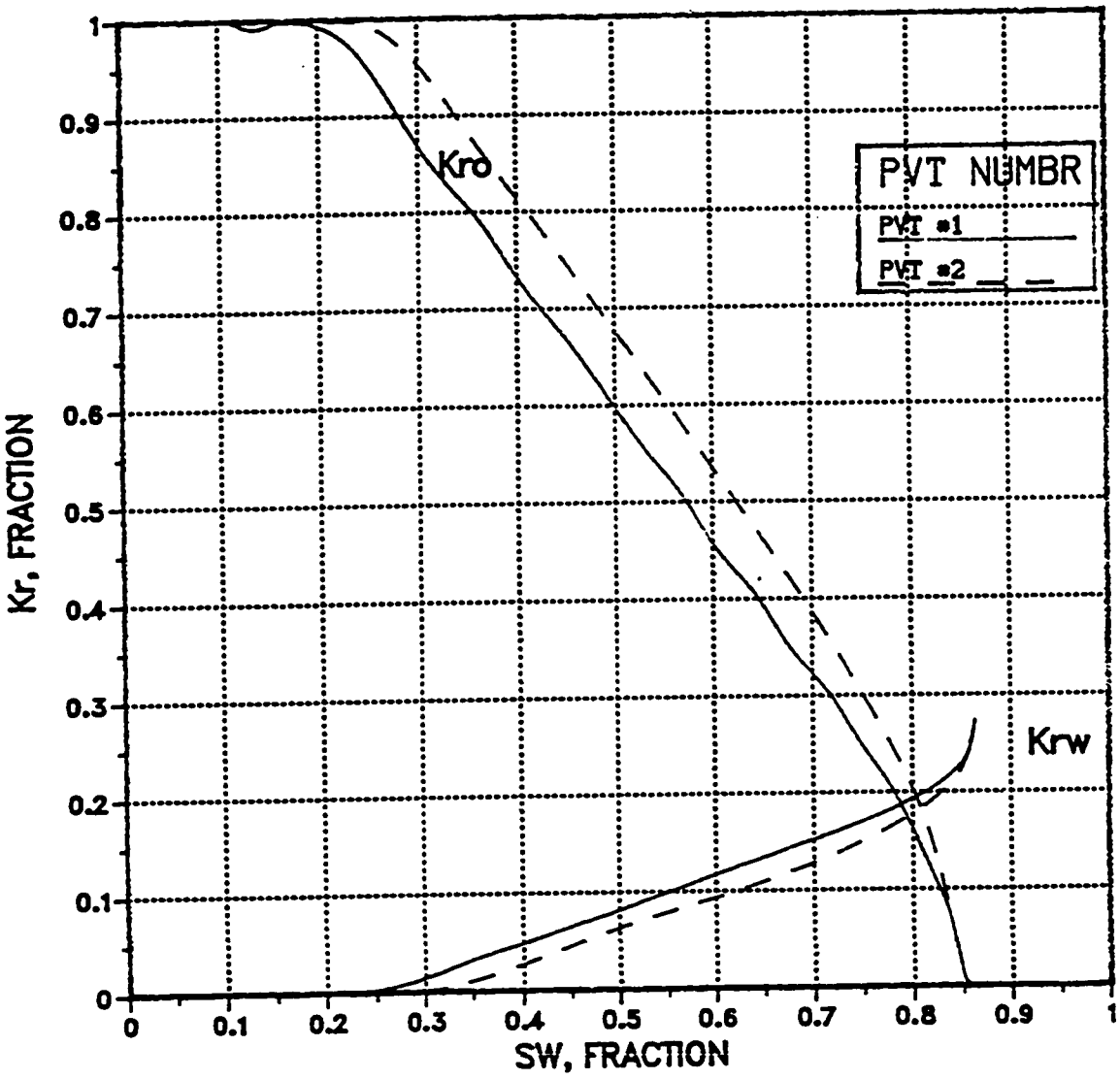

Fig.4.2: PVT data effect for the cross-section - thickness = 110', layers = 11-20, Kv/Kx = 0.7, cells = 71-80, angle 4.

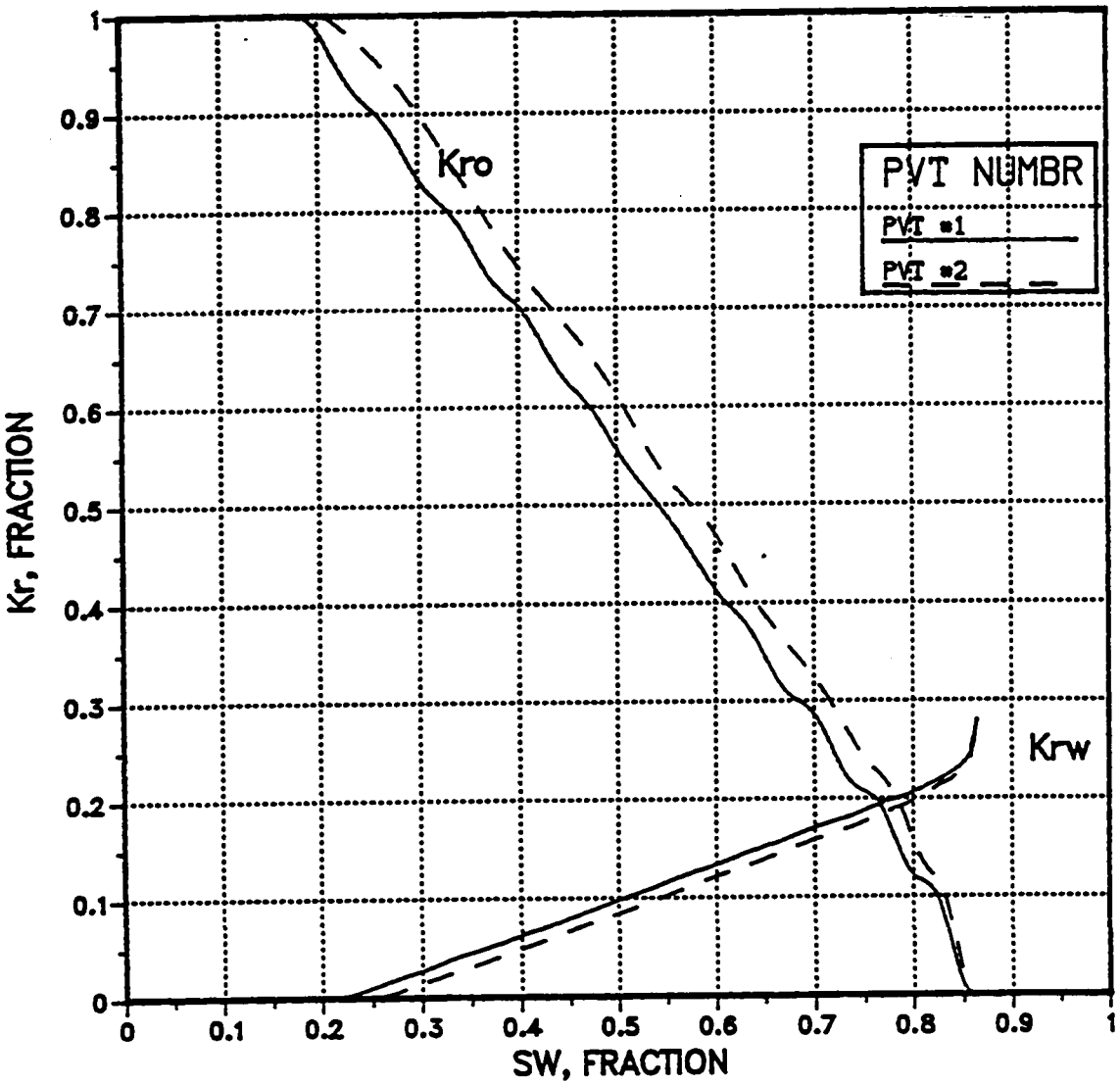

Fig.4.3: PVT data effect for the cross-section - thickness = 50', layers = 11-20, Kv/Kx = 0.7, cells = 71-80, angle 1.

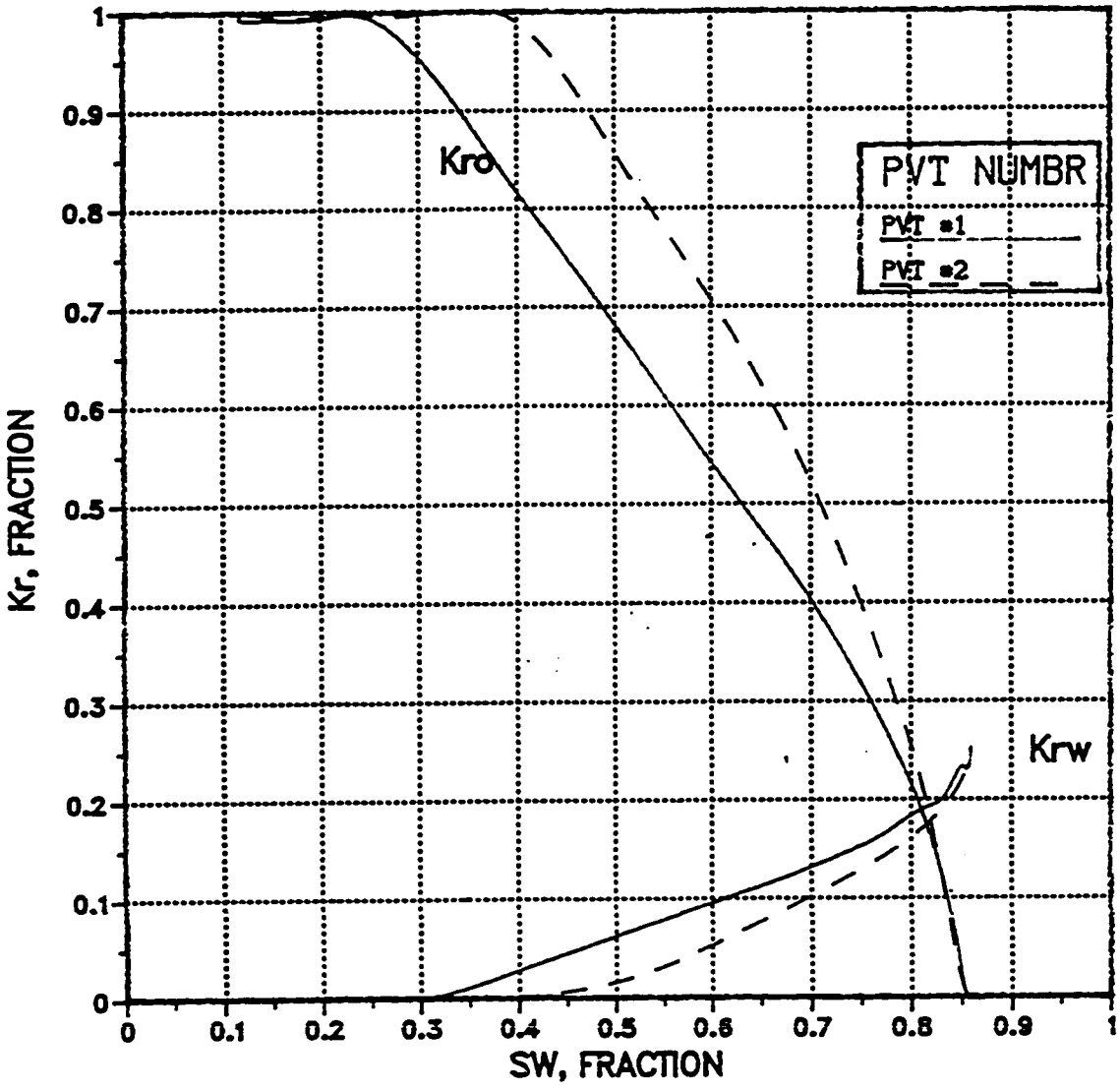

Fig.4.4: PVT data effect for the cross-section, thickness = 50', layers = 11-20, Kv/Kx = 0.7, cells = 71-80, angle 4.

To simulate the reservoir stringer effect a lower vertical to horizontal permeability ratio of 0.3 was used compared to a ratio of 0.7 for the main sand body of the reservoir. The horizontal permeability for the reservoir is considered constant for all cross-sectional cases and equals to 5 Darcys. For the stringer sands runs a vertical permeability value of 1.5 Darcy was used and for the main sand cases 3.5 Darcy.

The pseudo relative permeability curves generated for both the stringers and main sand are shown in Figs. 4.5 through 4.12.

It can be noticed from the figures that the pseudo relative permeability curves generated for the stringers are almost identical with the ones generated from the main sand. Apparently the ratio of vertical to horizontal permebility does not have an effect for this set of data.

For this reason, the cross-sectional models for the stringers were eliminated for the next parameters studied.

4.3 Effect of Layer Thickness

Two layer thicknesses of 50 ft and 110 ft were used to study their effect on pseudo relative permeability curves. The first value is 110 feet and the other one is 50 feet which are considered to be the layer thicknesses of the full-field model layers. Because each full-field model layer is divided in the fine gridded cross-section to 10 layers the fine

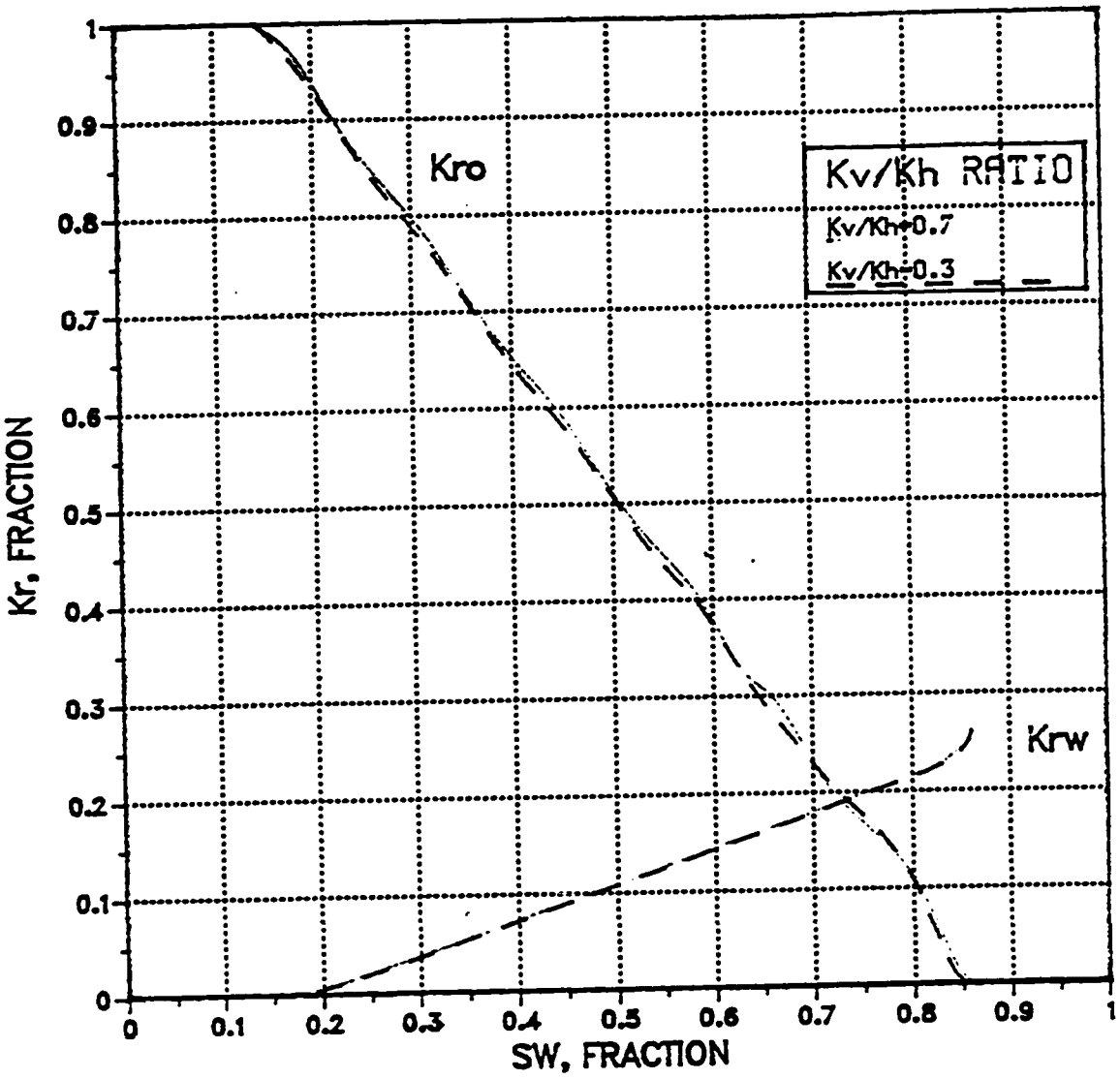

Fig.4.5: Kv/Kx Ratio effect for the cross-section - thickness = 110', layers = 11-20, angle 1, cells = 71-80, PVT No.1.

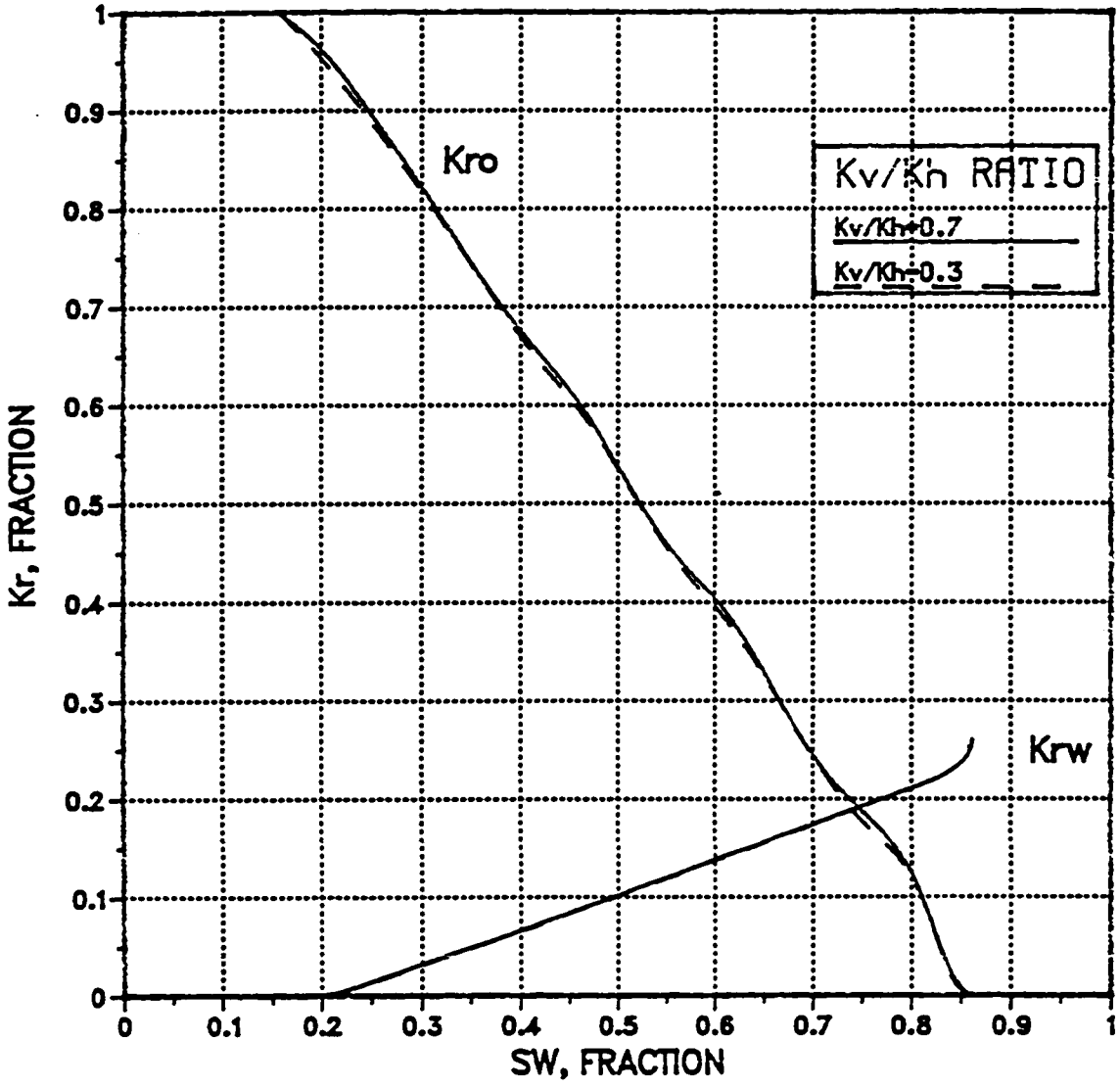

Fig.4.6: Kv/Kx Ratio effect for the cross-section - thickness = 110', layers = 11-20, angle 1, cells = 71-80, PVT No.2.

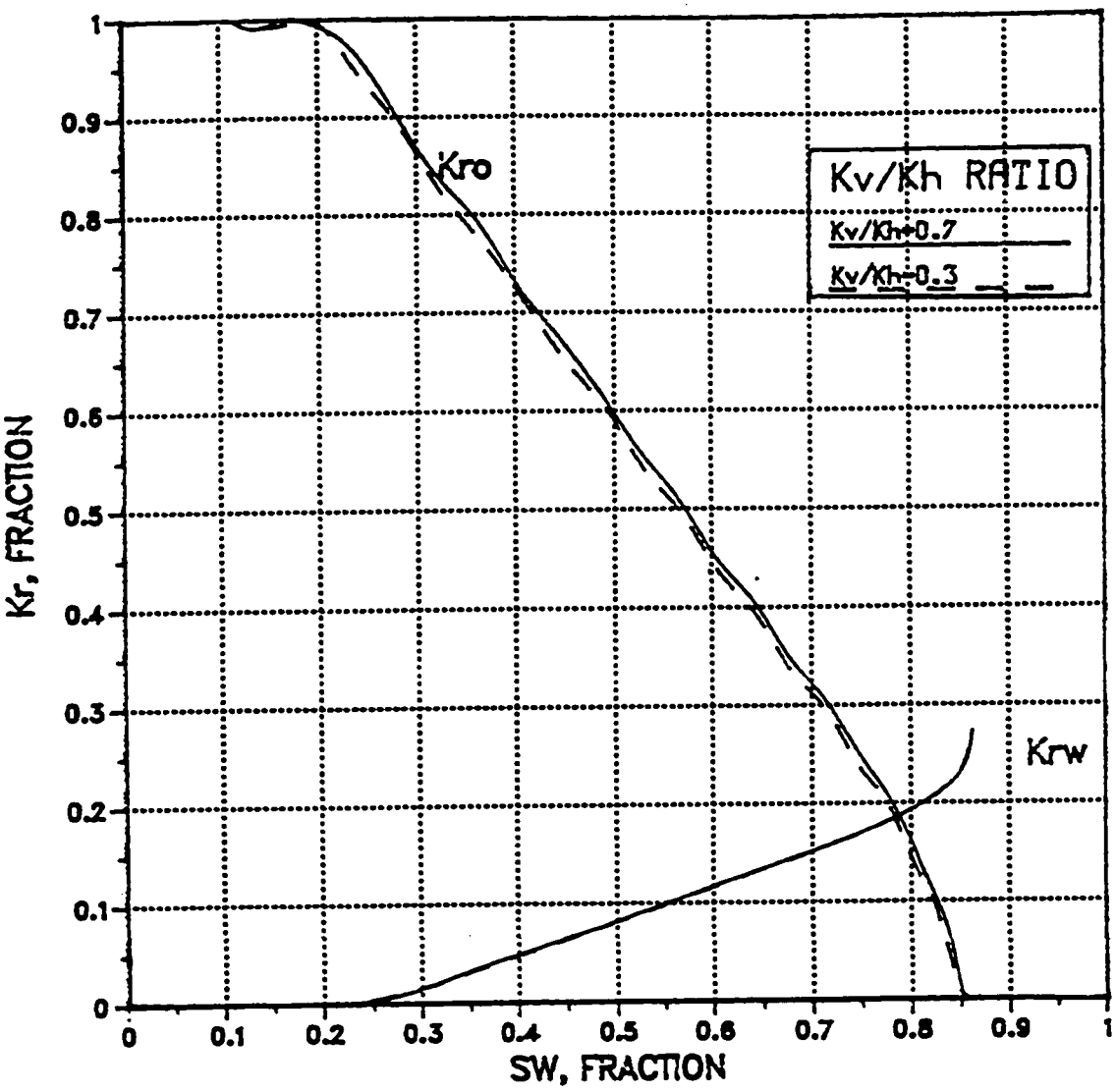

Fig.4.7: Kv/Kx Ratio effect for the cross-section - thickness = 110', layers = 11-20, angle 4, cells = 71-80, PVT No.1.

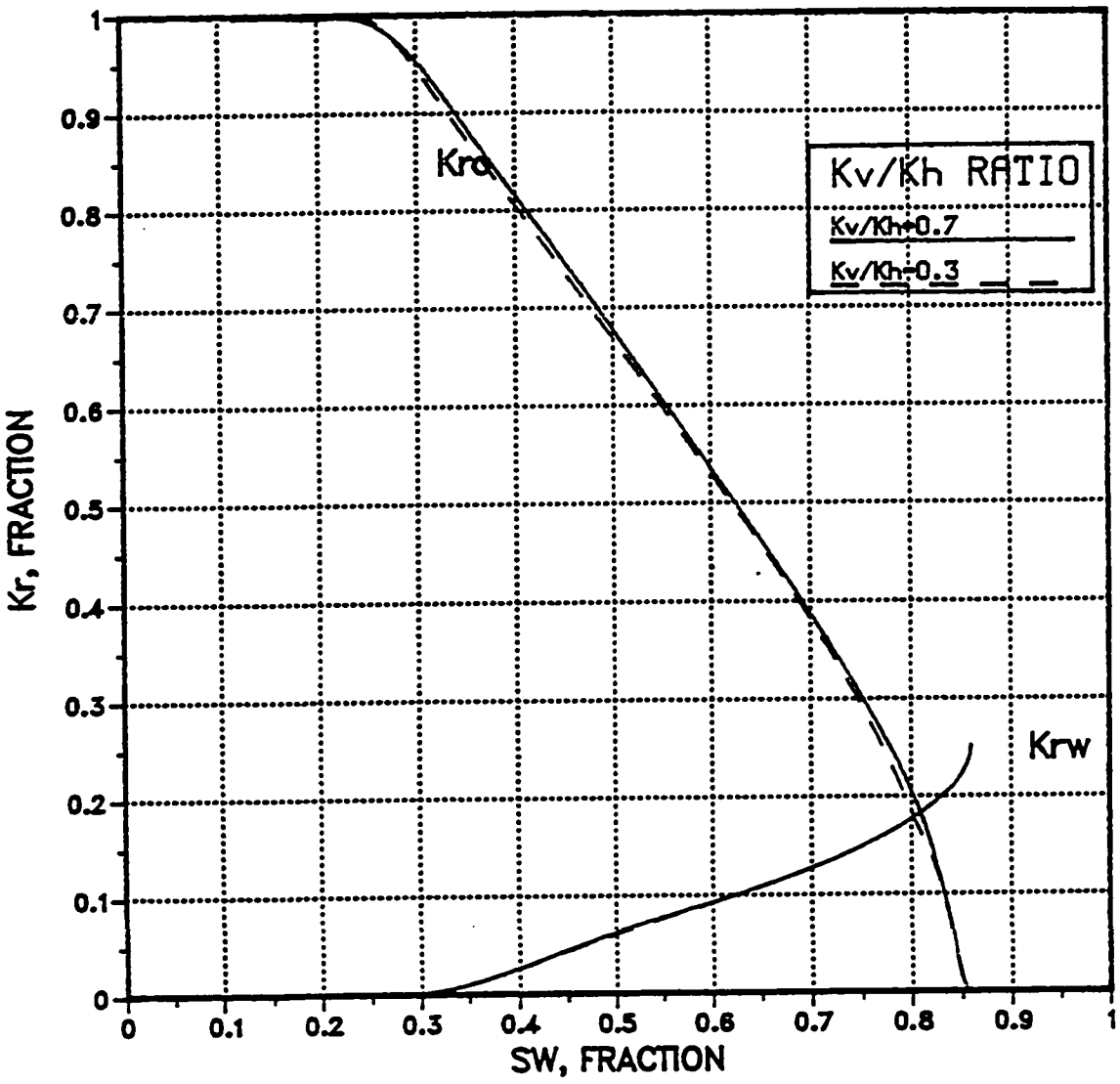

Fig.4.8: Kv/Kx Ratio effect for the cross-section - thickness = 110', layers = 11-20, angle 4, cells = 71-80, PVT No.2.

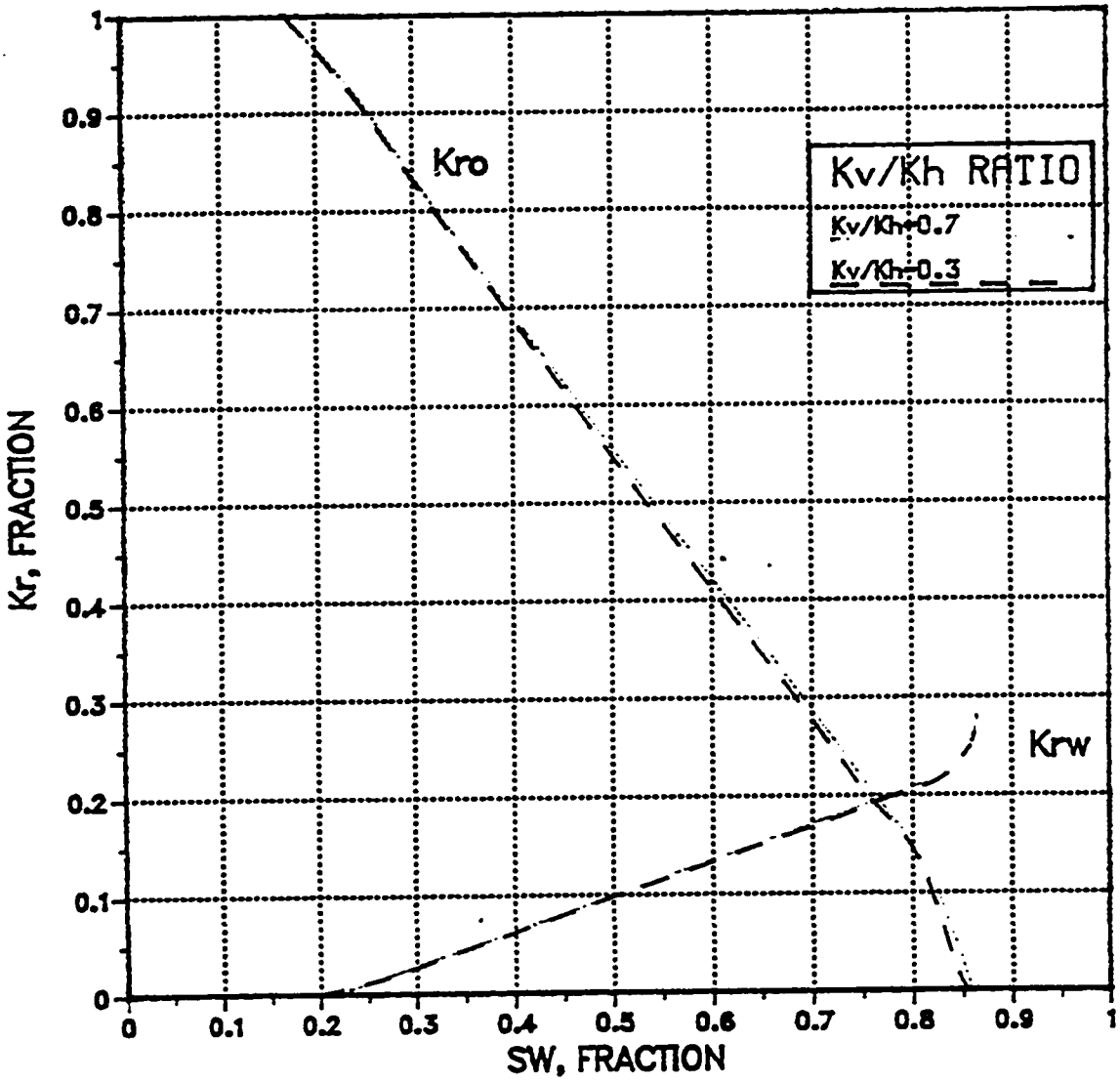

Fig.4.9: Kv/Kx Ratio effect for the cross-section - thickness = 50', layers = 11-20, angle 1, cells = 71-80, PVT No.1.

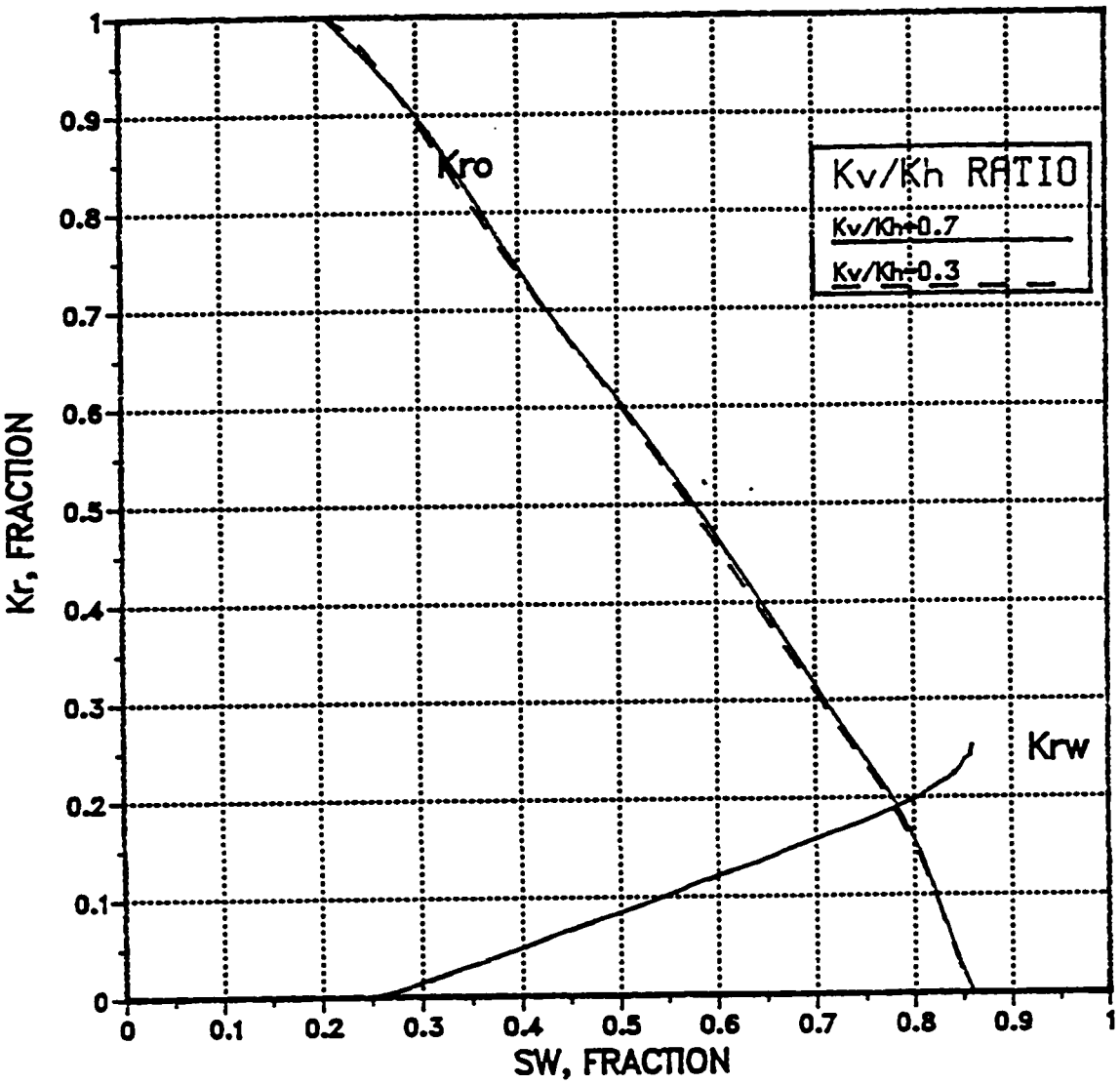

Fig.4.10: Kv/Kx Ratio effect for the cross-section - thickness = 50', layers = 11-20, angle 1, cells = 71-80, PVT No.2.

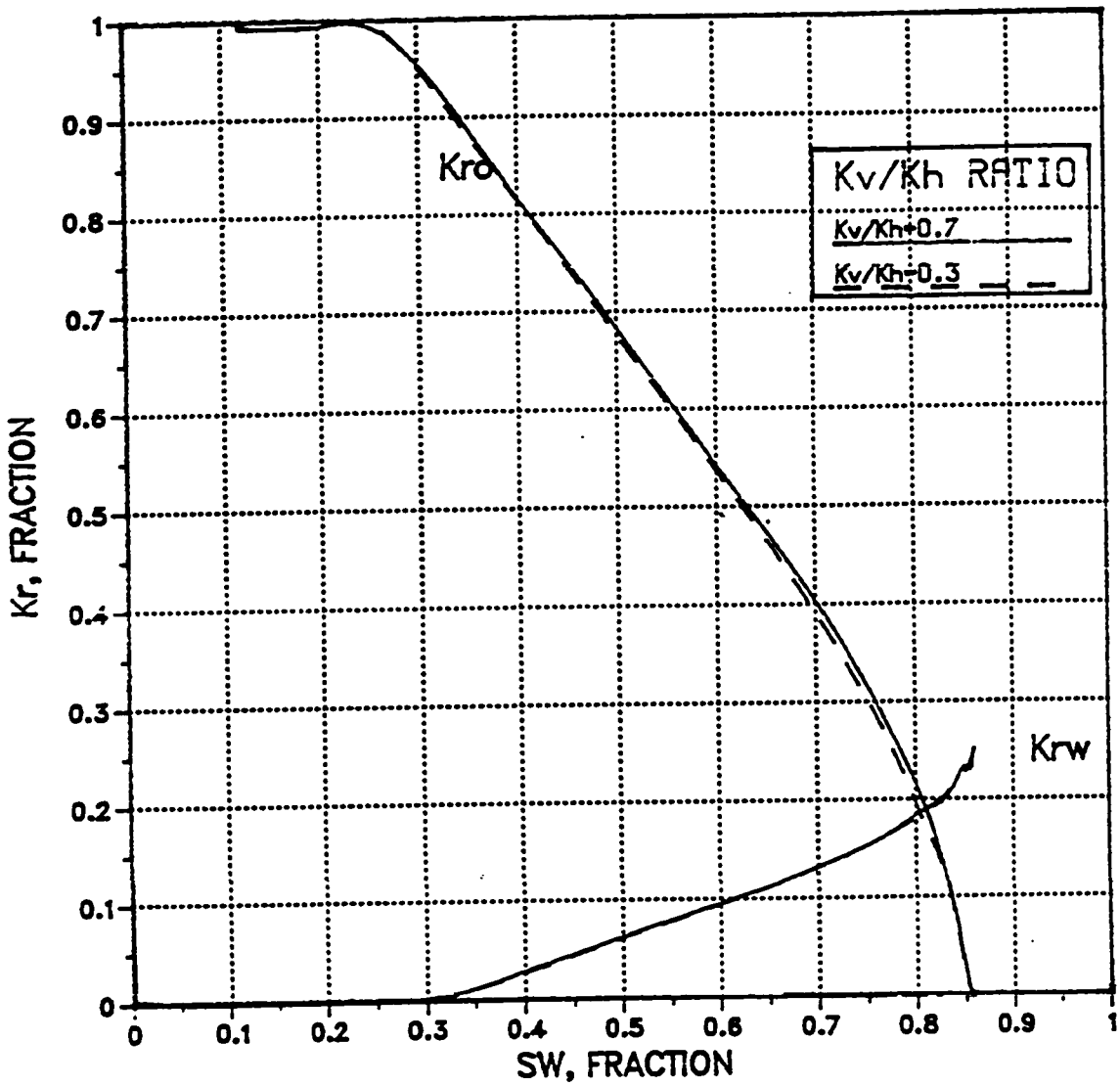

Fig.4.11: Kv/Kx Ratio effect for the cross-section - thickness = 50', layers = 11-20, angle 4, cells = 71-80, PVT No.1.

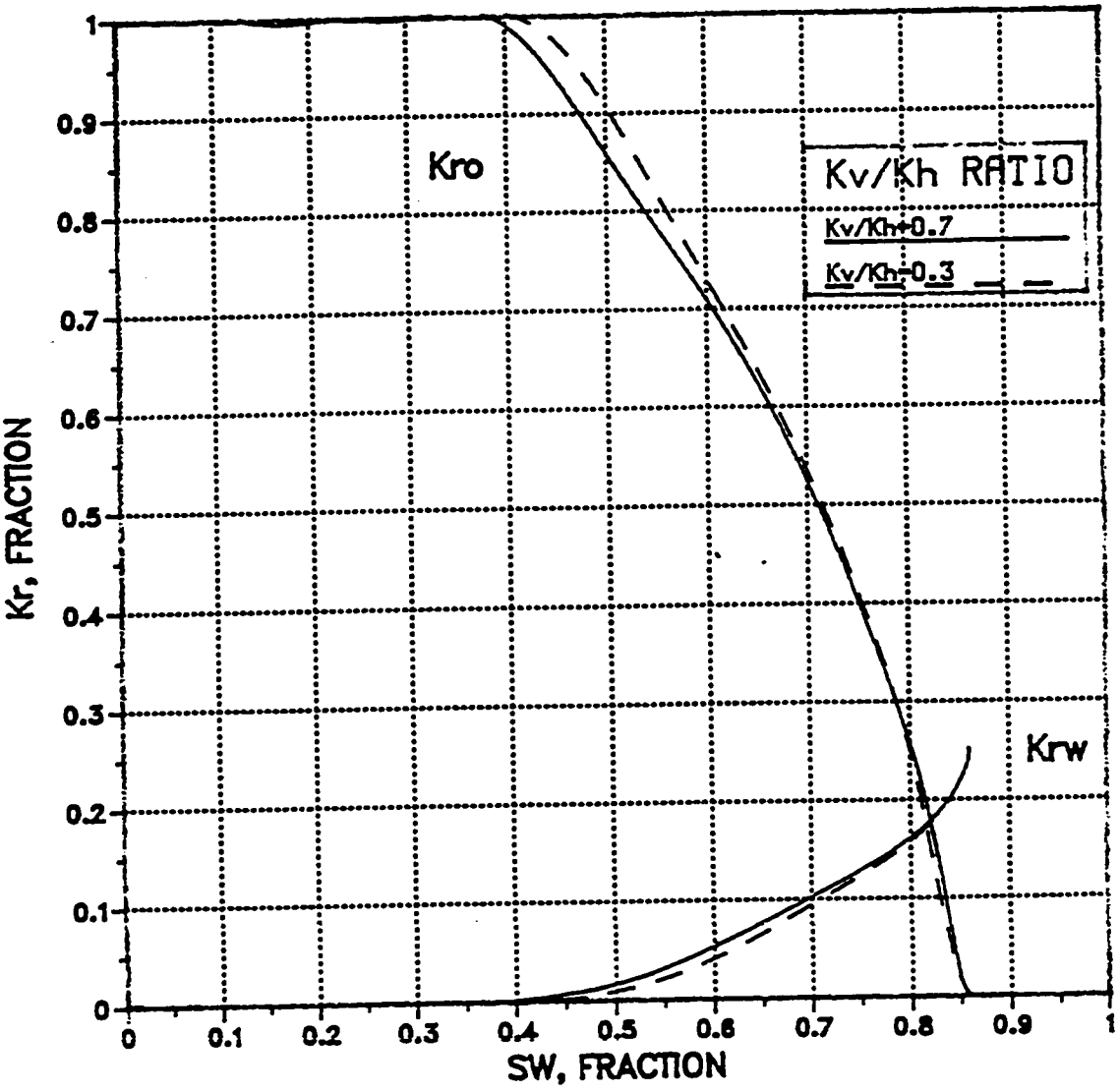

Fig.4.12: Kv/Kx Ratio effect for the cross-section - thickness = 50', layers = 11-20, angle, 4 cells = 71-80, PVT No.2.

grid layers are 11 feet for the maximum and 5 feet which is considered to be the minimum. The production rate was maintained at about 1.1 per cent of original oil in-place per year. Pseudo relative permeability curves generated from the cross-sectional models for these parameters are shown in Figs. 4.13 through 4.16. It can be noticed that the layer thickness always affects the pseudo relative permeability curves.

The most significant effect is caused by the combination of the smallest thickness and the highest dip angle of 4°. The minimum effect is noticed for the minimum dip angle and the highest thickness which is 110 feet.

4.4 Production Rate

The average production rate for all previous cases was kept constant at about 1.1% of original oil in-place per year. To study the effect of production rate on pseudo relative permeability curves the production rate was varied by a factor of 1.5. The cross-sectional models were run with the new rate and because the cross-sections were run in prediction mode, the oil production is replaced with a higher injection rate from the injectors which simulate the case of a very active water derive reservoir which is the case for most Saudi sandstone reservoirs. The resulting pseudo relative permeability curves are shown in Figs. 4.17 to 4.24.

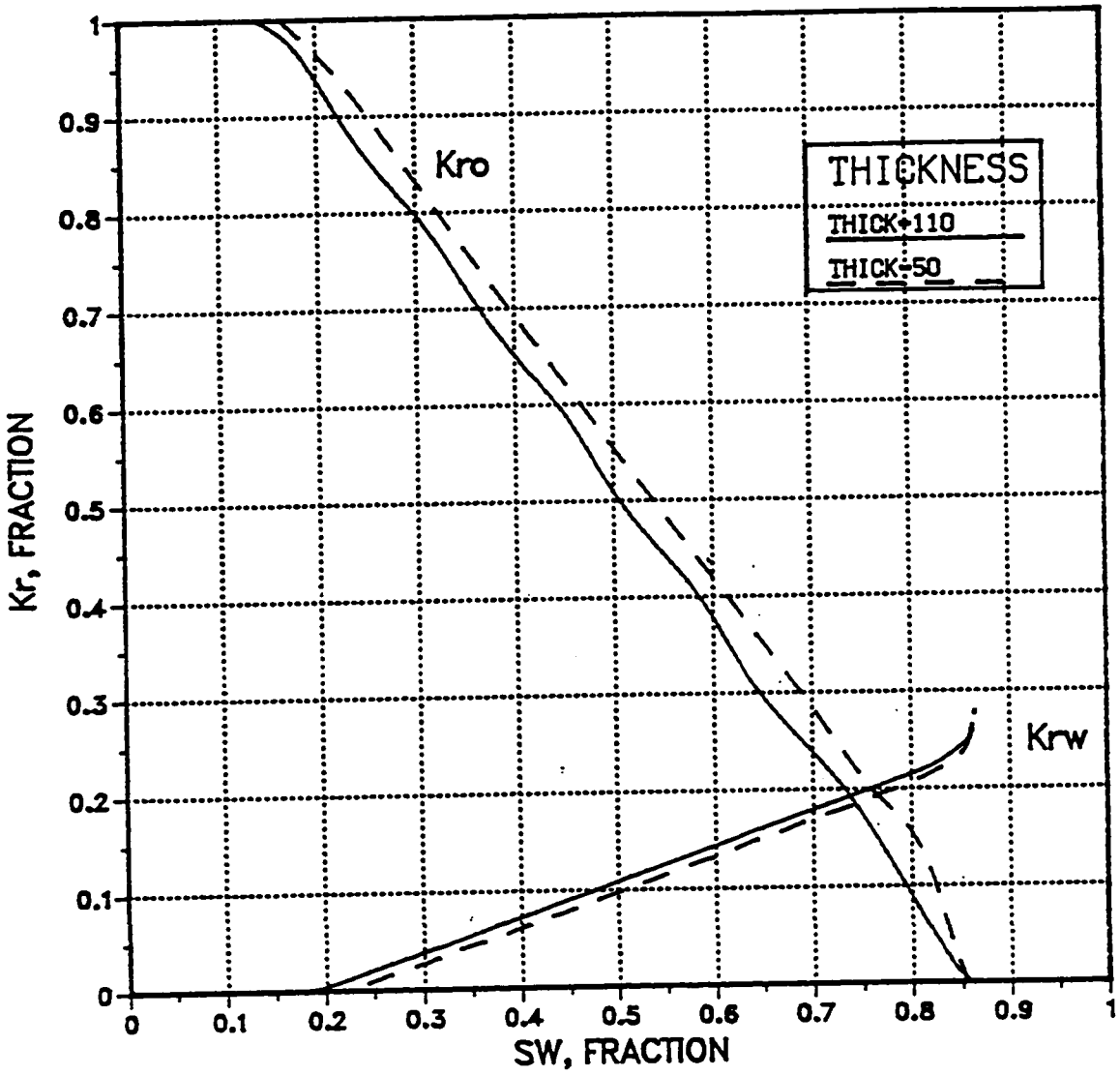

Fig.4.13: Layer thickness effect for the cross-section - angle 1, layers = 11-20, Kv/Kx = 0.7, cells = 71-80, PVT No.1.

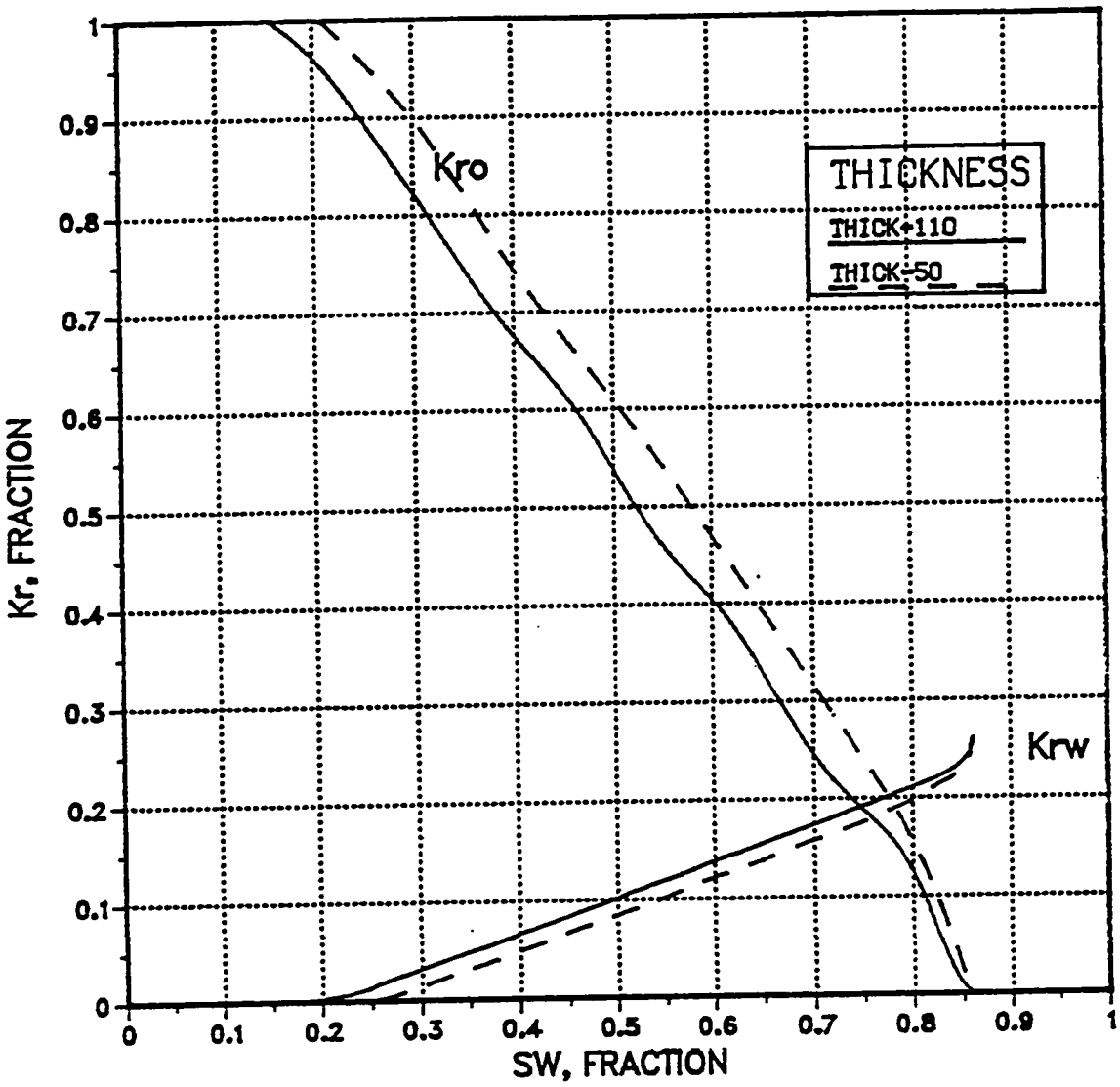

Fig.4.14: Layer thickness effect for the cross-section - angle 1, layers = 11-20, Kv/Kx = 0.7, cells = 71-80, PVT No.2.

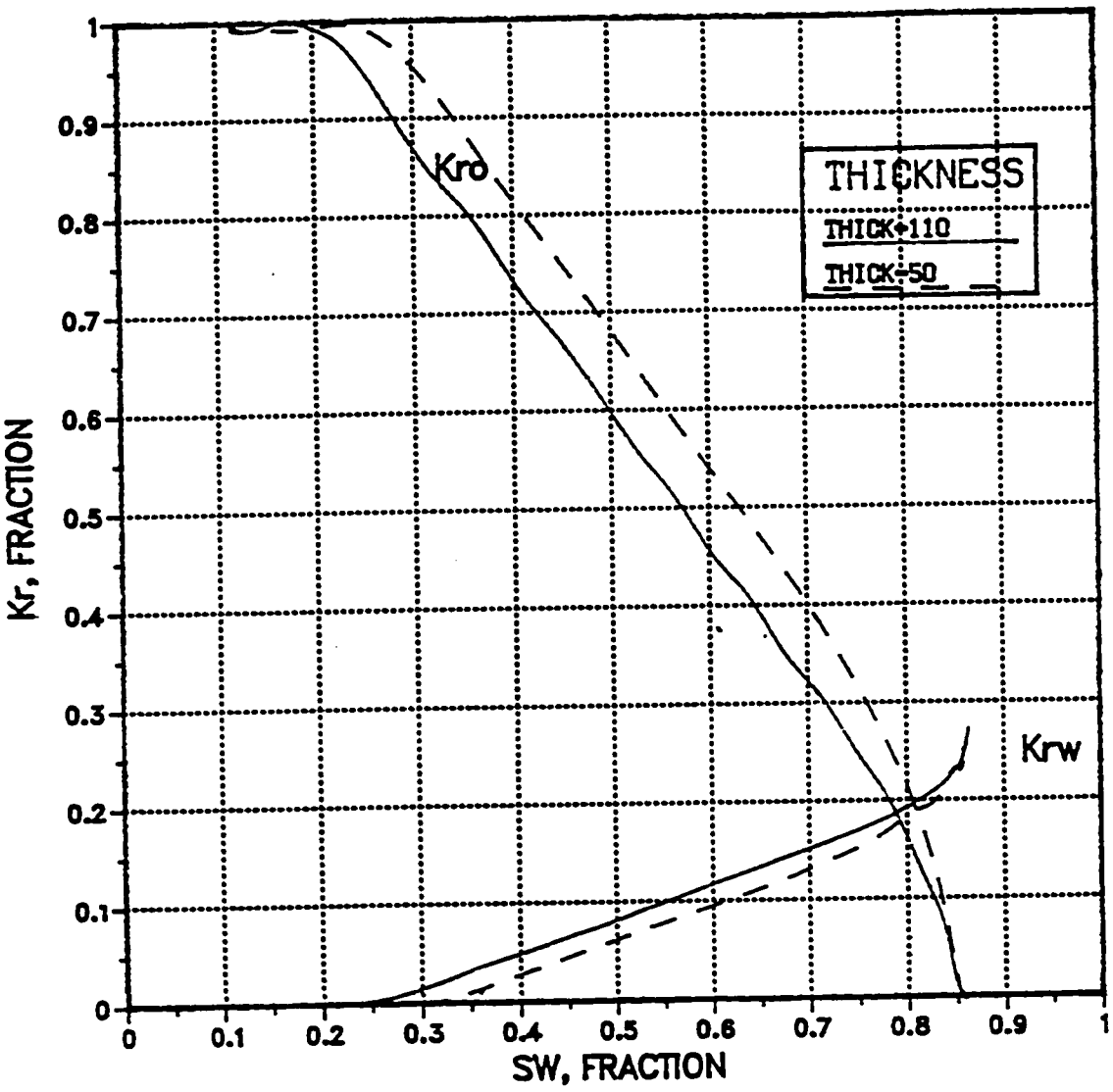

Fig.4.15: Layer thickness effect for the cross-section - angle 4, layers = 11-20, Kv/Kx = 0.7, cells = 71-80, PVT No.1.

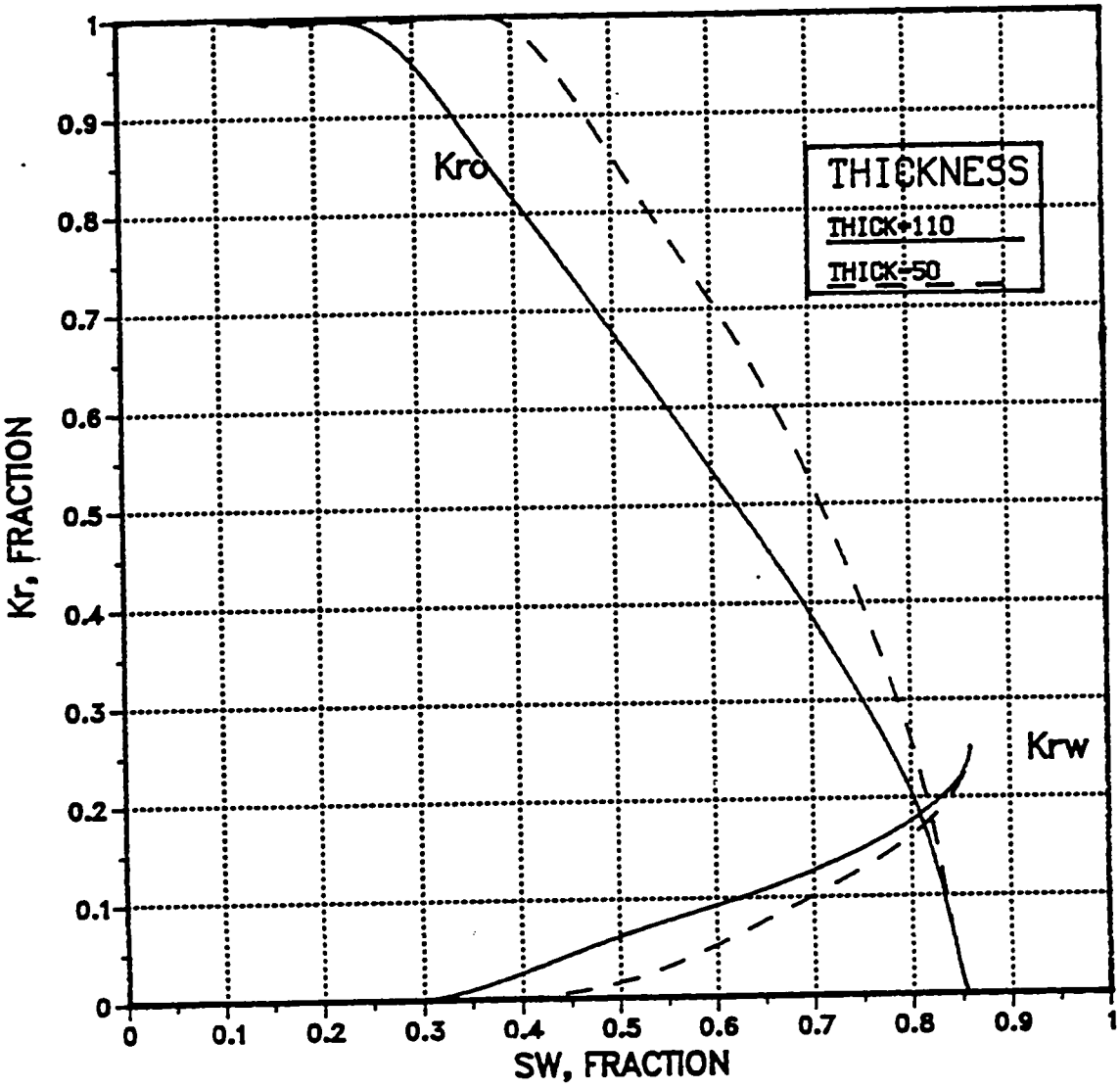

Fig.4.16: Layer thickness effect for the cross-section - thickness = 110', angle 4, layers = 11-20, Kv/Kx = 0.7, cells = 71-80, PVT No.2.

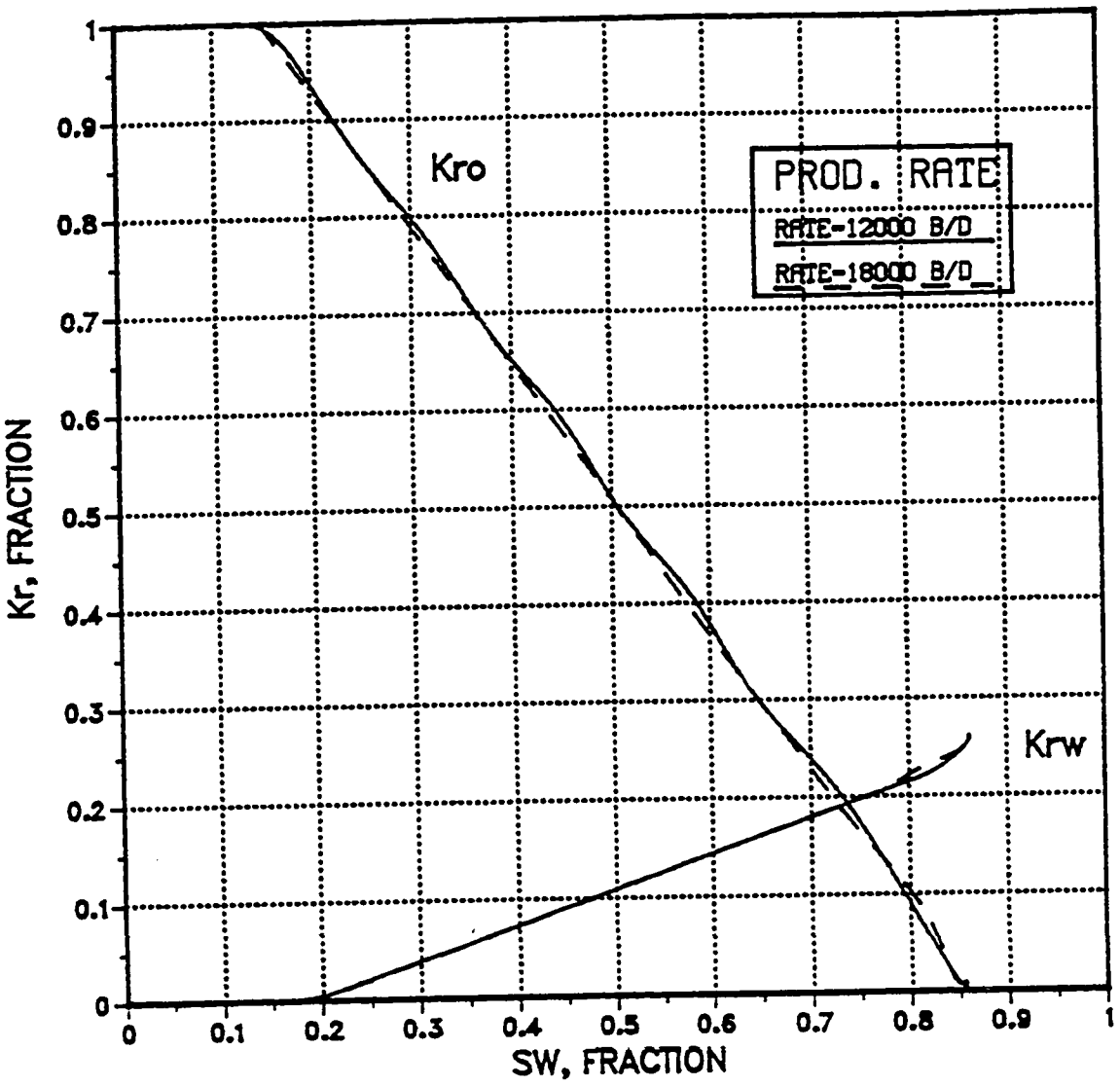

Fig.4.17: Production rate effect for the cross-section - thickness = 110', angle 1, layers = 11-20, Kv/Kx = 0.7, cells = 71-80, PVT No.1.

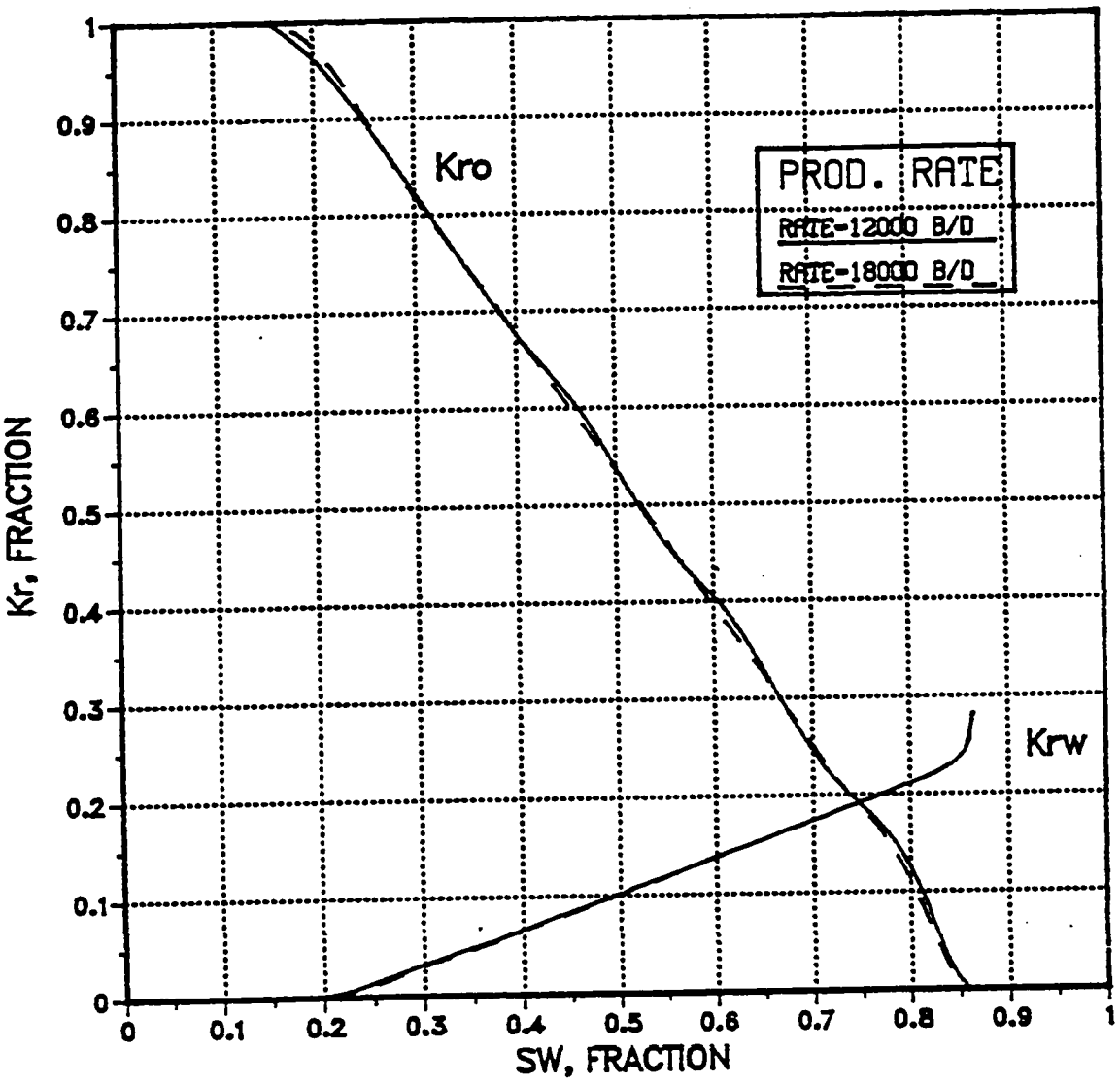

Fig.4.18: Production rate effect for the cross-section - thickness = 110', angle 1, layers = 11-20, Kv/Kx = 0.7, cells = 71-80, PVT No.2.

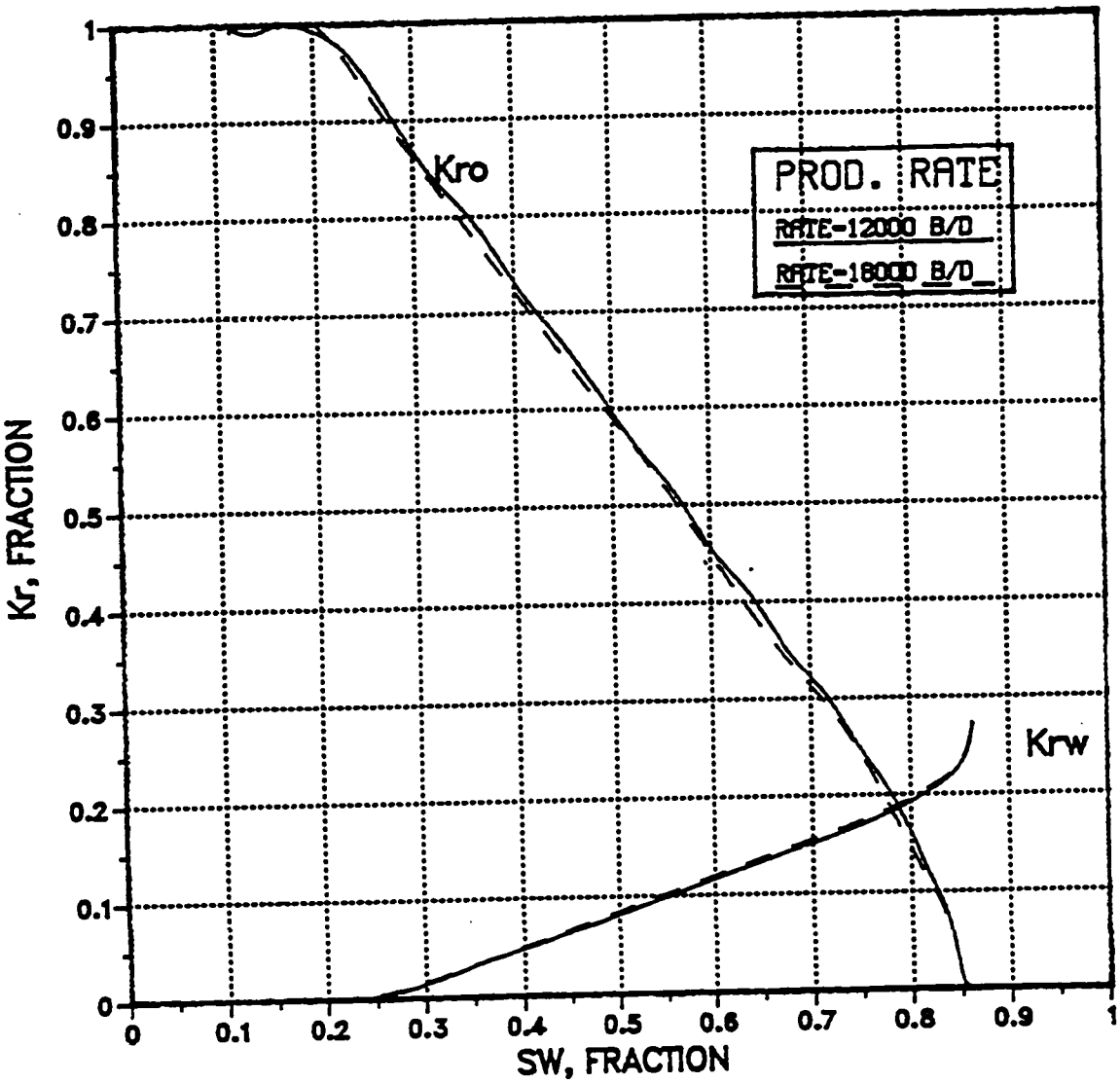

Fig.4.19: Production rate effect for the cross-section - thickness = 110', angle 4, layers = 11-20, Kv/Kx = 0.7, cells = 71-80, PVT No.1.

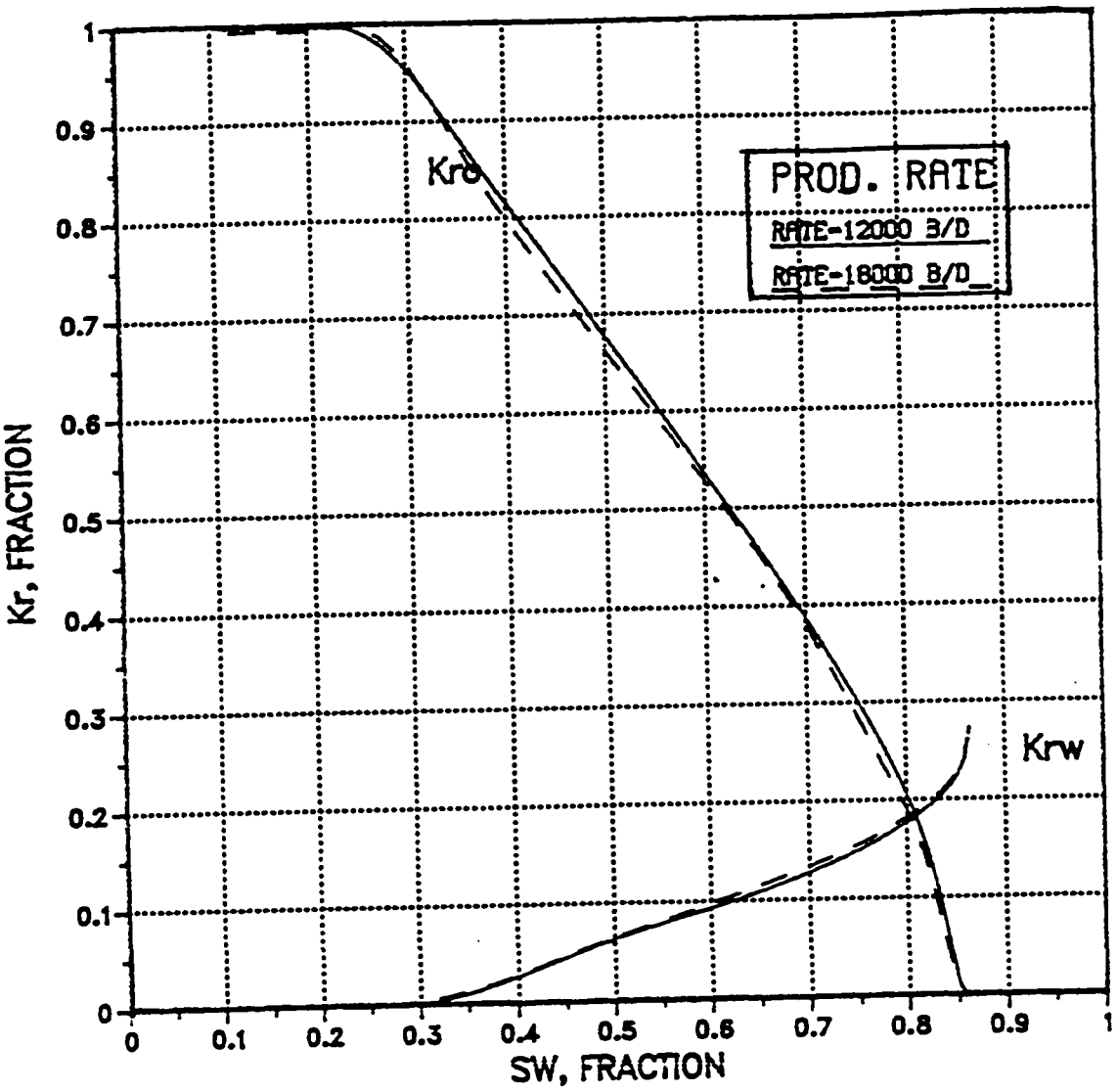

Fig.4.20: Production rate effect for the cross-section - thickness = 110', angle 4, layers = 11-20, Kv/Kx = 0.7, cells = 71-80, PVT No.2.

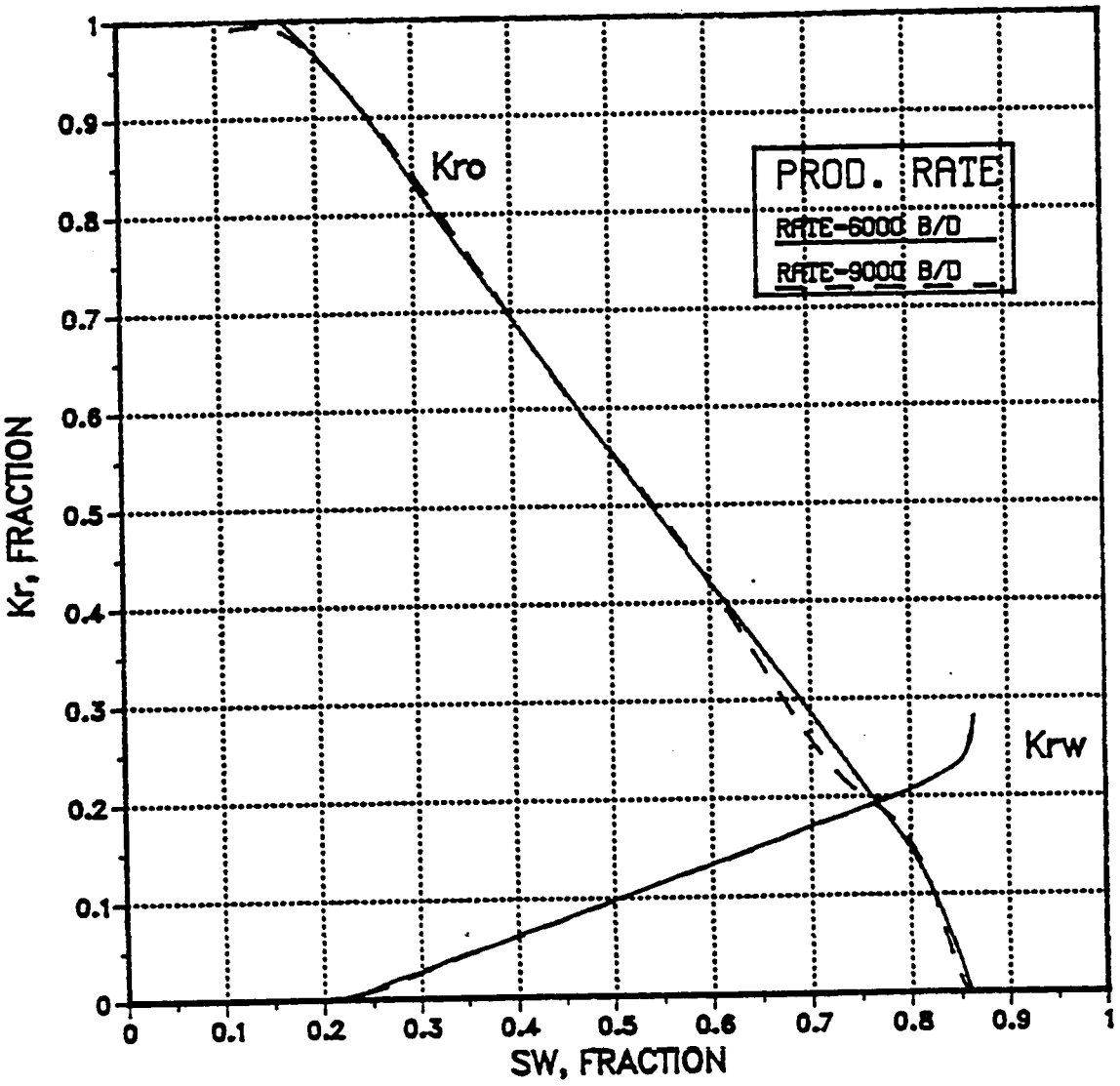

Fig.4.21: Production rate effect for the cross-section - thickness = 50', angle 1, layers = 11-20, Kv/Kx = 0.7, cells = 71-80, PVT No.1.

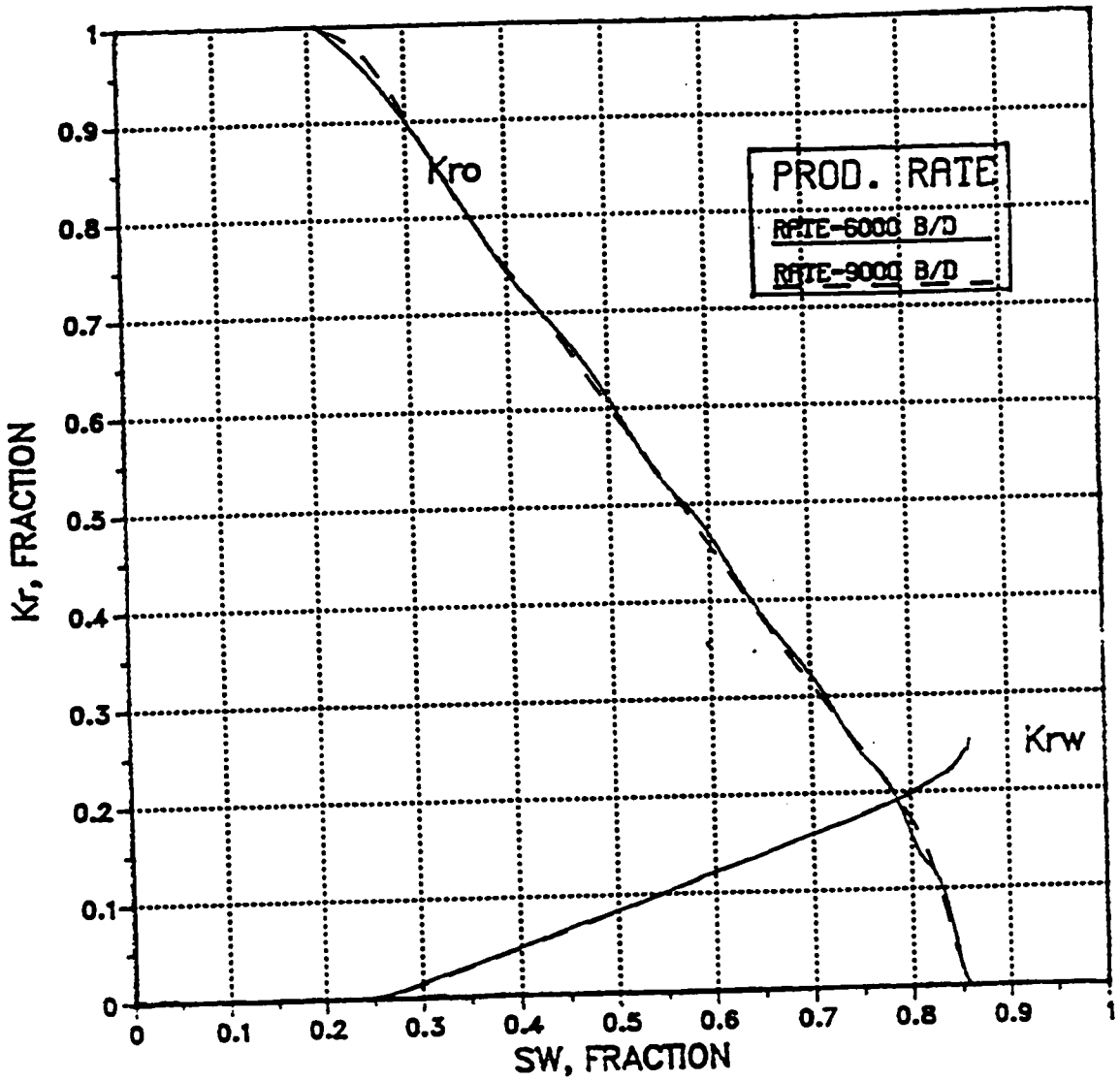

Fig.4.22: Production rate effect for the cross-section - thickness = 50', angle 1, layers = 11-20, Kv/Kx = 0.7, cells = 71-80, PVT No.2.

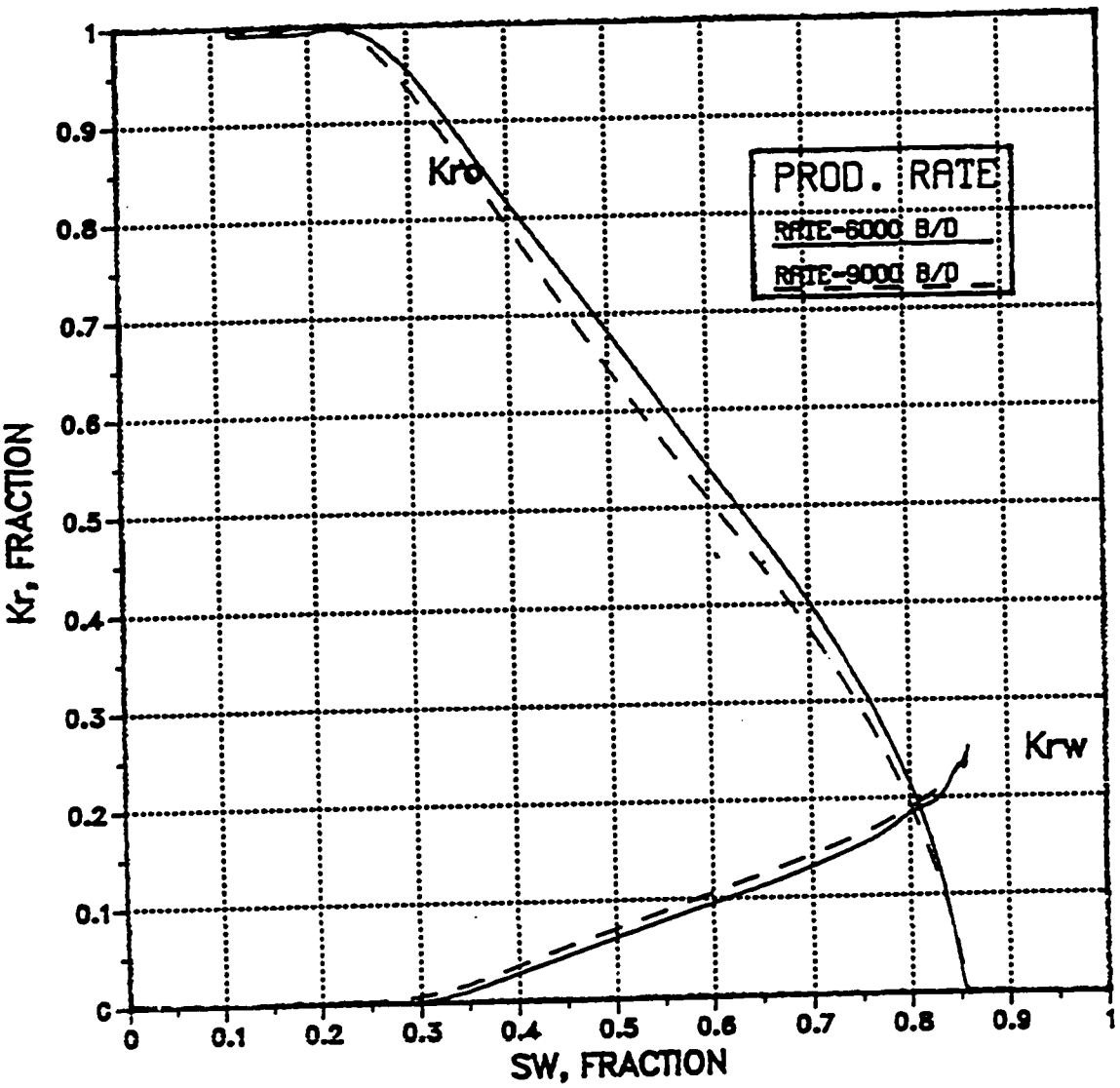

Fig.4.23: Production rate effect for the cross-section - thickness = 50', angle 4, layers = 11-20, Kv/Kx = 0.7, cells = 71-80, PVT No.1.

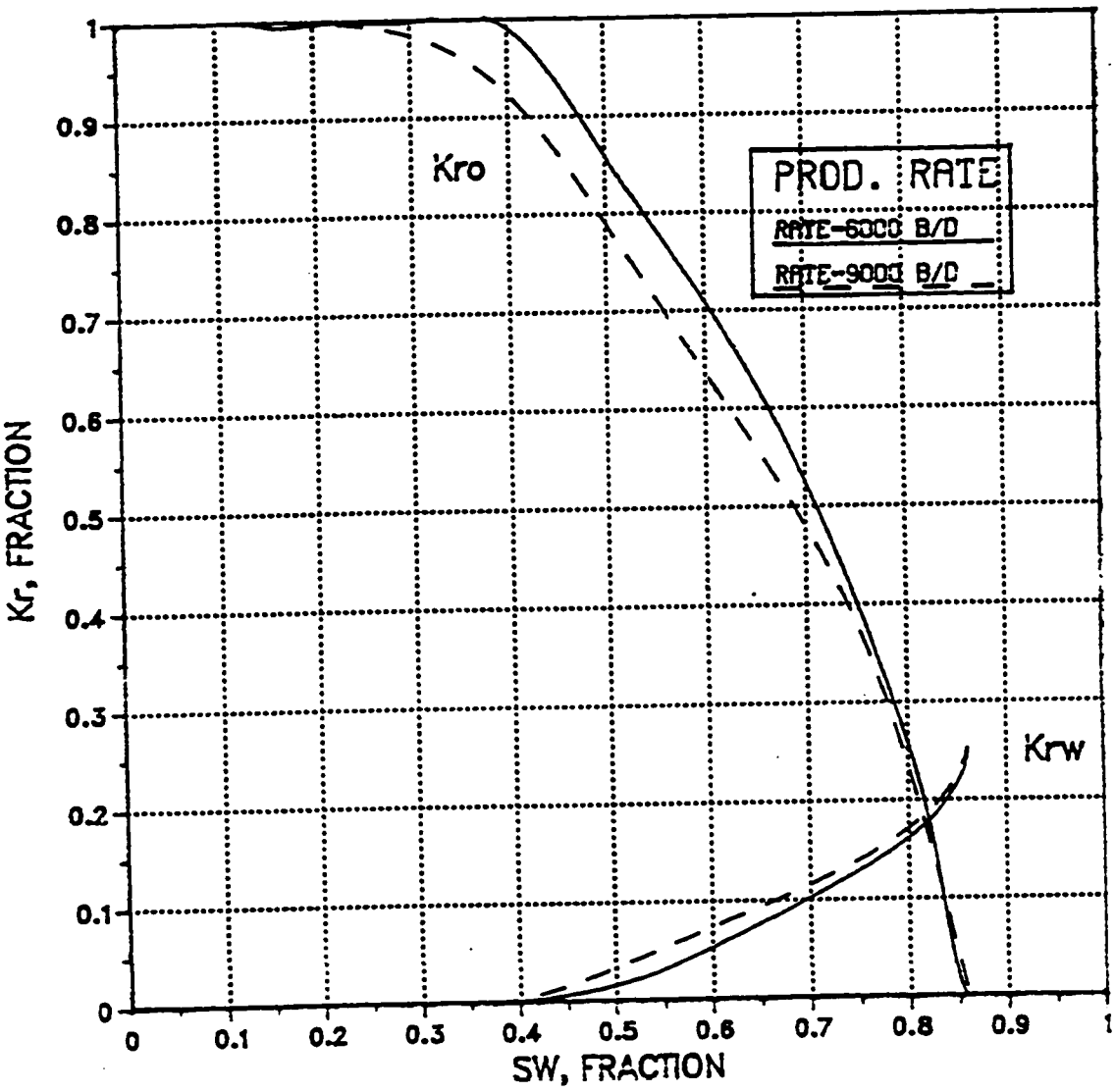

Fig.4.24: Production rate effect for the cross-section - thickness = 50', angle 4, layers = 11-20, Kv/Kx = 0.7, cells = 71-80, PVT No.2.

From the figures, it is clear that the production rates used have no effect on almost all generated pseudo relative permeability curves except for the case having the smallest layer thickness of 50 feet and the highest dip angle of 4°.

4.5 Reservoir Dip Angle

Two reservoir dip angles of 1° and 4° were investigated. The resulting pseudo relative permeability curves are shown in Figs. 4.25 through 4.28 The plot legend shows Angle 1 and Angle 2 which refers to reservoir dip angles of 1° and 4° respectively.

The dip angle has the most significant influence on pseudo relative permeability curves among the factors studied. The higher the angle the more hold-up is noticed because the tilt of the water front is lower and the resulting sweep is better. For waterflooding in a reservoir with significant dip, the magnitude of dip and the direction of water injection relative to the dip angle can have a considerable influence upon oil recovery. The effect of formation dip is dictated by the water and oil gravity difference and the angle direction. If water displaces oil up-dip, the oil displacement will improve and for this reason, all waterfloods are designed with the water injection up-dip to obtain maximum oil recovery. The dip angle effect becomes more pronounced for the small thickness cases and the maximum effect is shown for the case where maximum angle and smallest layer thickness exists.

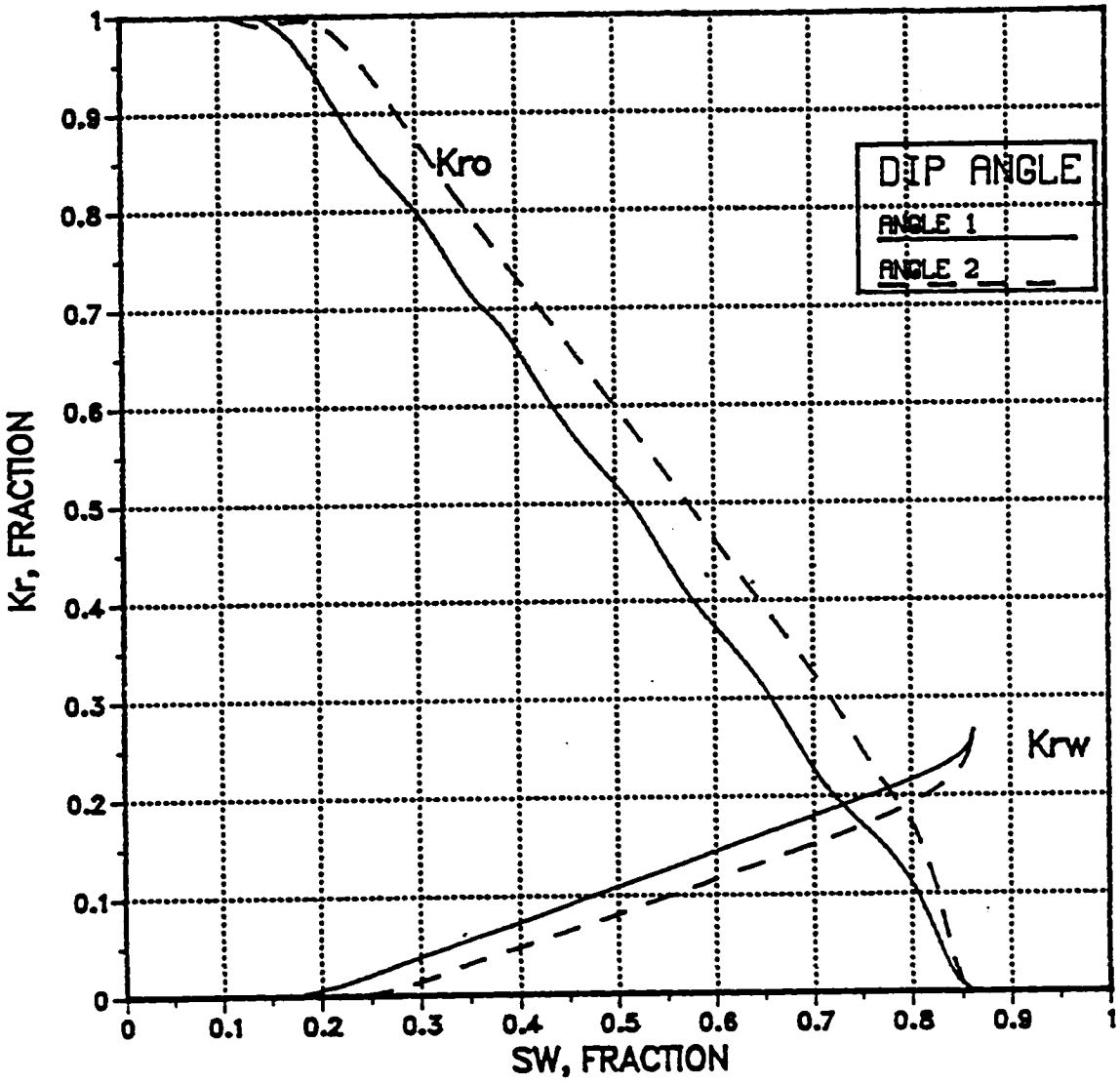

Fig.4.25: Dip angle effect for the cross-section - thickness = 110', layers = 11-20, Kv/Kx = 0.7, cells = 71-80, PVT No.1.

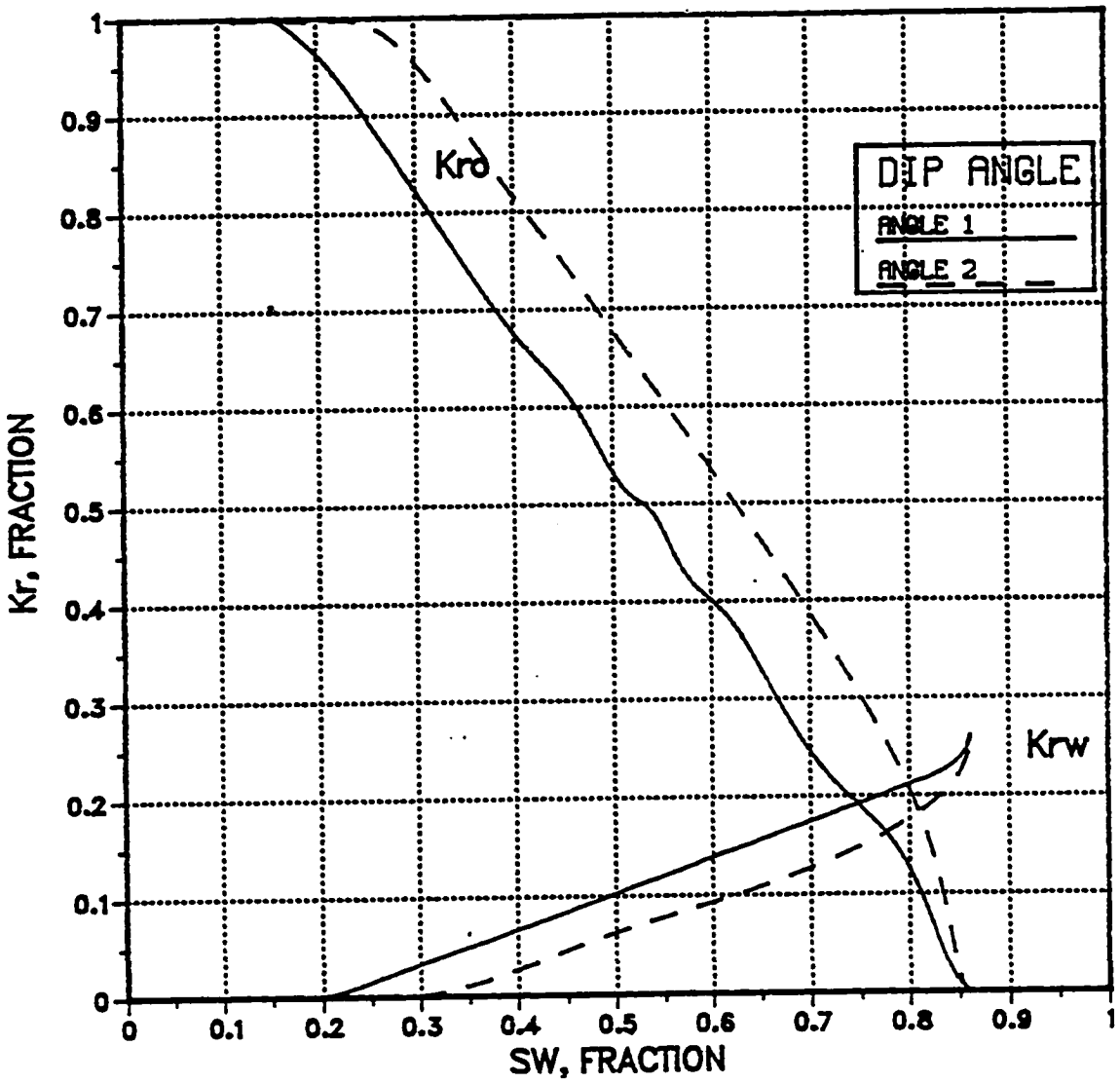

Fig.4.26: Dip angle effect for the cross-section - thickness = 110', layers = 11-20, Kv/Kx = 0.7, cells = 71-80, PVT No.2.

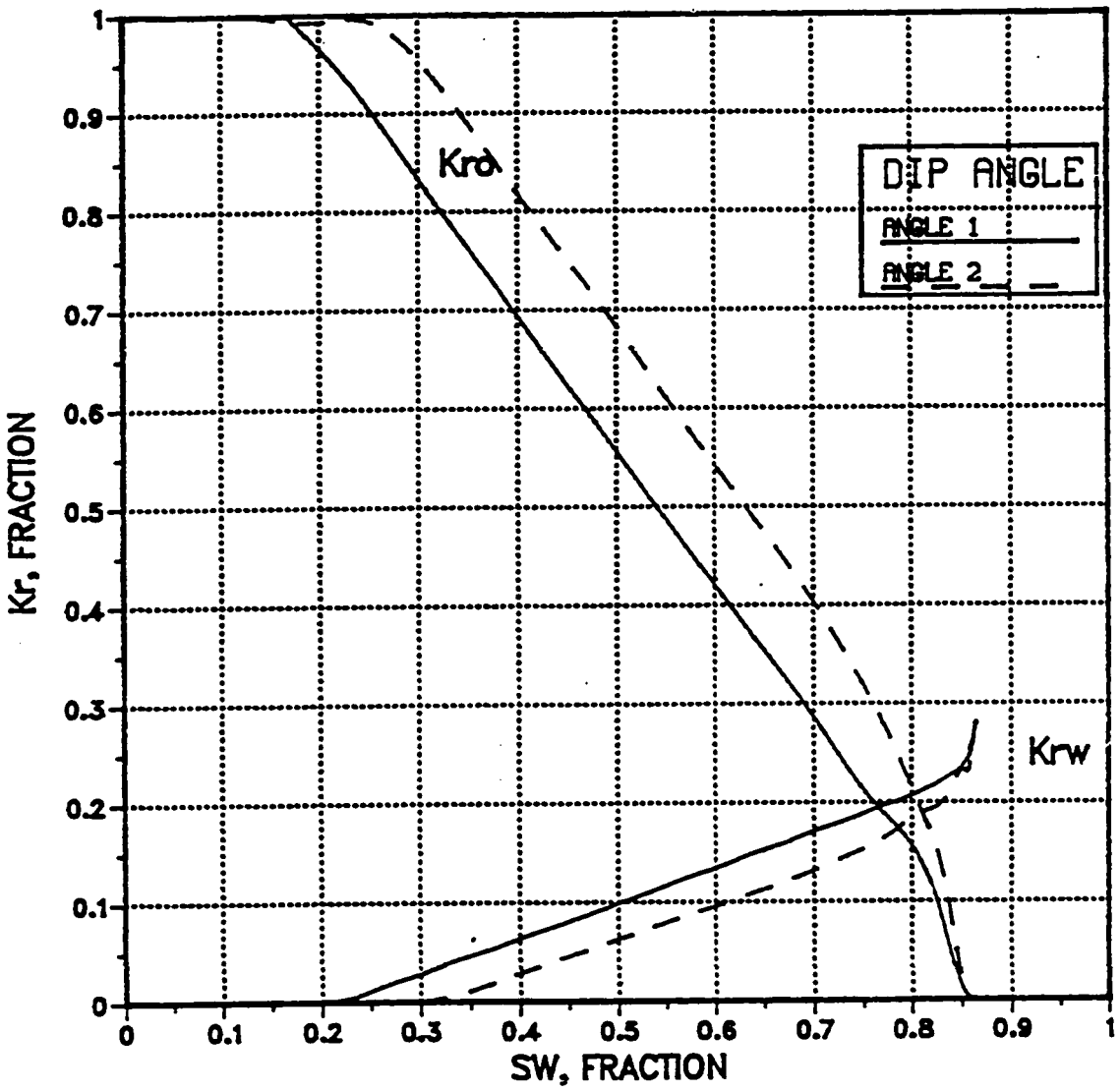

Fig.4.27: Dip angle effect for the cross-section - thickness = 50', layers = 11-20, Kv/Kx = 0.7, cells = 71-80, PVT No.1.

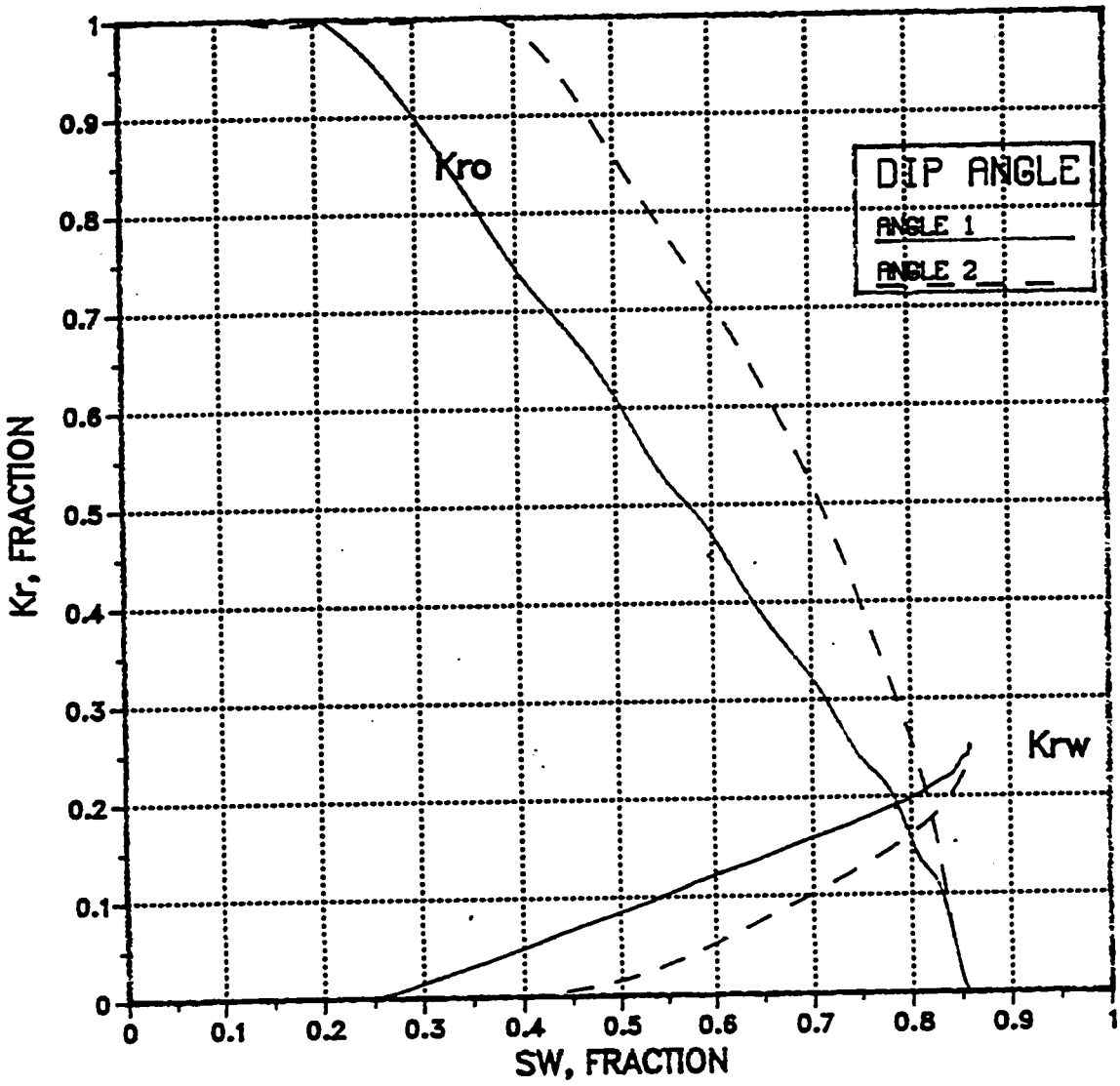

Fig.4.28: Dip angle effect for the cross-section - thickness = 50', layers = 11-20, Kv/Kx = 0.7, cells = 71-80, PVT No.2.

4.6 Absolute Permeability

The absolute permeability used in all basic cross-sectional runs was 5 Darcy. To study the effect of absolute permeability on the pseudo relative permeability curves, the absolute permeability was reduced to 1 Darcy.

Figs. 4.29 through 4.36 show the comparisons of the pseudo relative permeability curves for absolute permeabilities of 1 and 5 Darcies. For the eight comparisons shown, it can be noticed that the effect of absolute permeability is associated with the 4° angle. For the cases where the 1° angle is used, the effect is almost negligible. This observation suggests that for the horizontal reservoirs or reservoirs with low dip angles the absolute permeability is not a factor to be considered in the generation of pseudo relative permeability curves for these reservoirs. The maximum effect again is shown in the case with the lowest layer thickness and the highest dip angle.

The intersection of K_{ro} and K_{rw} exists at a lower water saturation reading for the lower absolute permeability case compared to the higher absolute permeability case.

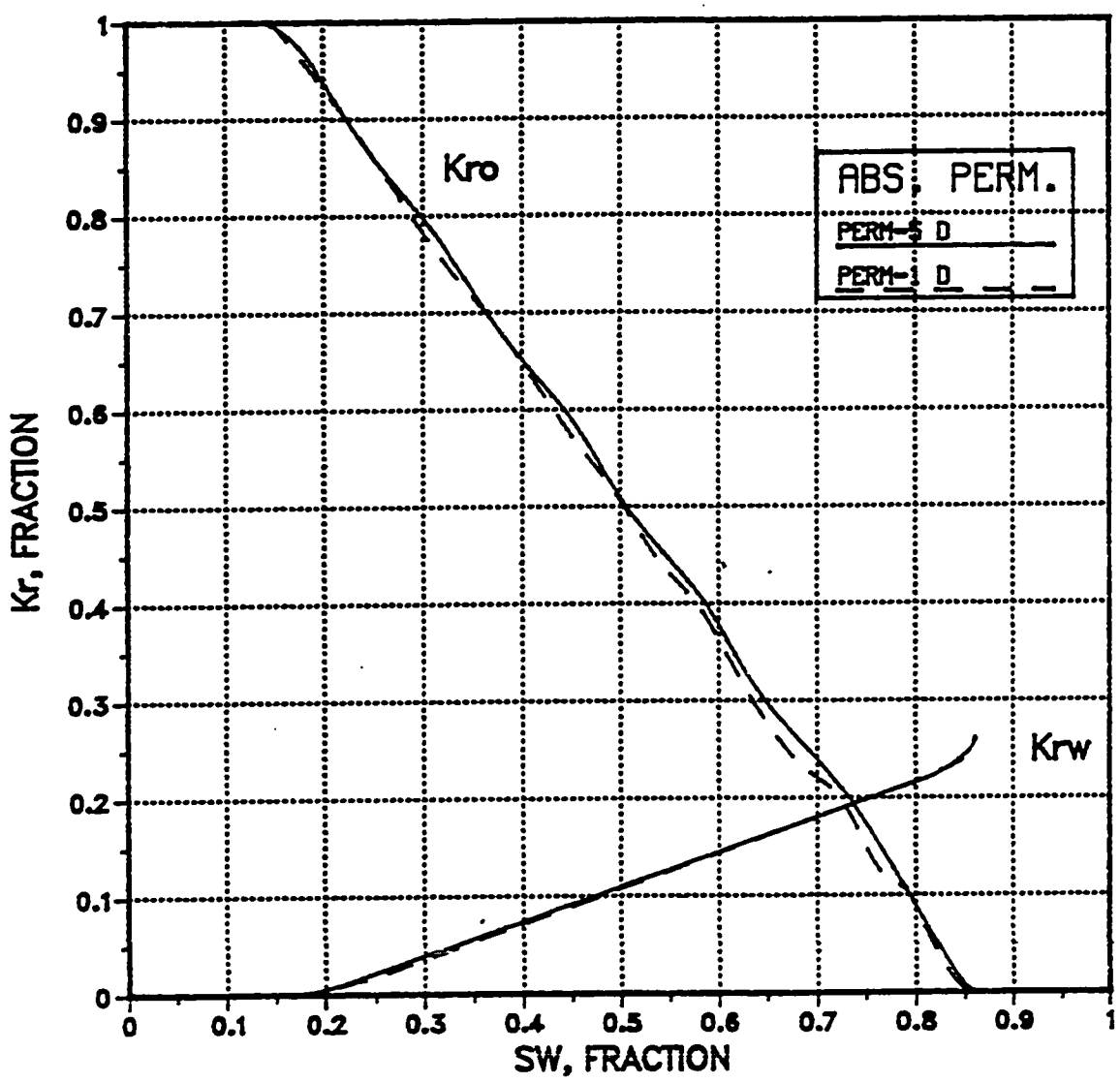

Fig.4.29: Absolute permeability effect for the cross-section - thickness = 110', layers = 11-20, angle = 1, cells = 71-80, PVT No.1.

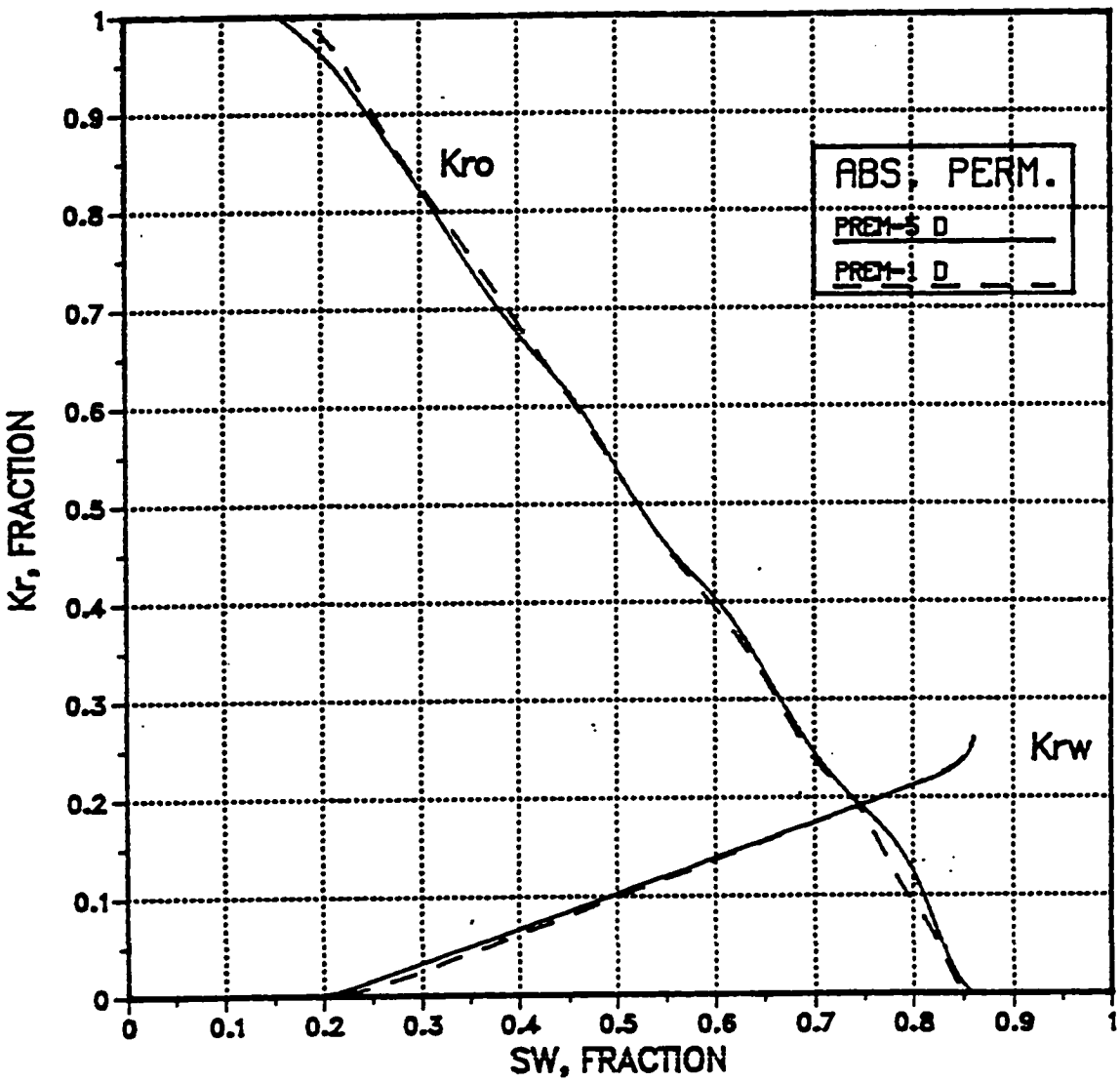

Fig.4.30: Absolute permeability effect for the cross-section - thickness = 110', layers = 11-20, angle = 1, cells = 71-80, PVT No.2.

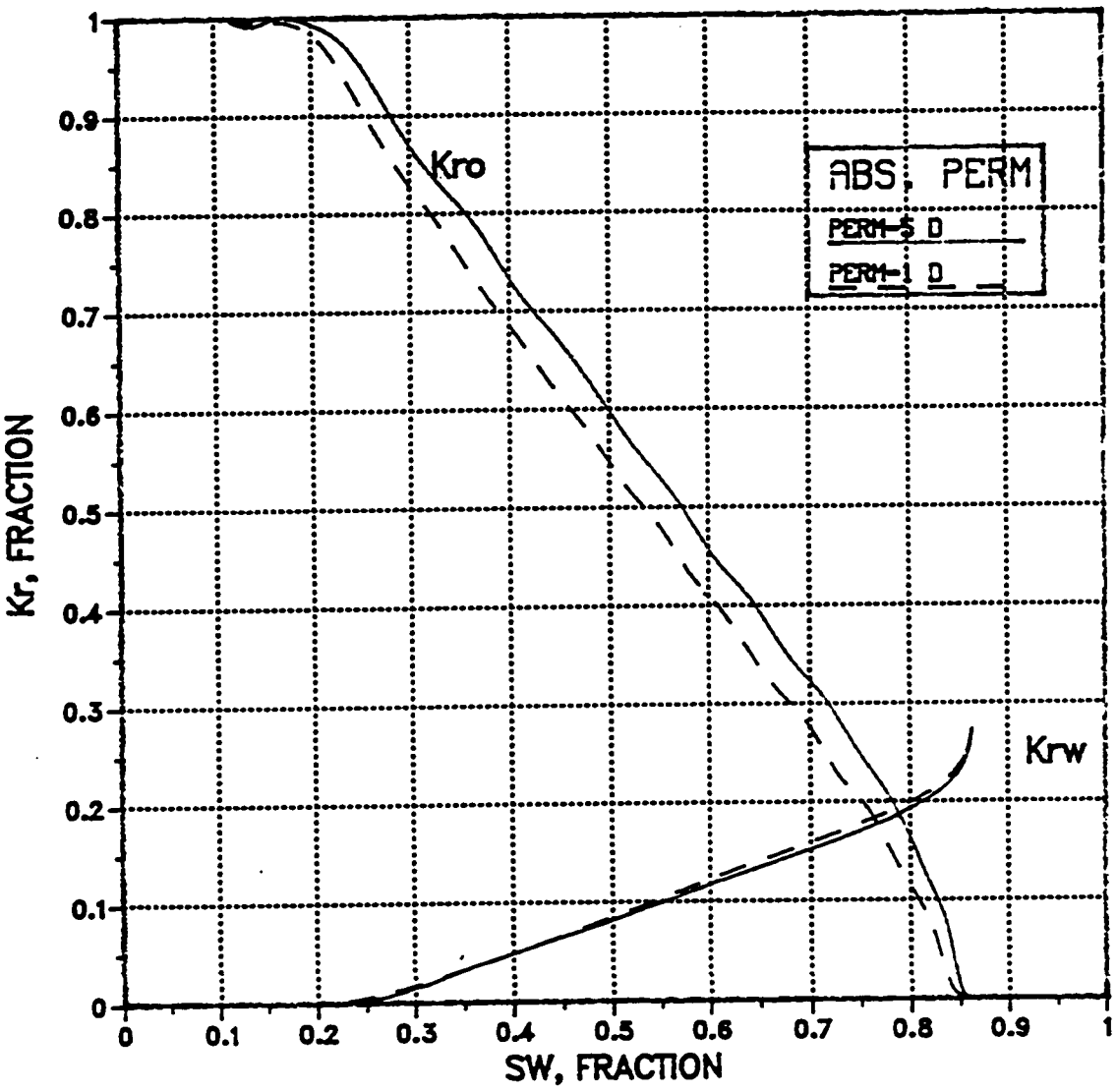

Fig.4.31: Absolute permeability effect for the cross-section - thickness = 110', layers = 11-20, angle = 4, cells = 71-80, PVT No.1.

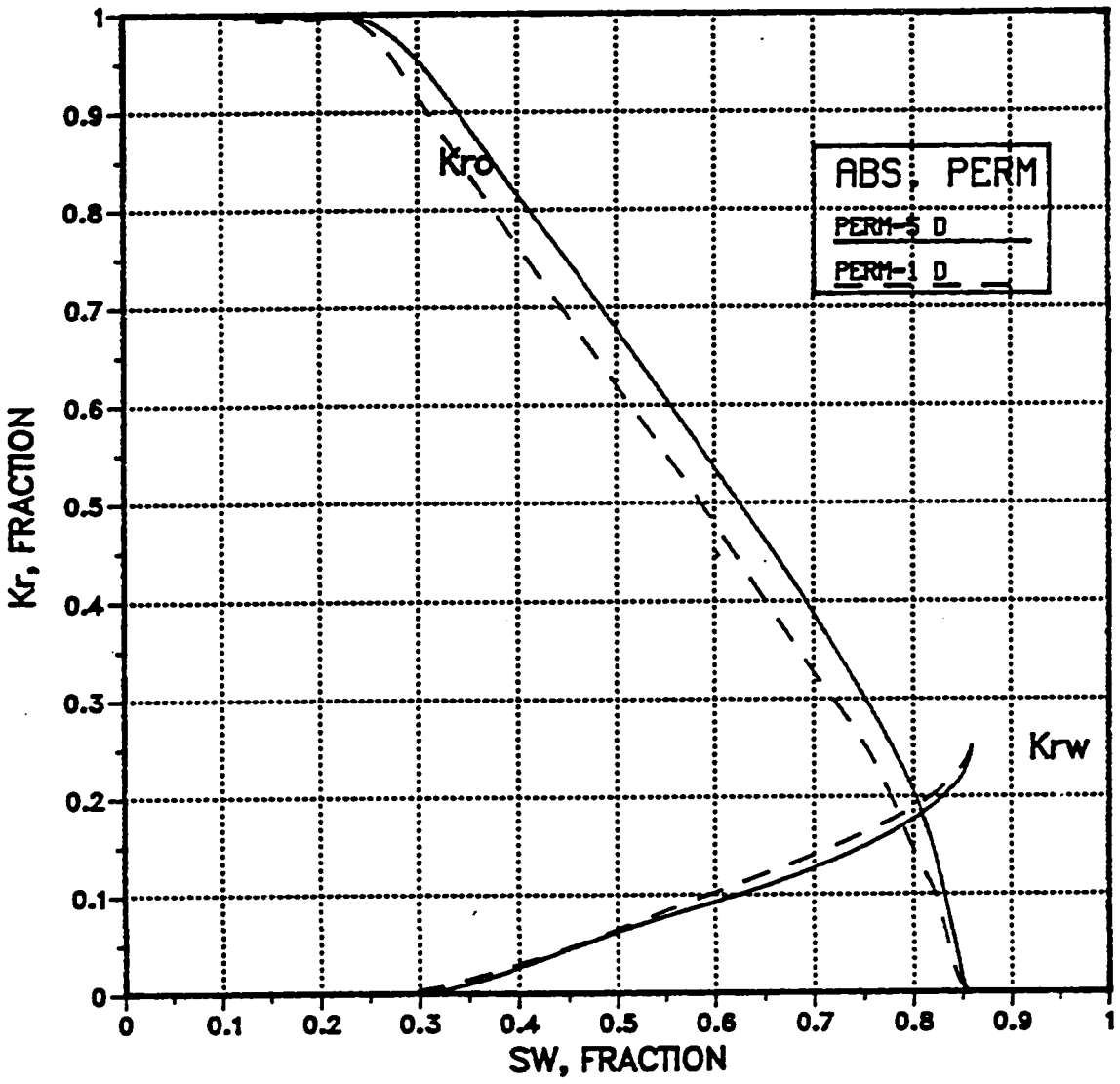

Fig.4.32: Absolute permeability effect for the cross-section - thickness = 110', layers = 11-20, angle = 4, cells = 71-80, PVT No.2.

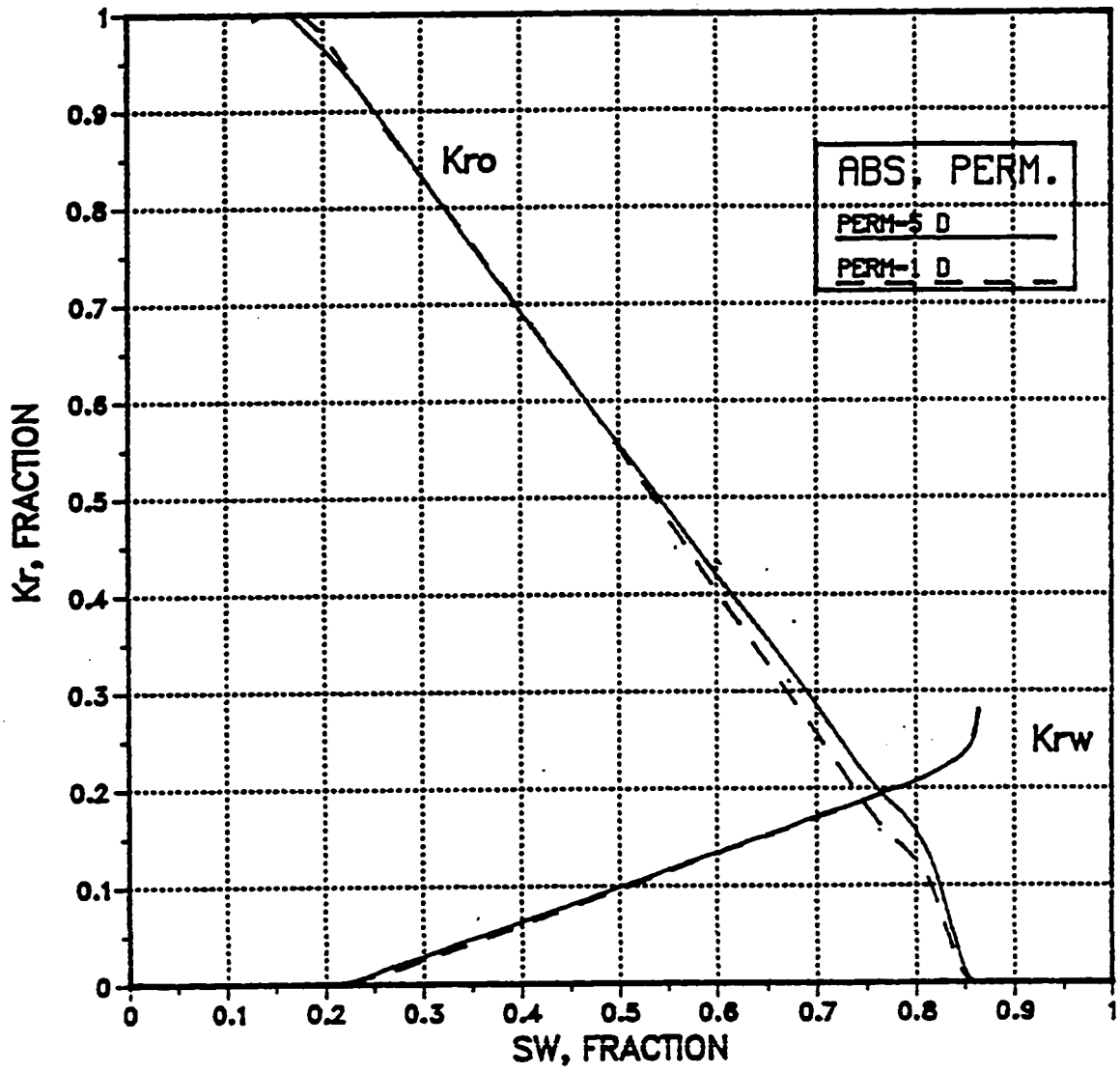

Fig.4.33: Absolute permeability effect for the cross-section - thickness = 50', layers = 11-20, angle = 1, cells = 71-80, PVT No.1.

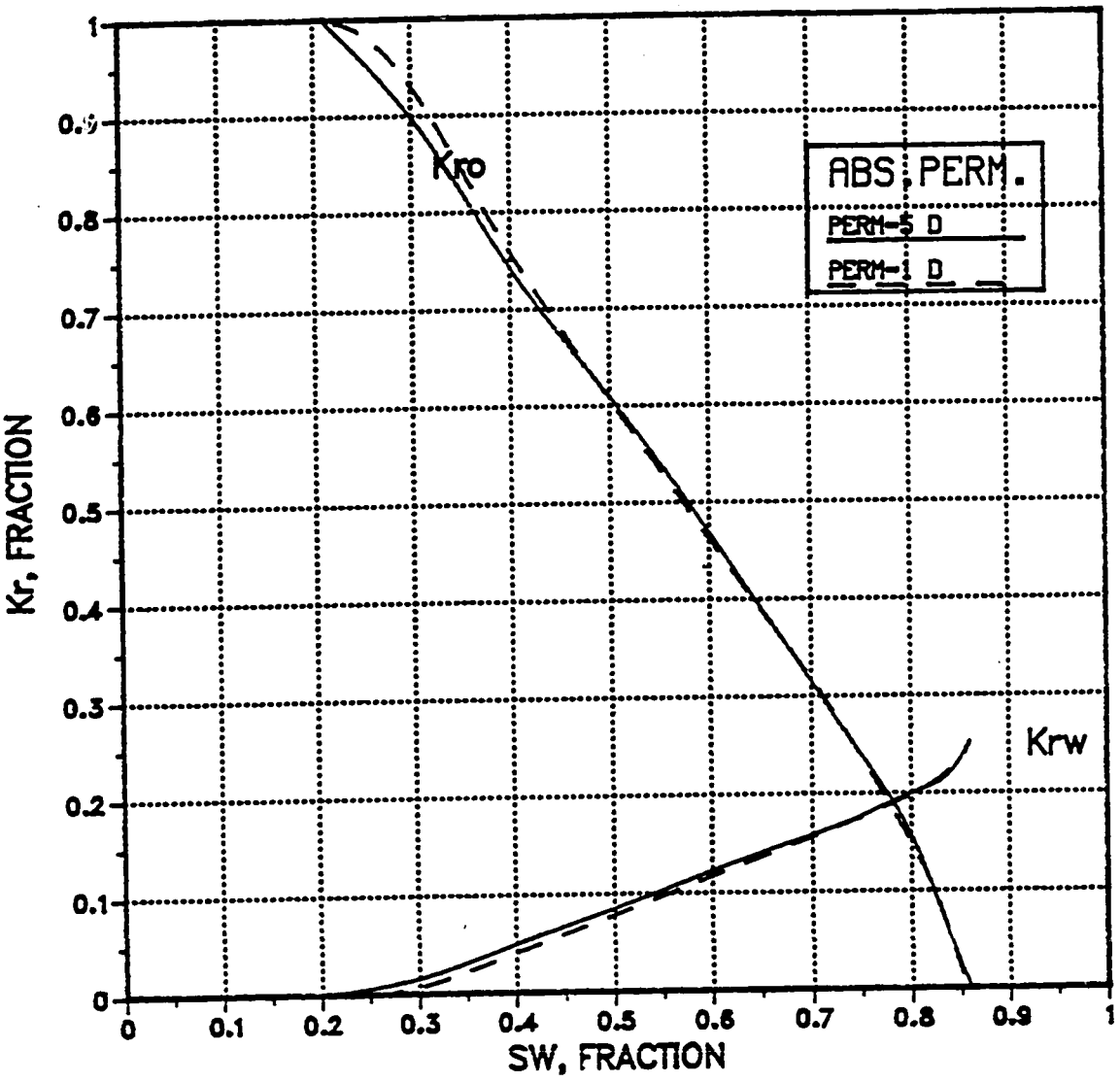

Fig.4.34: Absolute permeability effect for the cross-section - thickness = 50', layers = 11-20, angle = 1, cells = 71-80, PVT No.2.

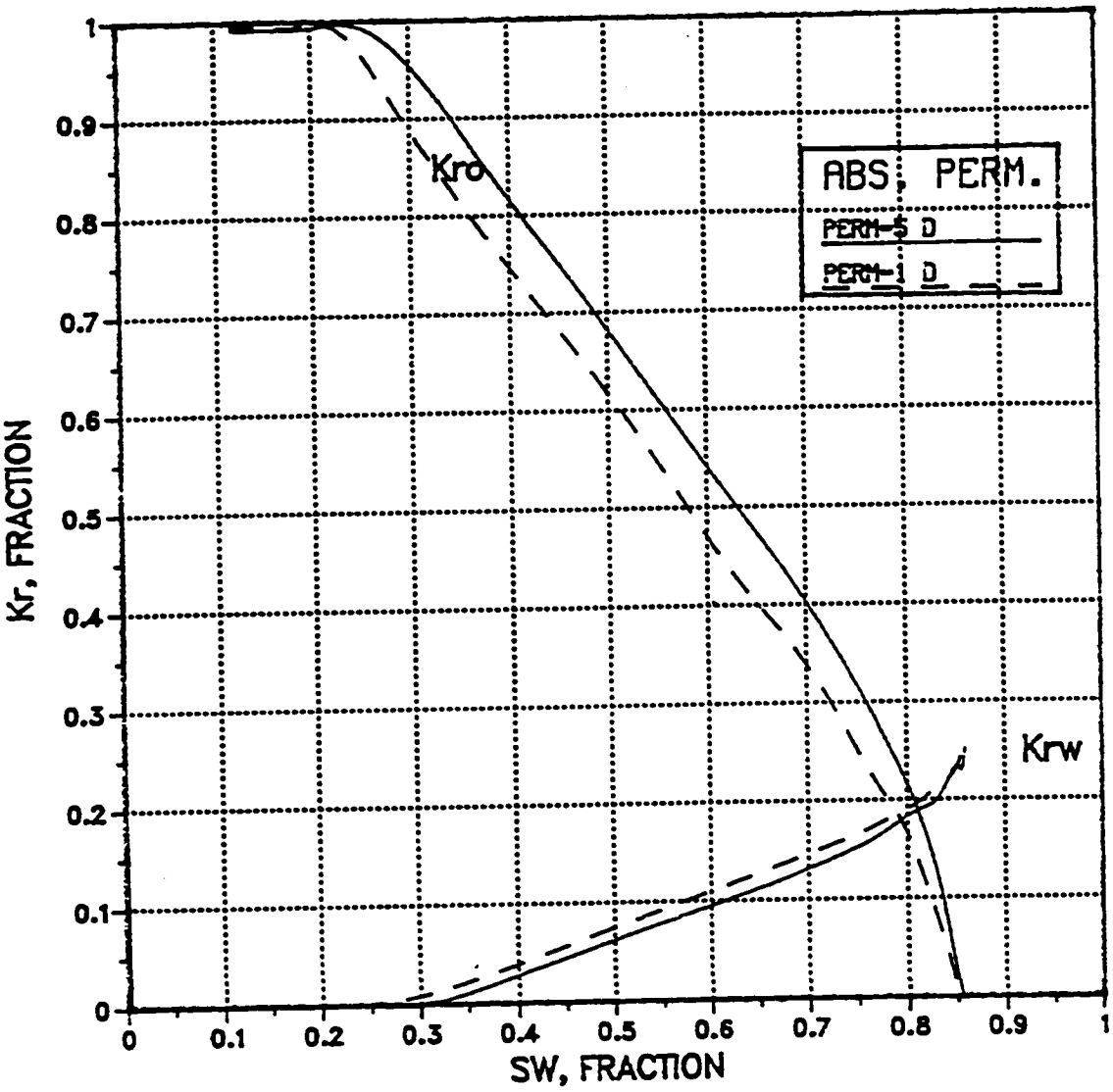

Fig.4.35: Absolute permeability effect for the cross-section - thickness = 50', layers = 11-20, angle = 4, cells = 71-80, PVT No.1.

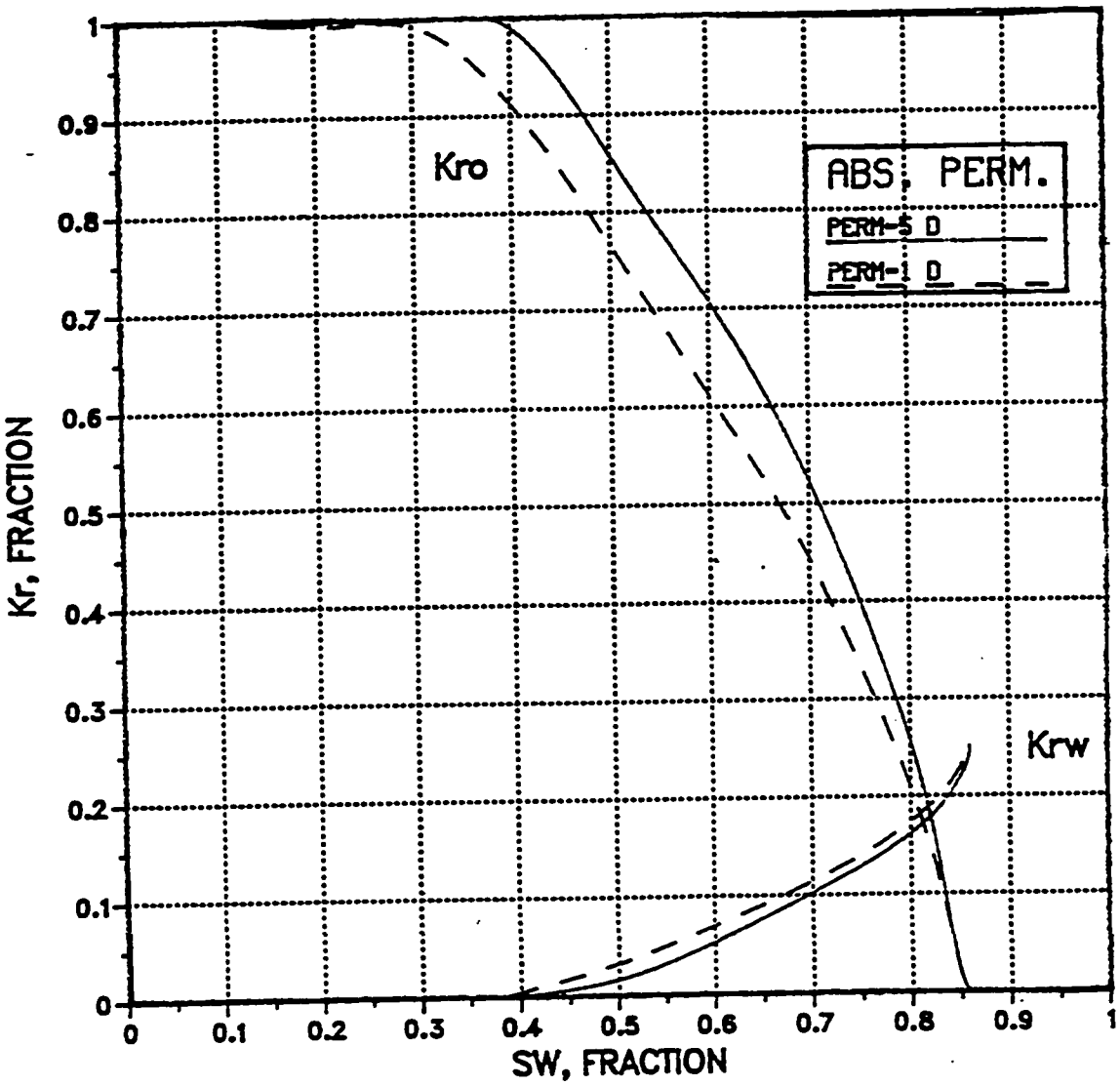

Fig.4.36: Absolute permeability effect for the cross-section - thickness = 50', layers = 11-20, angle = 4, cells = 71-80, PVT No.2.

4.7 Pseudo Relative Permeability Validation

To validate the pseudo relative permeability curves, large size 2-D models of equivalent cross-sections were built. Fig. 4.37 shows a schematic of the 2-D model used for validation. The coarser 2-D model has exactly the same reservoir and fluid properties except the grid sizes are larger than the fine gridded cross-sectional model used to generate the pseudo relative permeability curves. Each coarse grid is equal to five columns of the fine grid and each 10 layers of the fine grid cross-section is lumped to one layer as shown in the figure. Pseudo relative permeability curves generated from the equivalent fine gridded model were used in the coarse 2-D cross-sectional model to see the water saturation front location as a function of time and compare it with the water saturation front of the fine grid cross-sectional model where the rock relative permeability curves are used.

Two cases were chosen randomly for the validation purposes; one for 110 feet layer thickness and the other one for 50 feet layer thickness. Figures 4.38 and 4.39 show the water front location at different times for both the coarse 2-D model and the fine grid model where a close match can be seen. Furthermore, the rock relative permeability curve was used in a coarse 2-D model to show the water saturation front at different model times and is shown in Fig. 4.40.

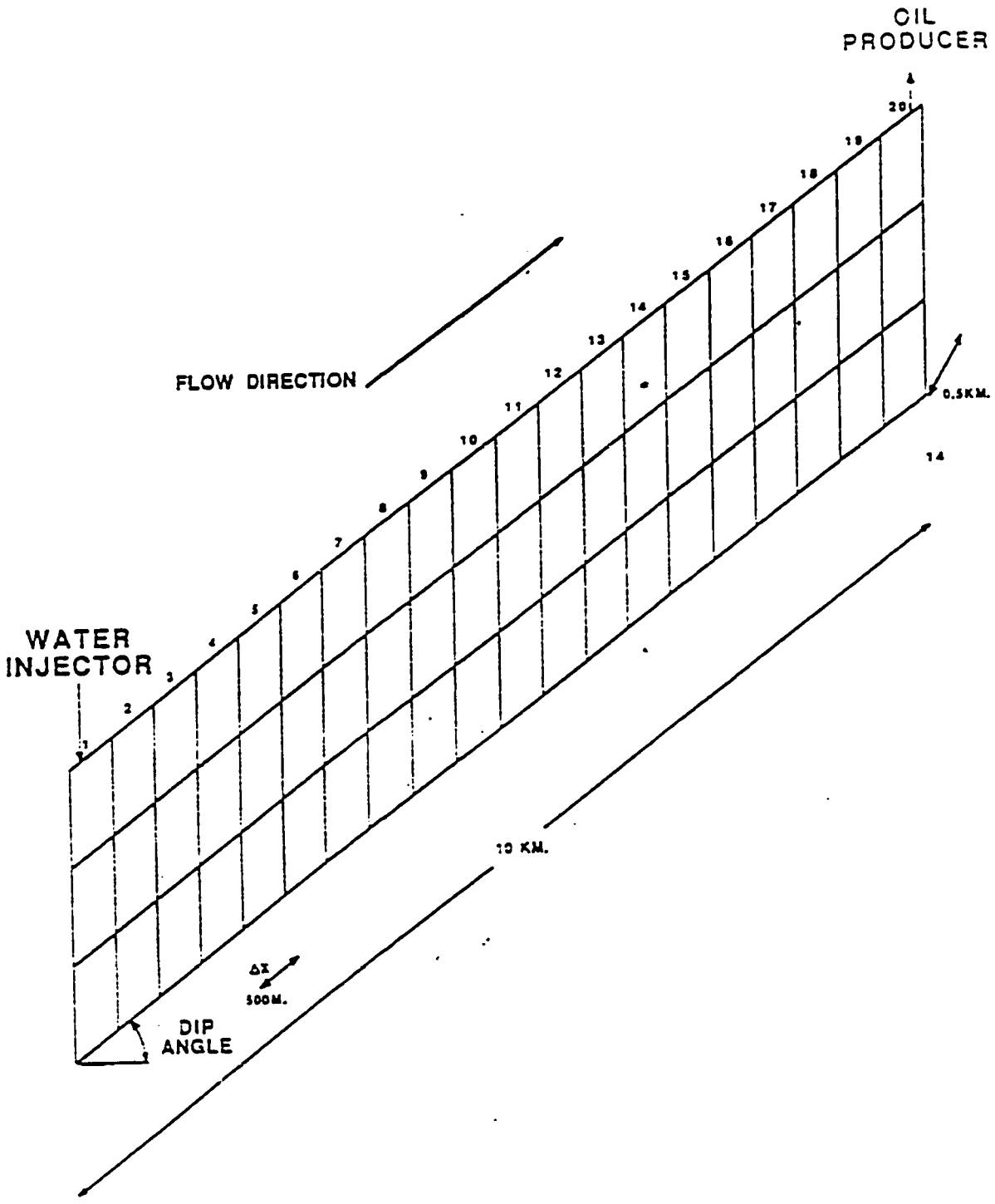

Fig.4.37: A schematic of the coarse cross-section used to validate pseudo relative permeability curves.

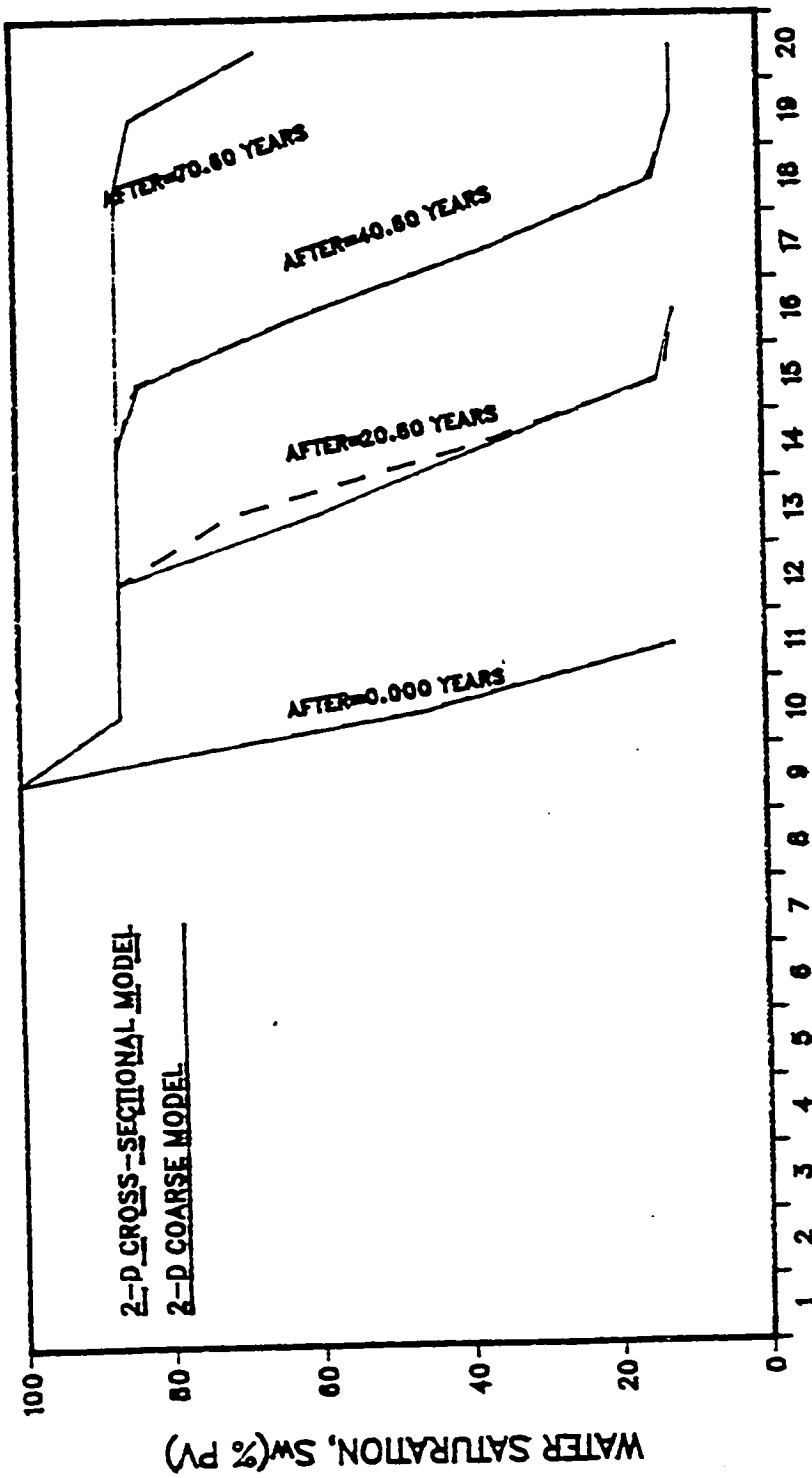

Fig.4.38: Average water saturation distributions calculated using 2-D fine-grid cross-section and 2-D coarse-grid cross-section models.

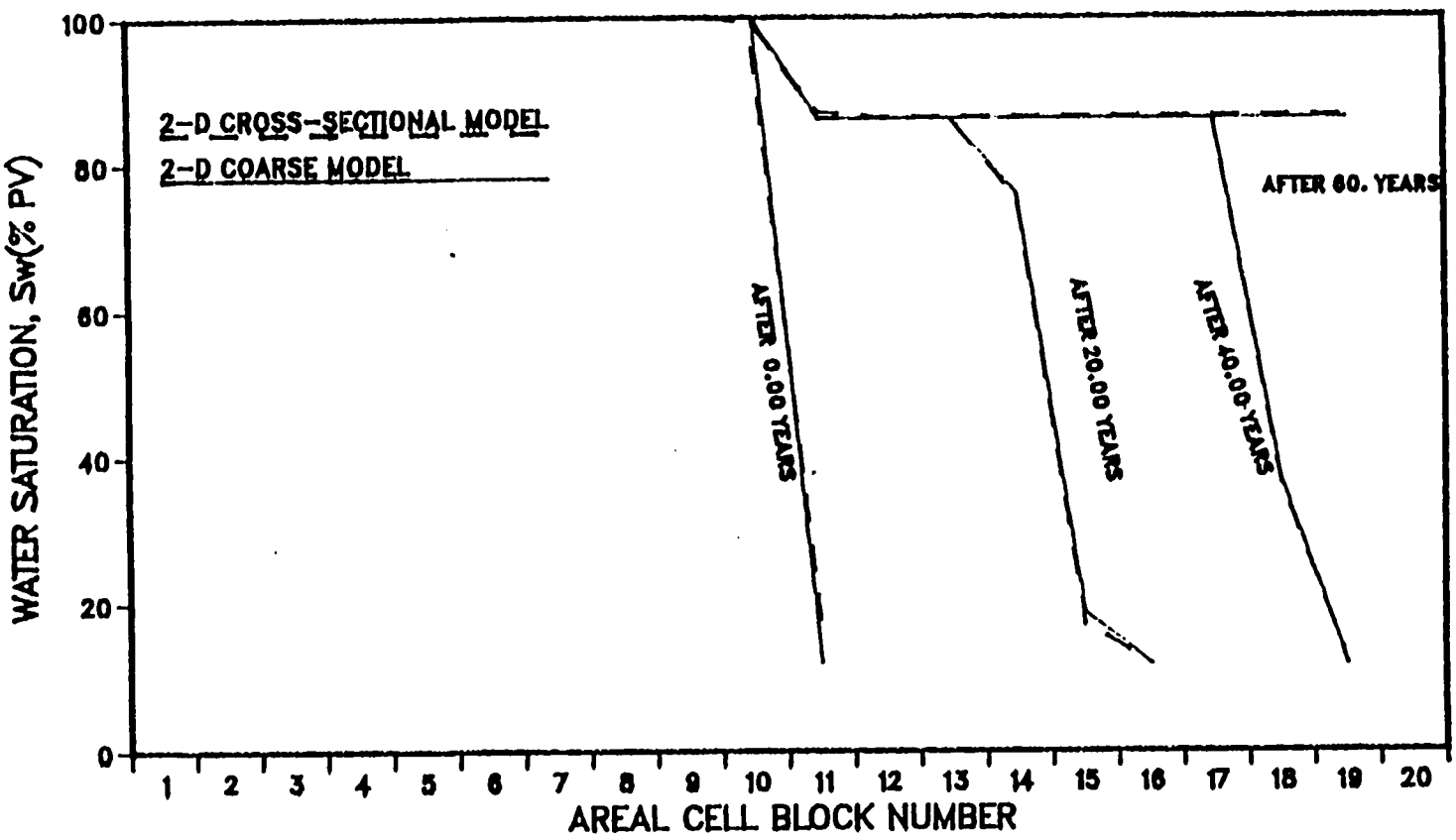

Fig.4.39: Average water saturation distributions calculated using 2-D fine-grid cross-section and 2-D coarse-grid cross-section models.

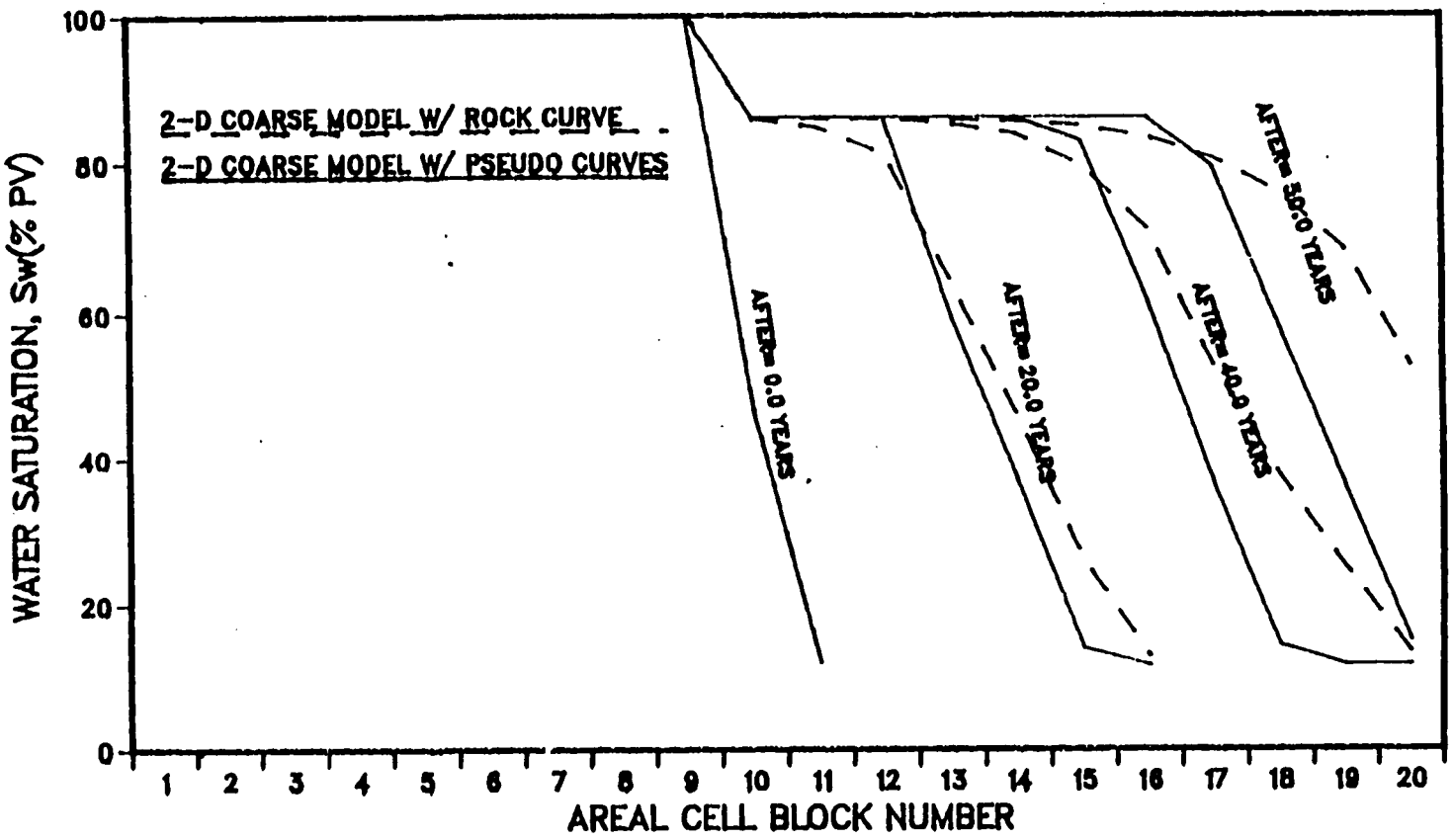

Fig.4.40: Average water saturation distributions calculated using 2-D fine-grid cross-section and 2-D coarse-grid cross-section models. (using rock relative permeability for both).

It can be noticed that using pseudo relative permeability in coarse grid models reproduces the water saturation movement in the model without using fine grid cross-sectional model. In the meantime, for the same case when rock relative permeability curves are used rather than the pseudo relative permeability curves, the water front moved faster which makes the coarse model or full-field model results significantly different.

Chapter 5

CONCLUSIONS AND RECOMMENDATIONS

Chapter 5

CONCLUSIONS AND RECOMMENDATIONS

5.1 Conclusions

Based on the discussion presented in Chapter 4, the following conclusions are drawn with regard to the factors affecting pseudo relative permeability curves. These conclusions apply to a typical sandstone reservoir and are valid for the parameter ranges studied.

1. PVT data has an effect on pseudo relative permeability curves. The effect is minimal when the reservoir dip angle is small and the reservoir thickness is high. The effect becomes more pronounced for the smaller thickness and higher dip angle. The smaller the mobility ratio, the better the sweep and the oil relative permeability value is higher at the same water saturation reading.

2. Vertical to horizontal permeability ratio has no effect on pseudo relative permeability curves regardless of reservoir dip angle or reservoir layer thickness.

3. Model layer thickness has an effect on pseudo relative permeability curves for all cases. The smaller the layer thickness, the better the sweep. For the same water saturation value, the oil relative permeability curve will be higher for the smaller layer thickness, and the relative permeability curves intersection will move towards the high water saturation reading.

4. No effect of the production rate on pseudo relative permeability curves was observed for the range of data used in this study.

5. The most pronounced effect on pseudo relative permeability curves is caused by the reservoir dip angle. The effect becomes more obvious for the low layer thickness and high reservoir dip angle. The higher the dip angle, the better the sweep through the cross-section. This will give a higher oil relative permeability reading for a certain water saturation value. The oil and water relative permeability curves intersection shifts towards the higher water saturation values as the dip angle increases.

6. Absolute permeability has an effect only for the cases where dip angle is high regardless of layer thickness changes, for low dip angles the absolute permeability effect on pseudo relative permeability curves is negligible.

5.2 Recommendations

1. For a sandstone reservoir where PVT data changes with depth a separate set of pseudo relative permeability curves is needed.

2. For reservoir simulation where the layer thickness changes, pseudo relative permeability curves for each layer thickness are needed.

3. Vertical permeability to horizontal permeability ratio and production rates have no effect on pseudo relative permeability curves for the ranges used in this study.

4. For reservoirs where absolute permeability changes, the pseudo relative permeability curves should be generated for the areas where reservoir dip angle changes.

NOMENCLATURE

h = vertical dimension at outflow face of a computing block, ft

K = horizontal permeability at outflow face of a computing block, md

K_r = calculated pseudo relative permeability

P = pressure at midpoint of a computing block, psi

q = horizontal flow rate between adjacent computing blocks, B/D/ft

S = saturation, fraction of pore volume

ΔX = horizontal dimension of a computing block, ft

$\Delta \overline{X}$ = horizontal distance between the midpoint of a computing block and the midpoint of the adjacent downstream block, ft

ΔZ = the distance upward from the cross-section midpoint of the block in the stack, ft

μ = fluid viscosity, cp

ρ = fluid density, lb-cu/ft

φ = porosity, fraction

Subscripts

i = average value for the ith vertical stack in the cross-section

j = average value in the Y-direction

k = average value in the vertical dimension

o = oil

w = water

II,III = cell number in the shown figure

REFERENCES

REFERENCES

1. Honarpour, M.M., Koederitz, L.F., and Harvey, A.H.: "Empirical Equations for Estimating Two-Phase Relative Permeability in Consolidated Rock," JPT, (Dec. 1982) 2905-08.
2. Trujillo, E.M.: "Simple Method for Calculating Pseudo Relative Permeability from Laboratory Water Floods," SPE 1127, 1982.
3. Osoba, J.S. et al.: "Laboratory Meausurements of Relative Permeability," Trans., AIME, (1951), 192, 47-56.
4. Jones, S.C. and Rozelle, W.O.: "Graphical Techniques For Determining Relative Permeability From Displacement Experiments," J. Pet. Tech. (May 1978) 807-817.
5. Fulcher, R.A. Jr., Ertekin, T. and Stahl, C.O.: "The Effect of the Capillary Number and Its Constituents on Two-Phase Relative Permeability Curves," JPT (Feb. 1985) 249-260.
6. Amyx, J.W. Bass, D.M. Jr. and Whiting, K.L.: Petroleum Reservoir Engineering, McGraw Hill Book Co. New York (1960).
7. Craft, B.C. and Hawkins, M.F.: Applied Petroleum Reservoir Engineering, Prentice Hall Inc., Englewood Ciffs, New Jersey (1973).
8. Nelson N. Molina: "Systematic Approach to the Relative Permeability Problem in Reservoir Simulation," SPE 9234 presented at 55th Annual Fall Technical Conference, Dallas, TX, (Sept. 1980).
9. Hales, H.B.: "Parameterization of Match-Derived Pseudo Relative

Permeabilities," SPE 6200 presented at Middle East Oil Technical Conference, Manama, Bahrain, (March 1983).

10. Coats, K.H., Nielsen, R.L., Terhune, M.H. and Weber, A.G.: "Simulation of Three-Dimensional, Two-Phase Flow in Oil and Gas Reservoirs," SPEJ (Dec. 1967), 377-88.
11. Hearn, C.L.: "Simulation of Stratified Waterflood by Pseudo Relative Permeability Curves," JPT (Jul. 1971) 805-13.
12. Martin, J.C.: "Partial Integration of Equations of Multiphase Flow," SPEJ (Dec. 1968) 370-81.
13. Coats, K.H., Dempsey, J.R. and Henderson, J.H.: "The Use of Vertical Equilibrium in Two-Dimensional Simulation of Three-Dimensional Reservoir Performance, SPEJ (March 1971) 63-71.
14. Jacks, H.H., Smith, O.J. and Mattax, C.C.: "The Modeling of Three-Dimensional Reservoir with a Two-Dimensional Reservoir Simulator - The Use of Dynamic Pseudo Functions," SPEJ (June 1973) 173-185.
15. Kyte J.R. and Berry, D.W.: "New Pseudo Functions to Control Numerical Dispersion," SPEJ (Aug. 1975) 269-75.
16. Killough, J.E. and Foster Jr., H.P.: "Reservoir Simulation of the Empire Abo Field : The Use of Pseudos in Multilayered System," SPEJ (Oct. 1979) 279-88.
17. Andrew, D.S. and Koederitz, L.F.: "An Improved Method for the Determination of Pseudo-Relative Permeability Data for Stratified Systems," SPE 10975, presented at 57th Annual Fall Technical Conference, New Orleans, L.A. (Sept. 1982).

18. Starley, G.P.: "A Material-Balance Method for Deriving Interblock. Water/Oil Pseudofunctions for Coarse-Grid Reservoir Simulations," SPE 15821, presented at SPE Annual Technical Conference, New Orleans, (Oct. 1986).

19. Thomas, G.W.: "An Extension of Pseudofunction Concept," SPE (12274), Reservoir Simulation Symposium, San Fransisco, CA, (Nov. 1983).

20. Davis, B.J. and Haldorsen, H.H.: "Pseudofunctions in Formations Containing Discontinuous Shales: A Numerical Study," SPE (16012), presented at 9th Symposium on Reservoir Simulation, San Antinio, TX, (Feb. 1987).

21. Poolen, H.K., Breitenback, E.A., and Thurnan, D.H.: "Treatment of Individual Wells and Grids in Reservoir Modeling," paper SPE 2022 presented at SPE Symposium on Numerical Simulation of Reservoir Performance held in Dallas, TX, (April 1968).

22. Hillestad, J.G.: "Techniques for Simulating Complex Reservoirs," paper SPE 14109 presented at SPE International Meeting on Petroleum Engineering held in Beijing, (March 1986).

23. Emanuel, A.S., and Cook, G.W.: "Pseudo-Relative Permeability for Well Modeling," Soc. Pet. Engs., J., (Feb. 1974), 7-9.

24. Woods, E.G., and Khurana, A.K.: "Pseudo functions for Water Coning in 3-D Reservoir Simulation," SPEJ (August 1977), 251-262.

25. Al-Yousef, H.Y.: "An Improved Method to Calculate Pseudo Relative Permeability to Model Gravity and Capillary Effects in

Reservoir Simulation," Ph.D. Dissertation, Stanford University, (June 1985).

26. Stone, H.L.: "Rigorous Black Oil Pseudo Functions," paper SPE 21207 presented at the 11th SPE Symposium on Reservoir Simulation held in Anaheim, Ca., (February 1991).

APPENDIX

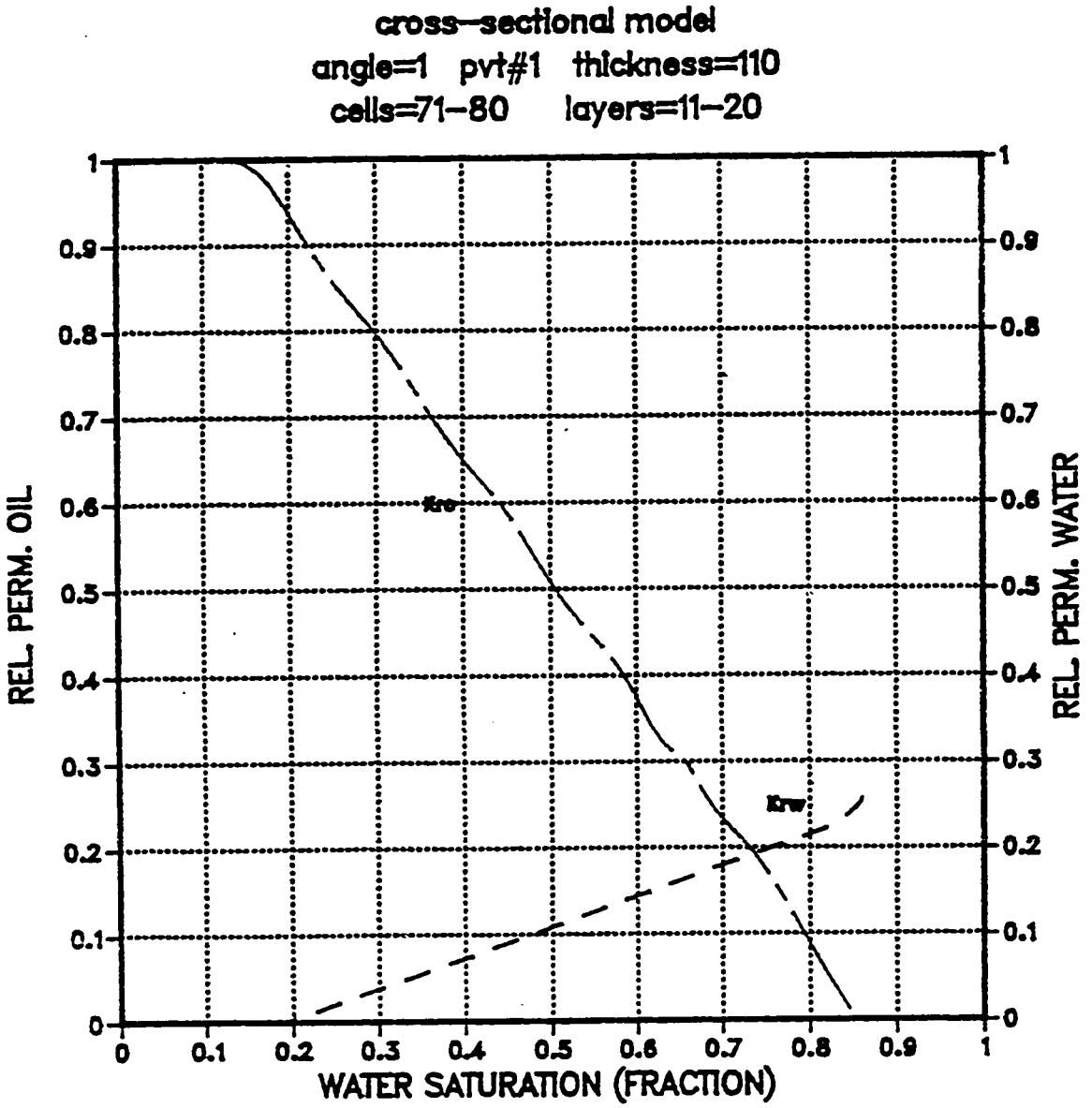
cross-sectional model
angle=1 pvt#1 thickness=110
cells=71-80 layers=11-20
REL. PERM. OIL
REL. PERM. WATER
WATER SATURATION (FRACTION)
kro
krw
0
0.1
0.2
0.3
0.4
0.5
0.6
0.7
0.8
0.9
1

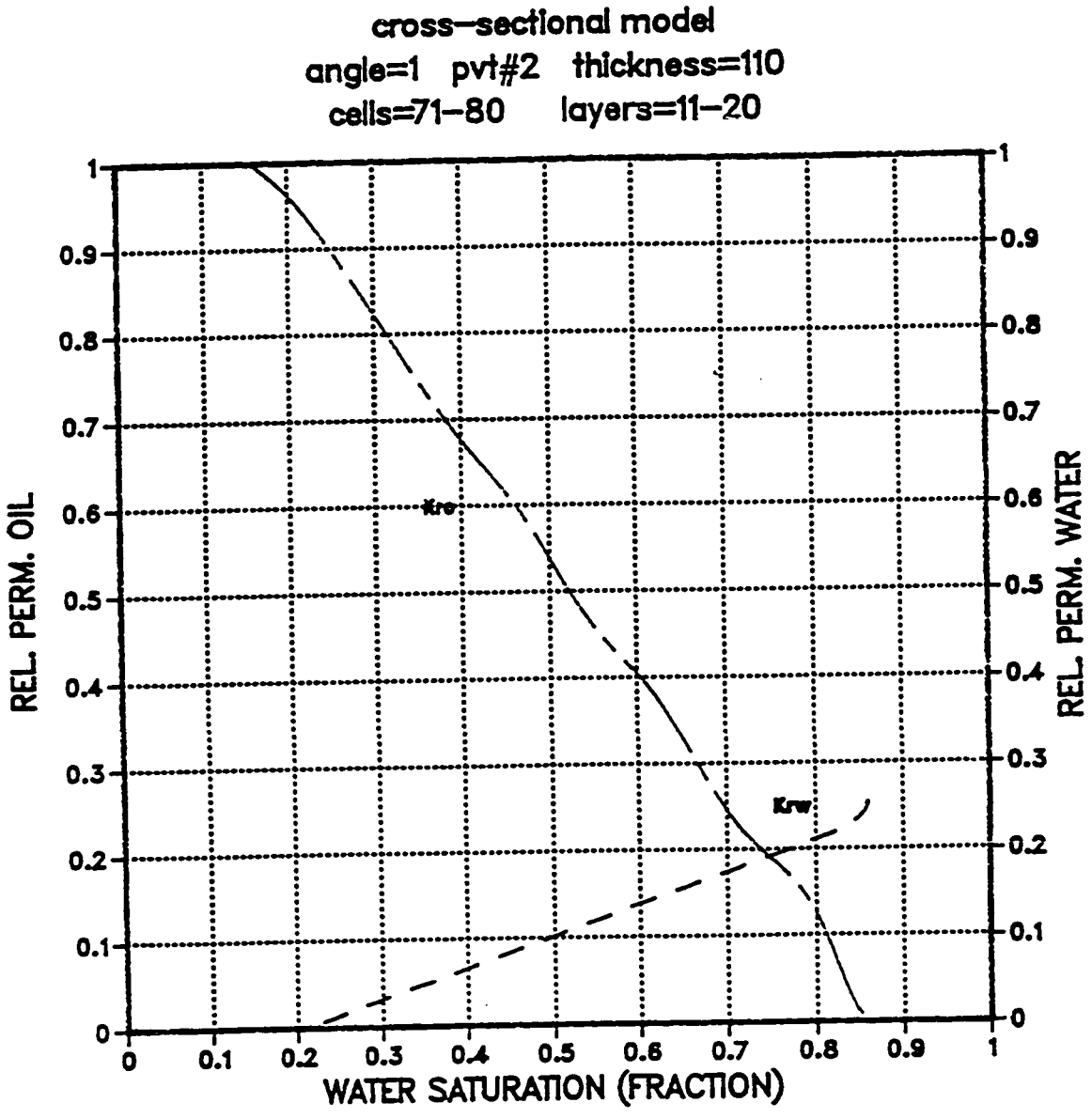
cross-sectional model
angle=1 pvt#2 thickness=110
cells=71-80 layers=11-20
REL. PERM. OIL
REL. PERM. WATER
WATER SATURATION (FRACTION)
Kro
Krw
0
0.1
0.2
0.3
0.4
0.5
0.6
0.7
0.8
0.9
1

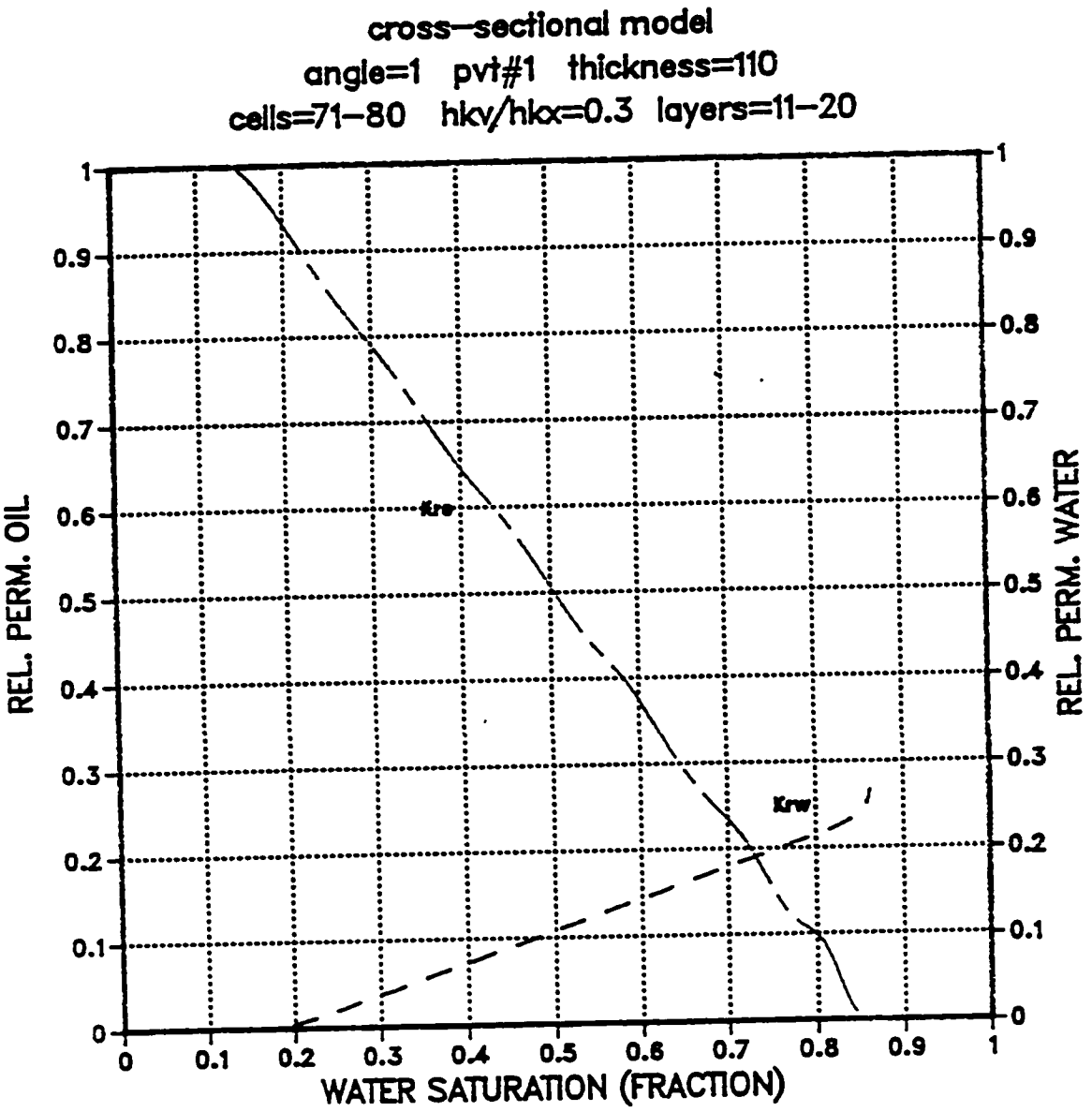
cross-sectional model
angle=1 pvt#1 thickness=110
cells=71-80 hkv/hkx=0.3 layers=11-20
REL. PERM. OIL
REL. PERM. WATER
WATER SATURATION (FRACTION)
Kro
Krw
0
0.1
0.2
0.3
0.4
0.5
0.6
0.7
0.8
0.9
1

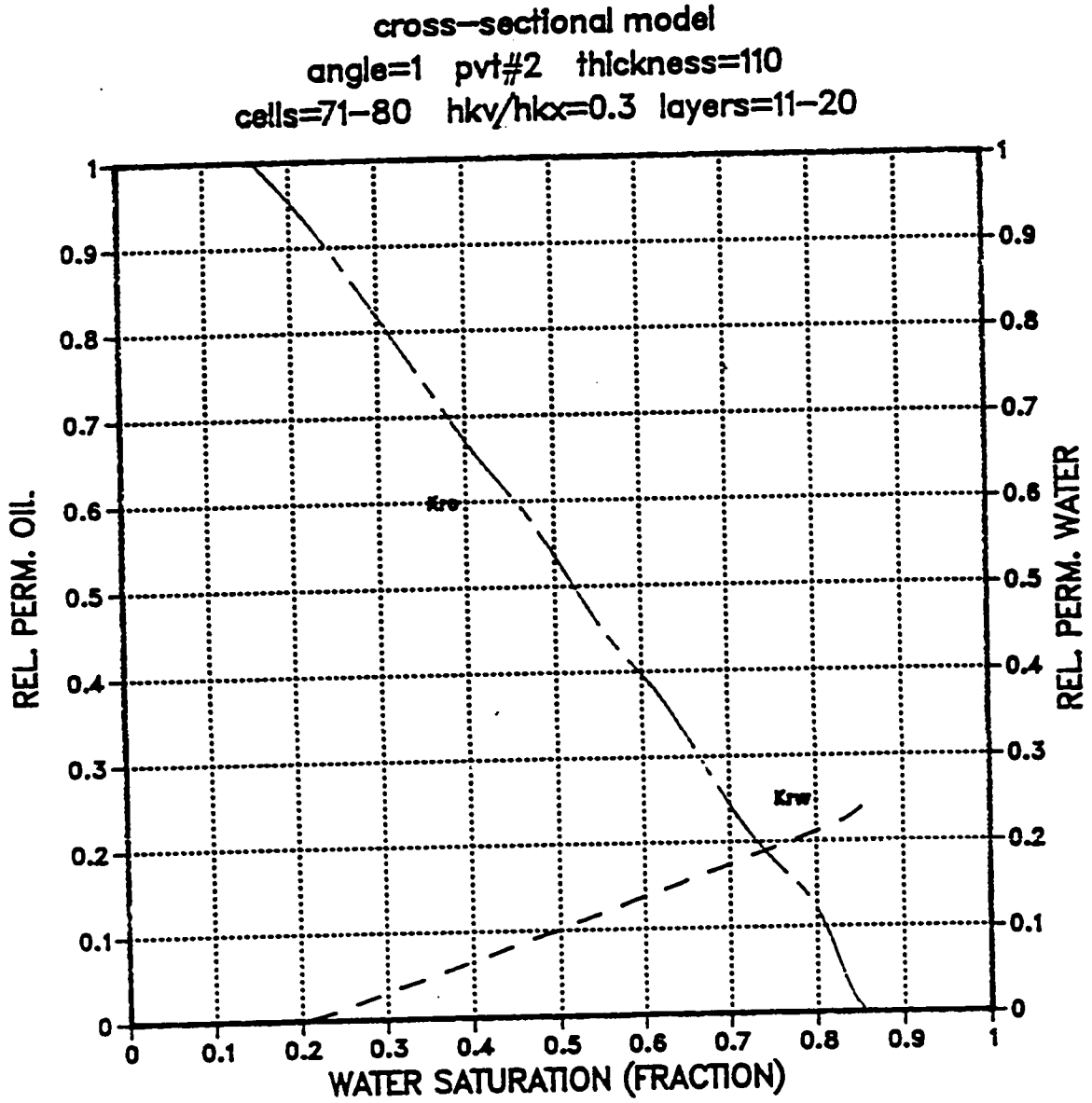
cross-sectional model
angle=1 pvt#2 thickness=110
cells=71-80 hkv/hkx=0.3 layers=11-20
REL. PERM. OIL.
REL. PERM. WATER
WATER SATURATION (FRACTION)
Kro
Krw
0
0.1
0.2
0.3
0.4
0.5
0.6
0.7
0.8
0.9
1

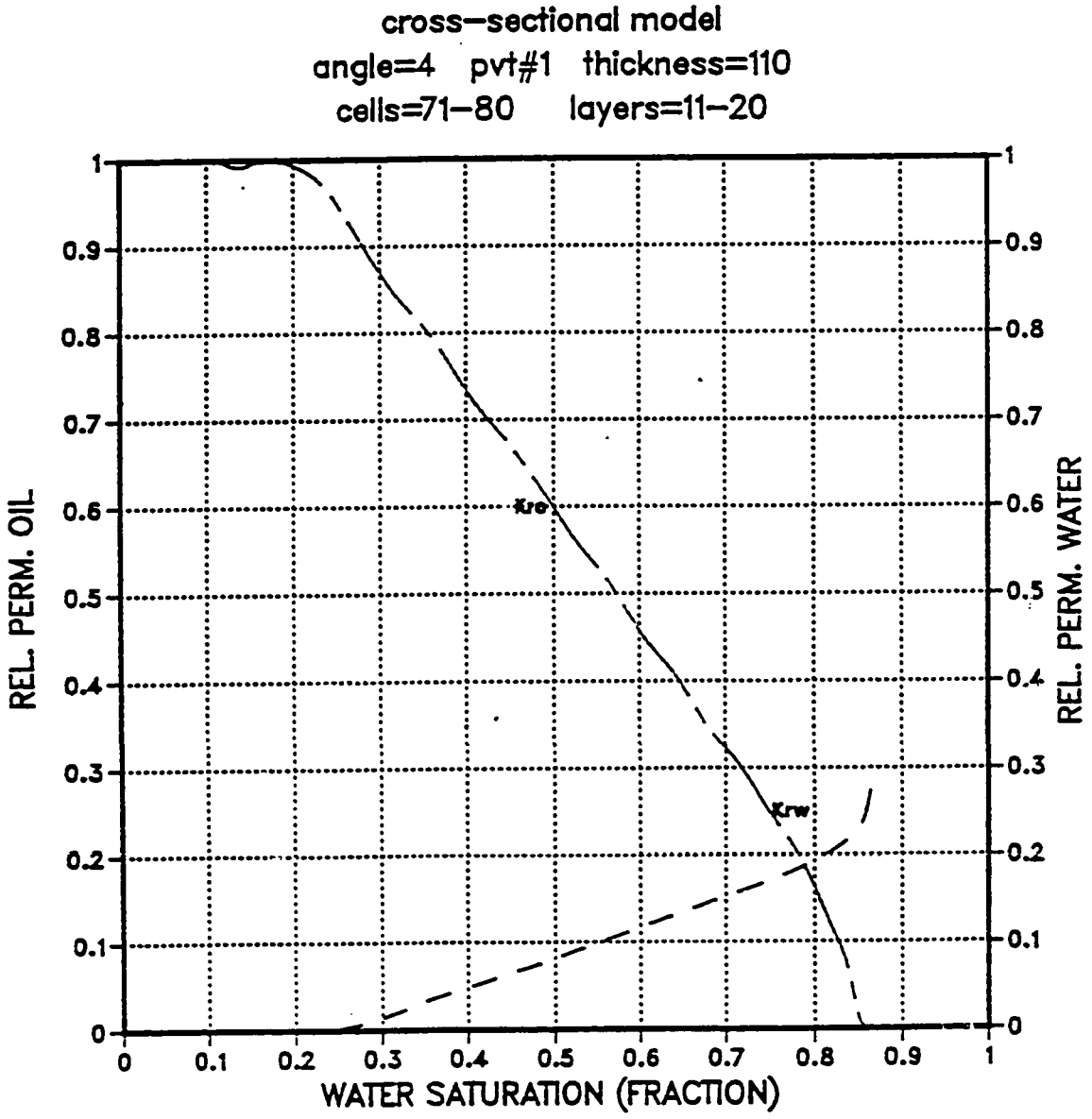
cross-sectional model
angle=4 pvt#1 thickness=110
cells=71-80 layers=11-20
REL. PERM. OIL
REL. PERM. WATER
WATER SATURATION (FRACTION)
Kro
Krw
0
0.1
0.2
0.3
0.4
0.5
0.6
0.7
0.8
0.9
1

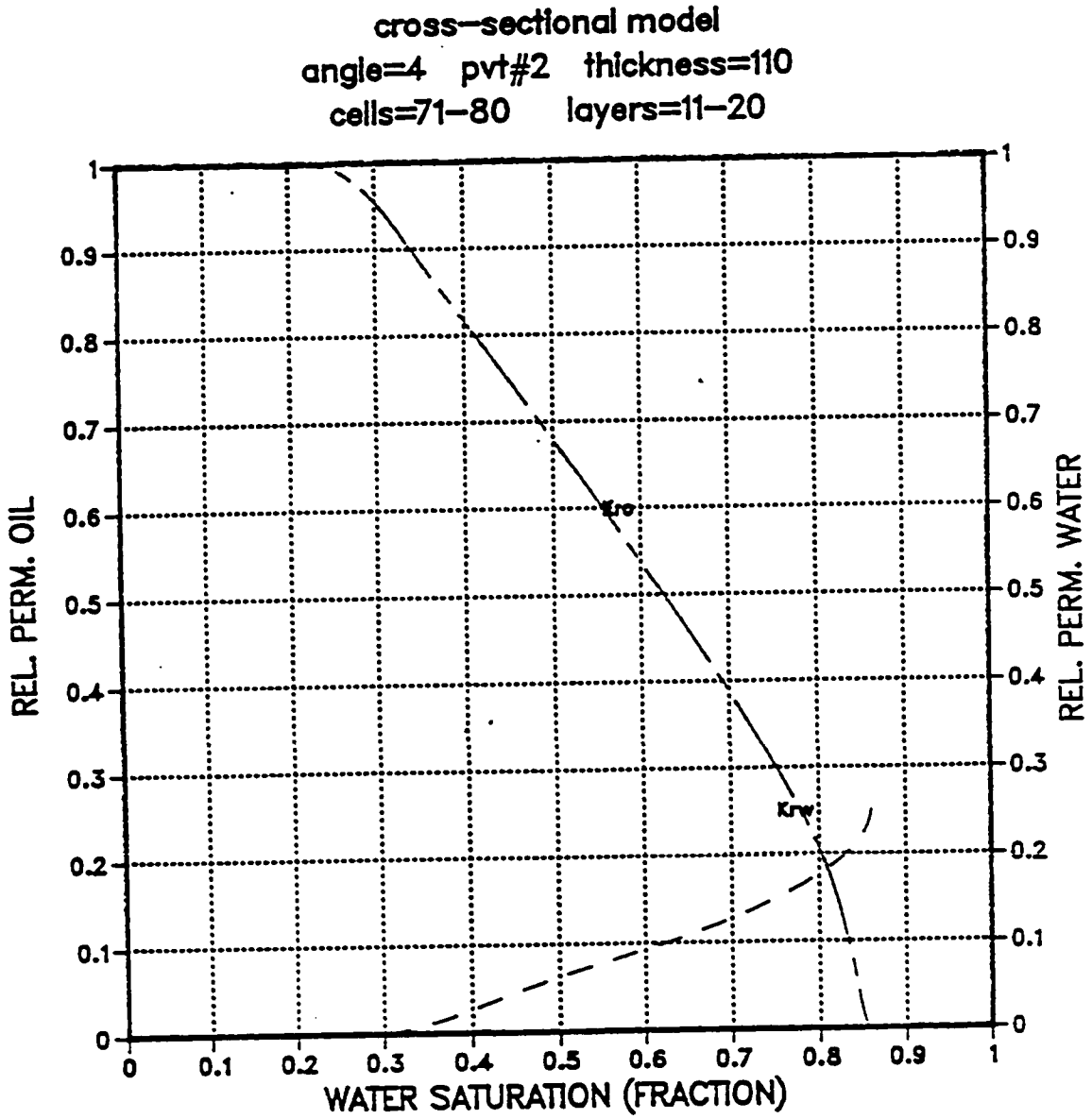
cross-sectional model
angle=4 pvt#2 thickness=110
cells=71-80 layers=11-20
REL. PERM. OIL
REL. PERM. WATER
WATER SATURATION (FRACTION)
Kro
Krw
0
0.1
0.2
0.3
0.4
0.5
0.6
0.7
0.8
0.9
1

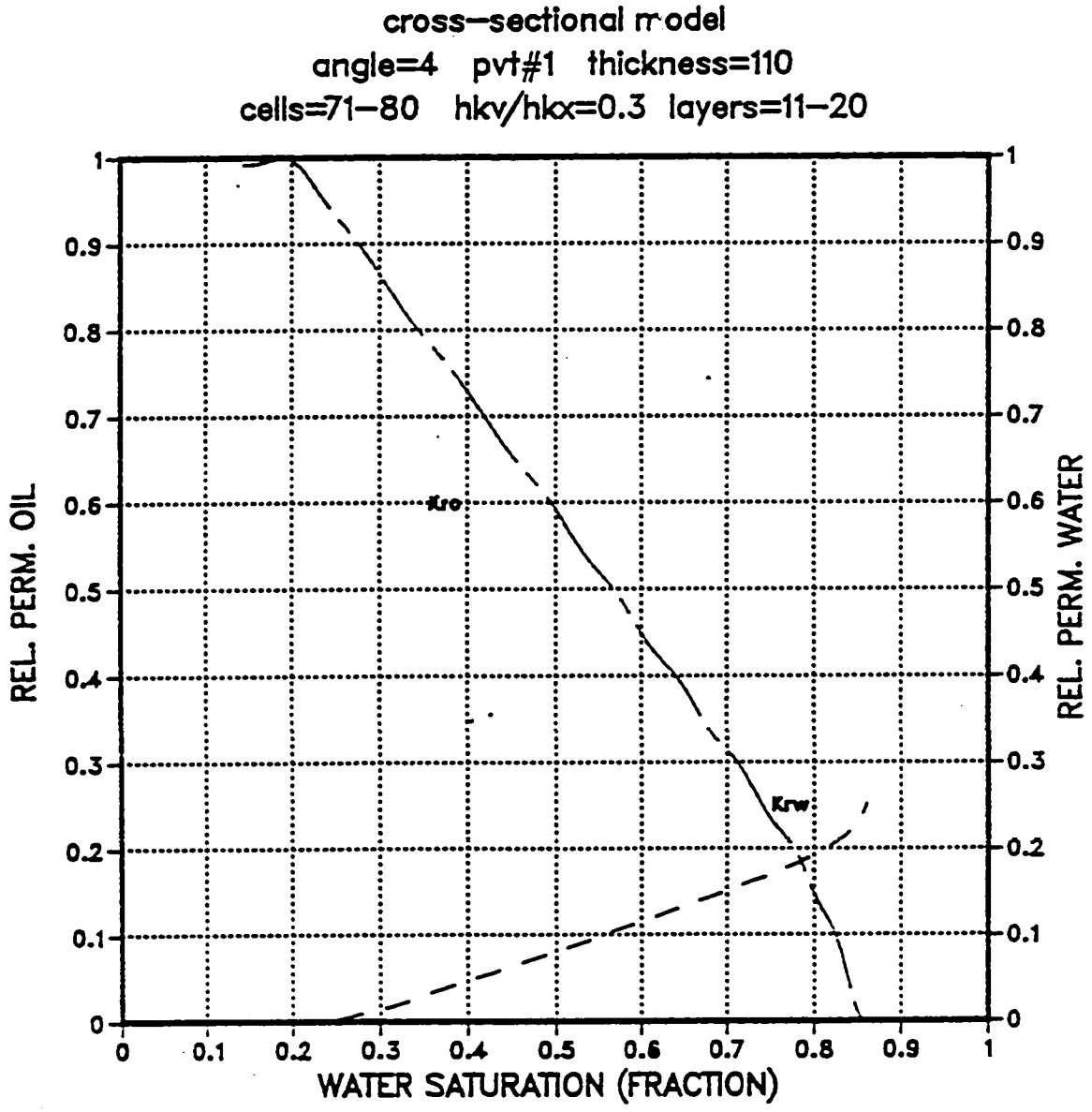
cross-sectional model
angle=4 pvt#1 thickness=110
cells=71-80 hkv/hkx=0.3 layers=11-20
REL. PERM. OIL
REL. PERM. WATER
WATER SATURATION (FRACTION)
Kro
Krw
0
0.1
0.2
0.3
0.4
0.5
0.6
0.7
0.8
0.9
1

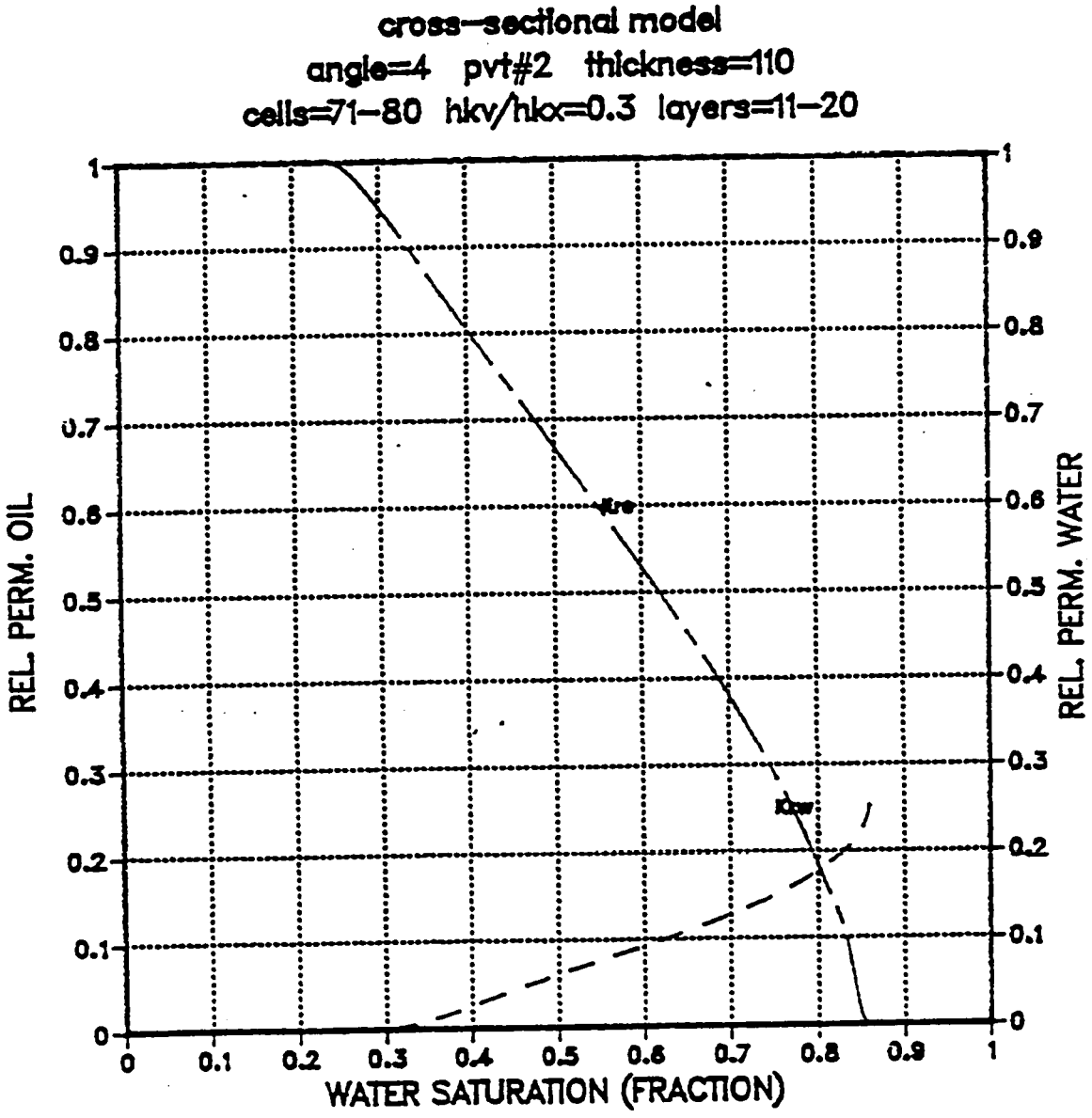
cross-sectional model
angle=4 pvt#2 thickness=110
cells=71-80 hkv/hkx=0.3 layers=11-20
REL. PERM. OIL
REL. PERM. WATER
WATER SATURATION (FRACTION)
0
0.1
0.2
0.3
0.4
0.5
0.6
0.7
0.8
0.9
1

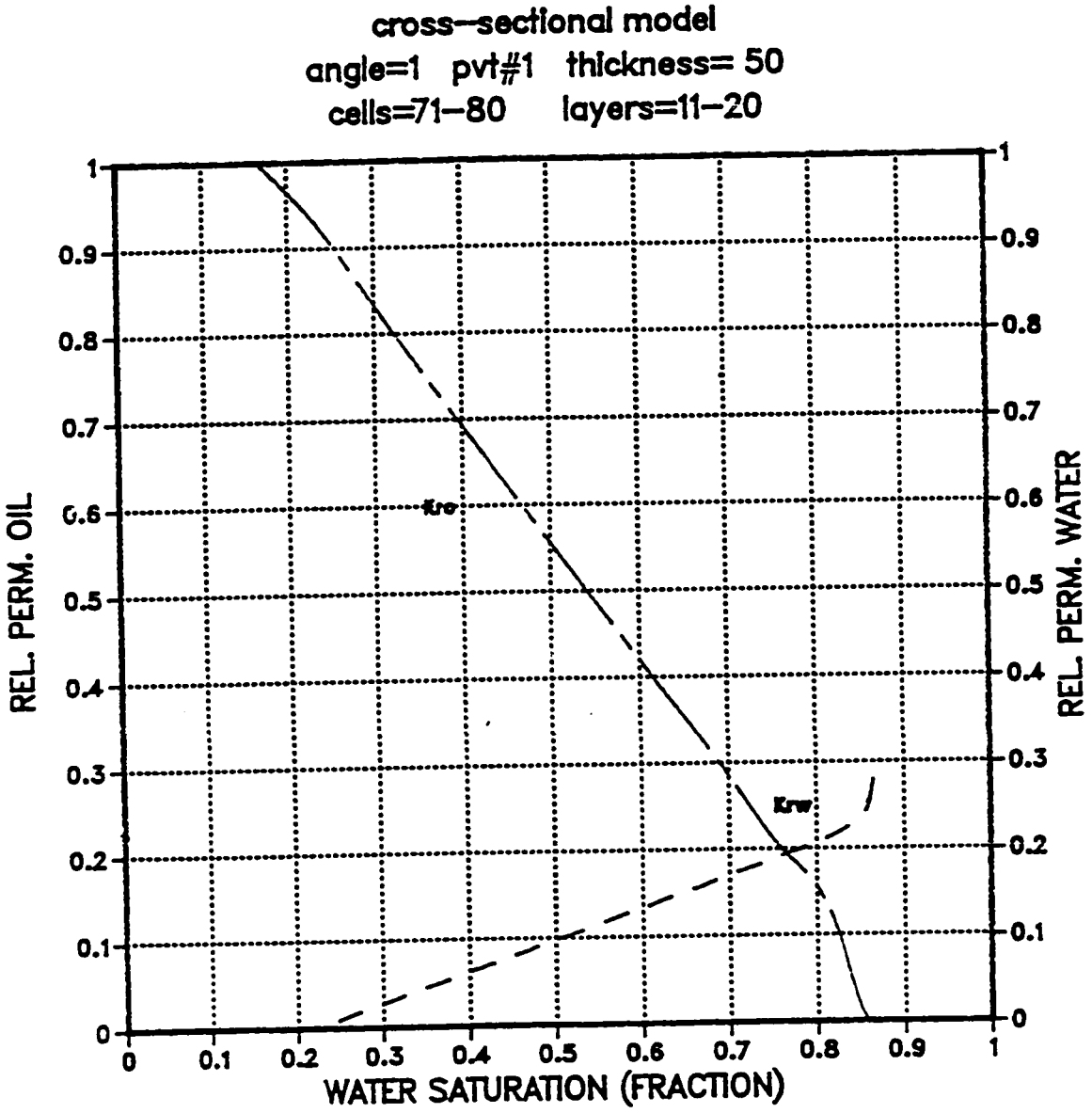
cross-sectional model
angle=1 pvt#1 thickness= 50
cells=71-80 layers=11-20
REL. PERM. OIL
REL. PERM. WATER
WATER SATURATION (FRACTION)
Kro
Krw
0
0.1
0.2
0.3
0.4
0.5
0.6
0.7
0.8
0.9
1

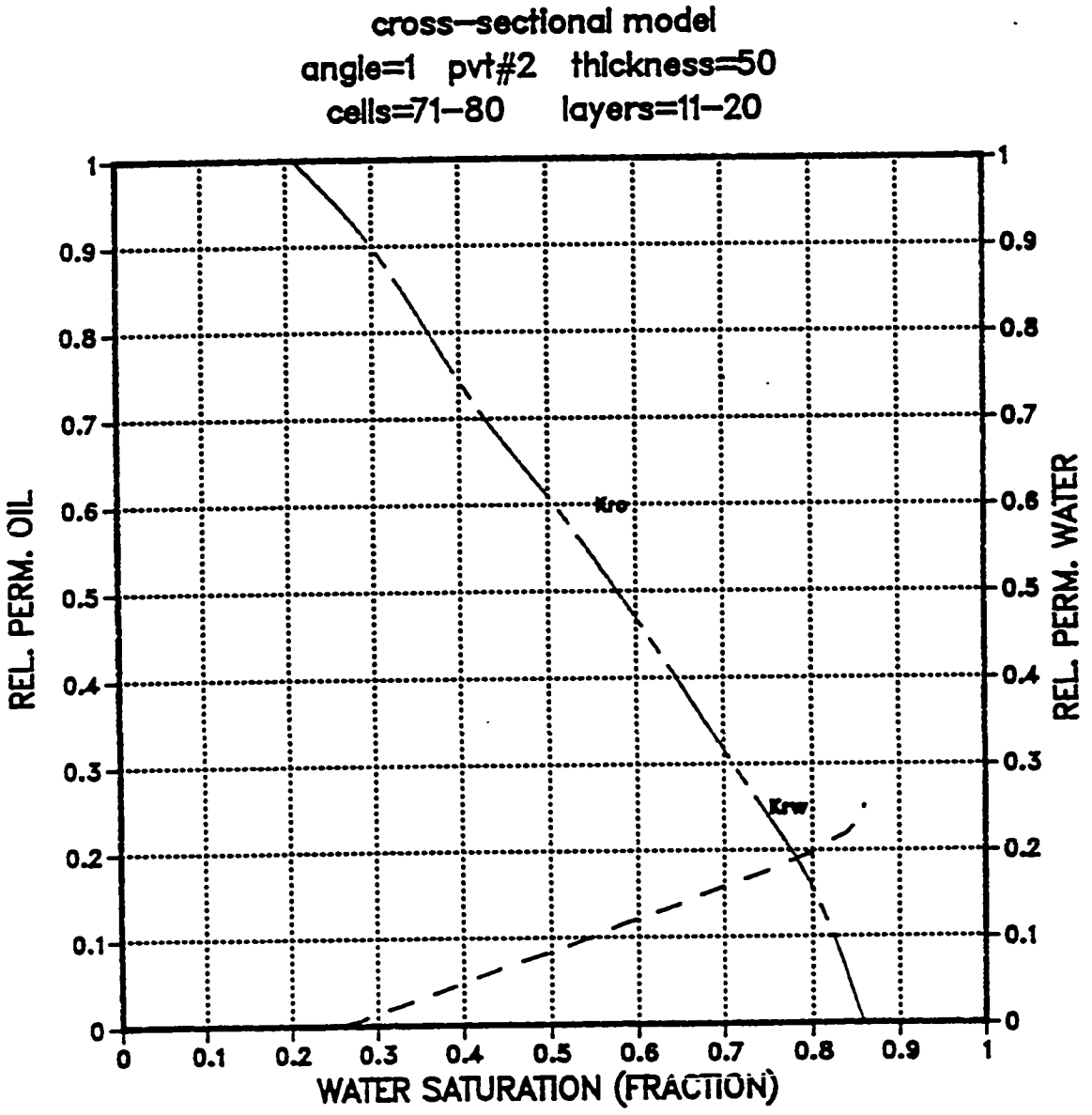
cross-sectional model
angle=1 pvt#2 thickness=50
cells=71-80 layers=11-20
REL. PERM. OIL
REL. PERM. WATER
WATER SATURATION (FRACTION)
Kro
Krw
0
0.1
0.2
0.3
0.4
0.5
0.6
0.7
0.8
0.9
1

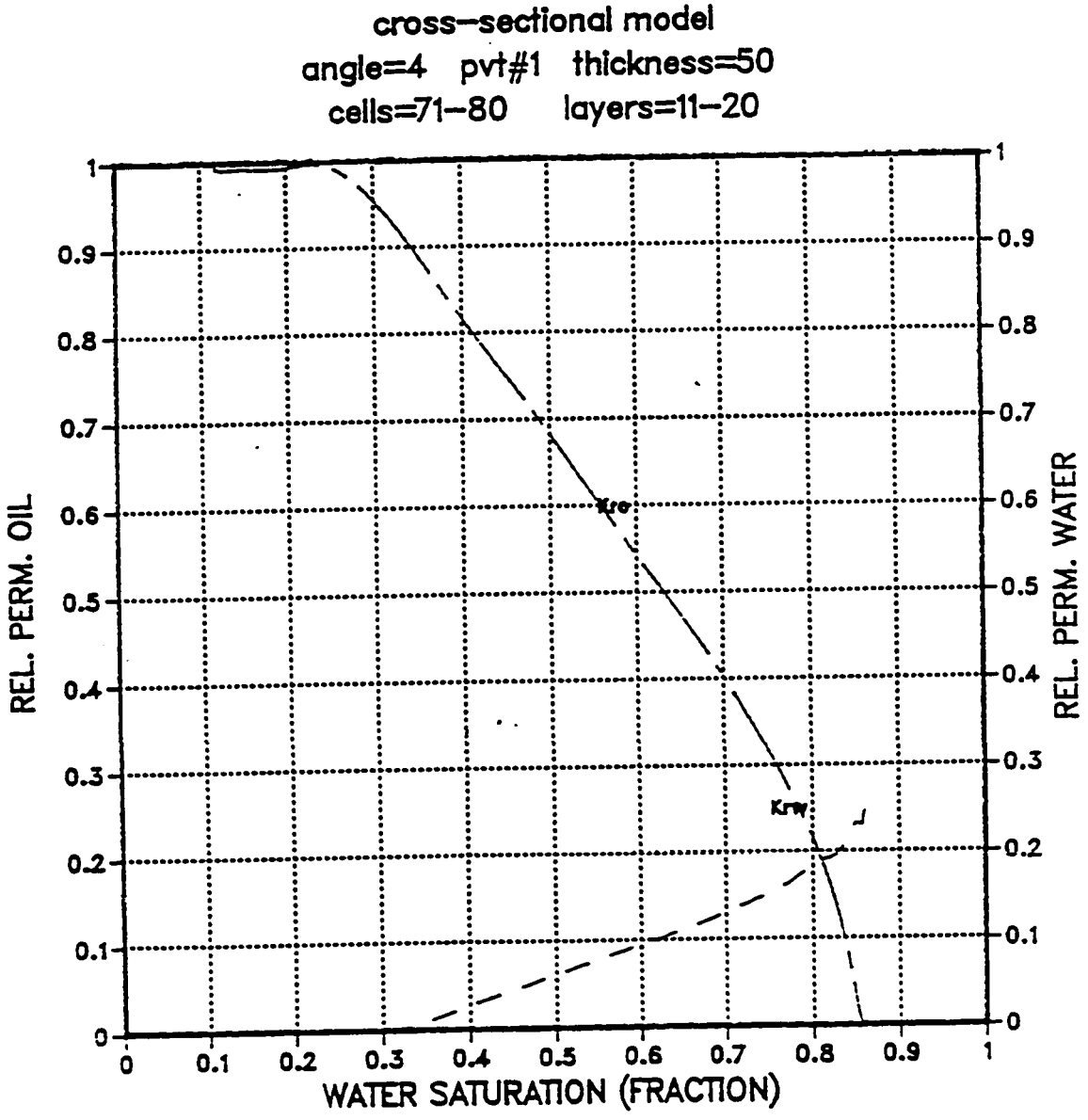
cross-sectional model
angle=4 pvt#1 thickness=50
cells=71-80 layers=11-20
REL. PERM. OIL
REL. PERM. WATER
WATER SATURATION (FRACTION)
Kro
Krw
0
0.1
0.2
0.3
0.4
0.5
0.6
0.7
0.8
0.9
1

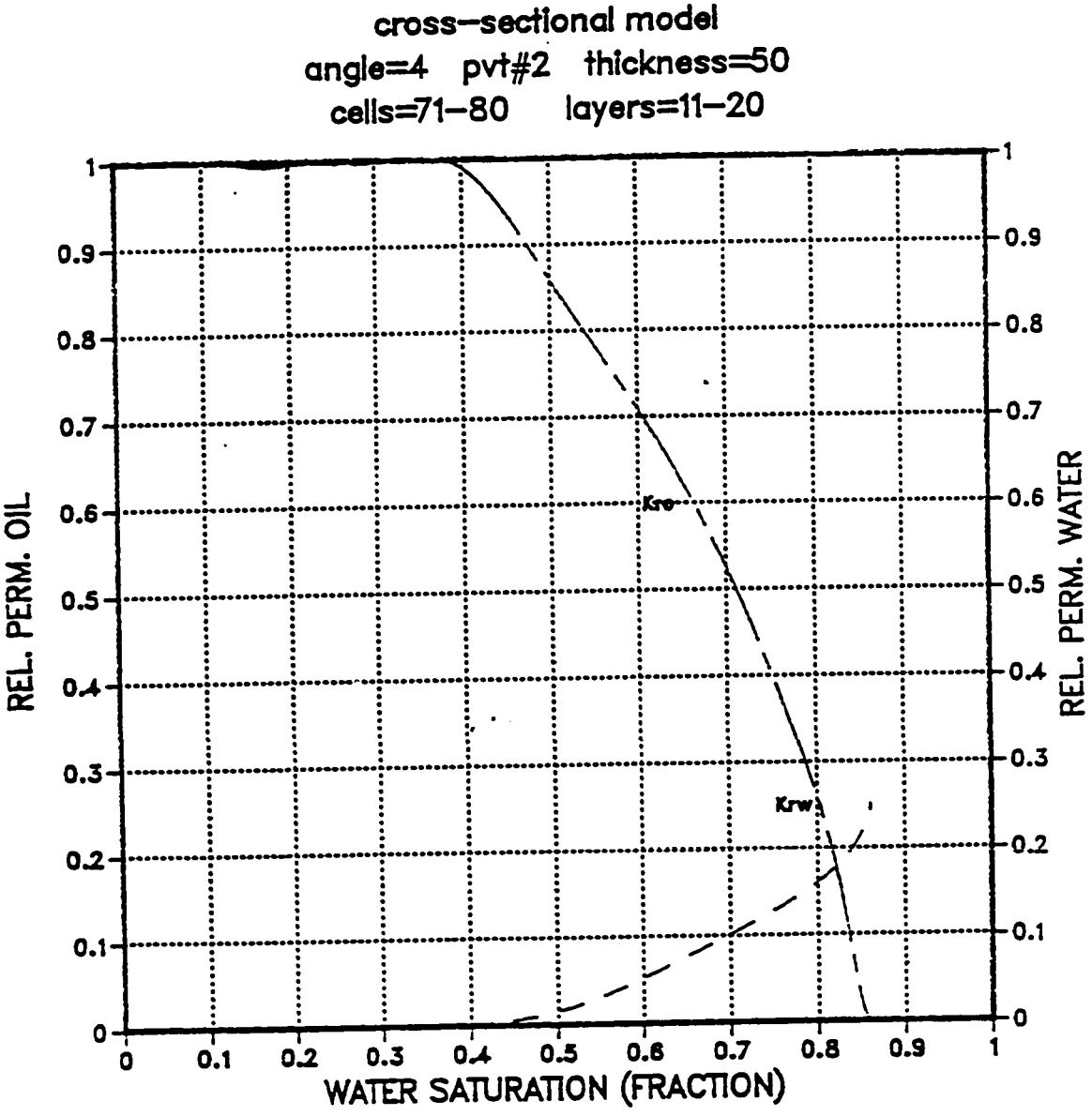
cross-sectional model
angle=4 pvt#2 thickness=50
cells=71-80 layers=11-20
REL. PERM. OIL
REL. PERM. WATER
WATER SATURATION (FRACTION)
Kro
Krw
0
0.1
0.2
0.3
0.4
0.5
0.6
0.7
0.8
0.9
1

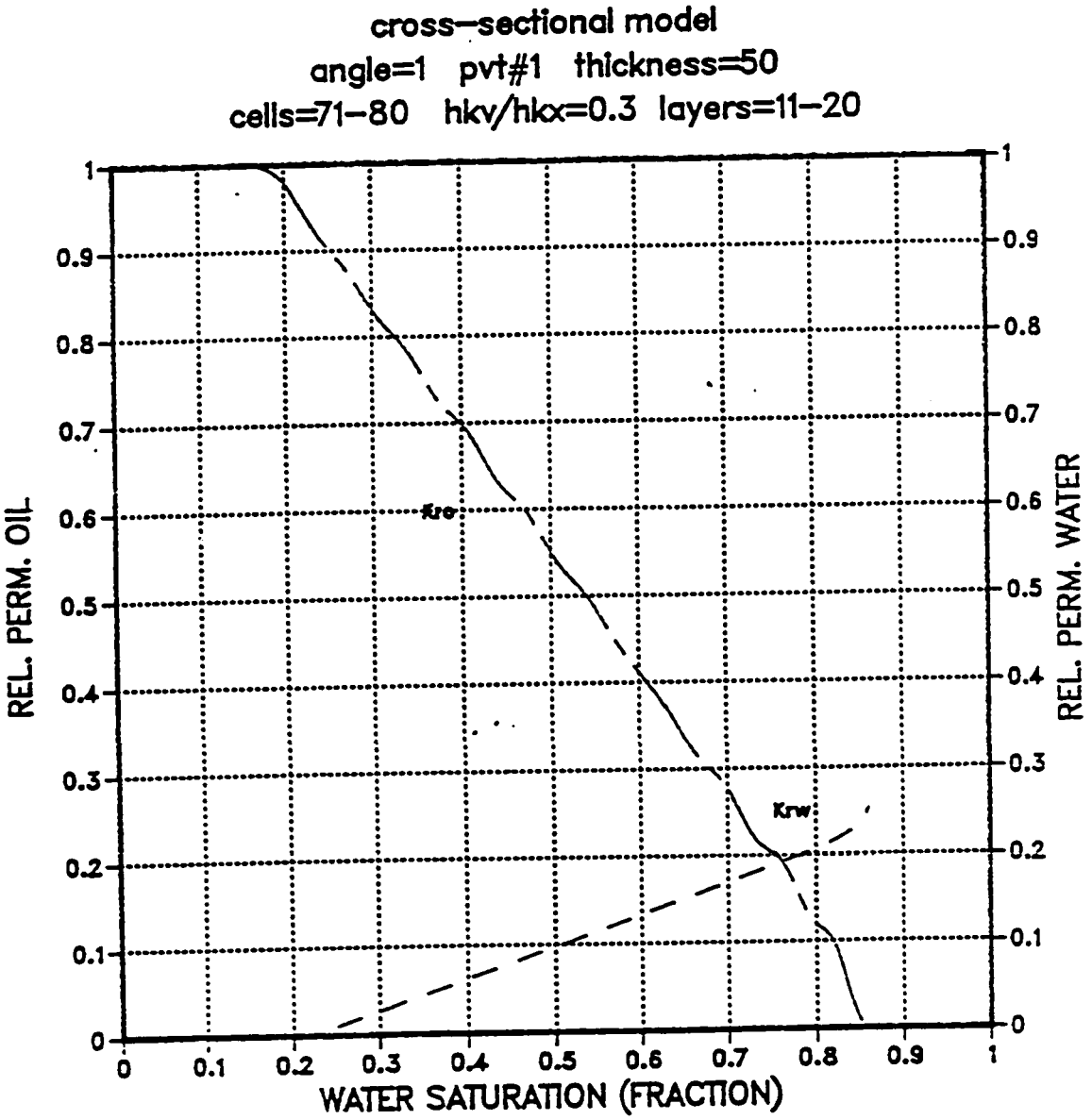
cross-sectional model
angle=1 pvt#1 thickness=50
cells=71-80 hkv/hkx=0.3 layers=11-20
REL. PERM. OIL
REL. PERM. WATER
WATER SATURATION (FRACTION)
Kro
Krw
0
0.1
0.2
0.3
0.4
0.5
0.6
0.7
0.8
0.9
1

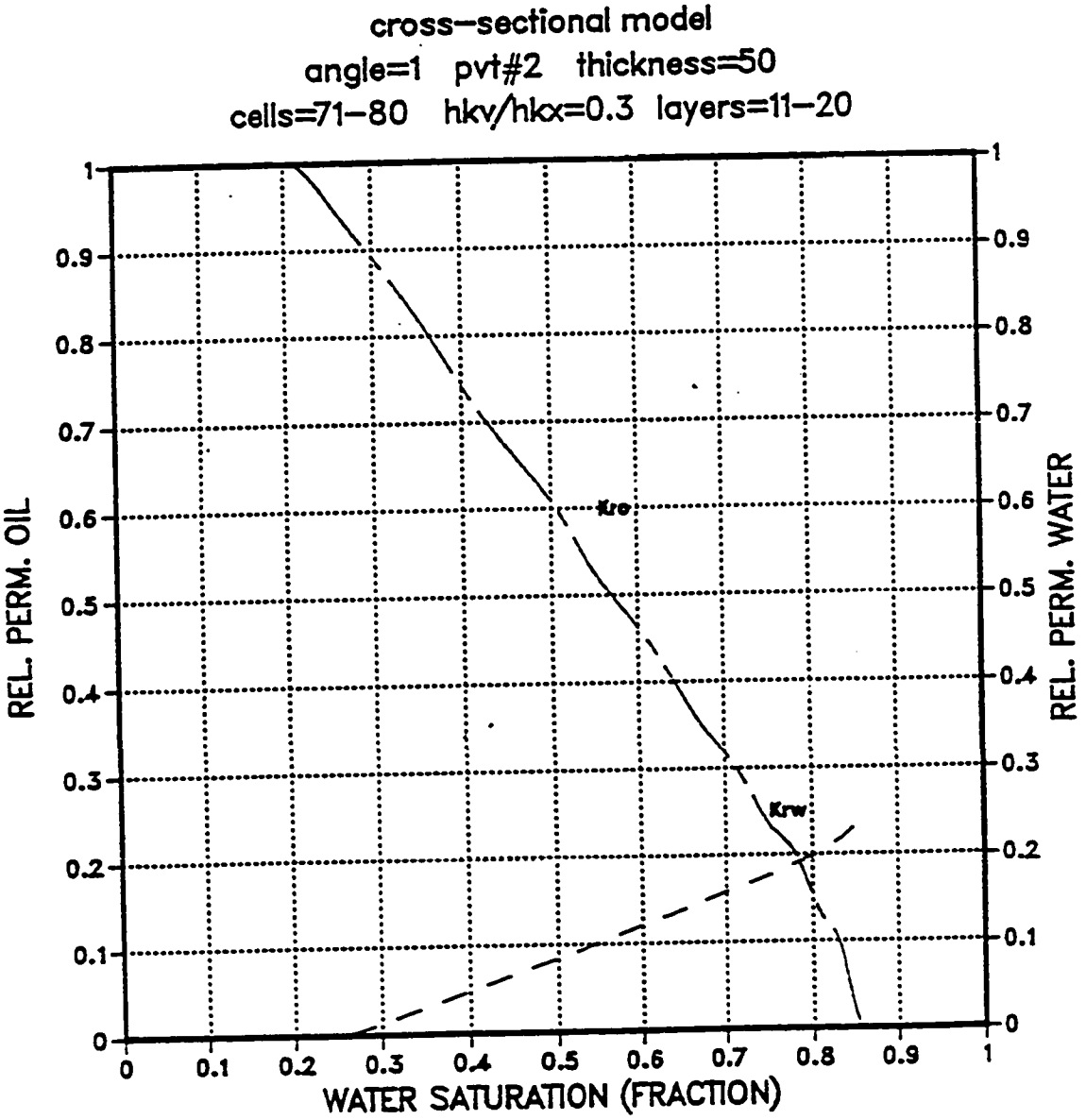
cross-sectional model
angle=1 pvt#2 thickness=50
cells=71-80 hkv/hkx=0.3 layers=11-20
REL. PERM. OIL
REL. PERM. WATER
WATER SATURATION (FRACTION)
Kro
Krw
0
0.1
0.2
0.3
0.4
0.5
0.6
0.7
0.8
0.9
1

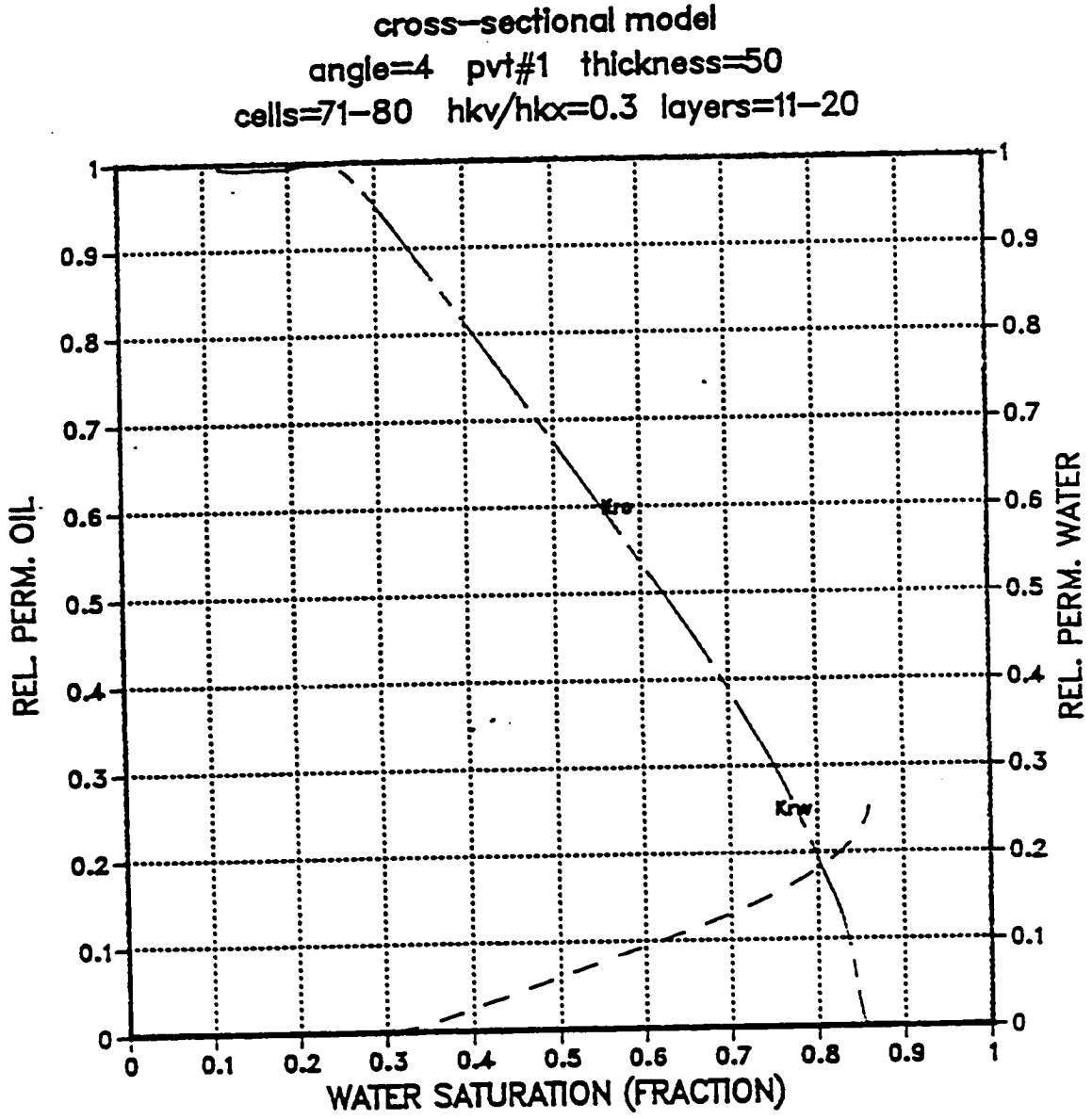
cross-sectional model
angle=4 pvt#1 thickness=50
cells=71-80 hkv/hkx=0.3 layers=11-20
REL. PERM. OIL
REL. PERM. WATER
WATER SATURATION (FRACTION)
Kro
Krw
0
0.1
0.2
0.3
0.4
0.5
0.6
0.7
0.8
0.9
1

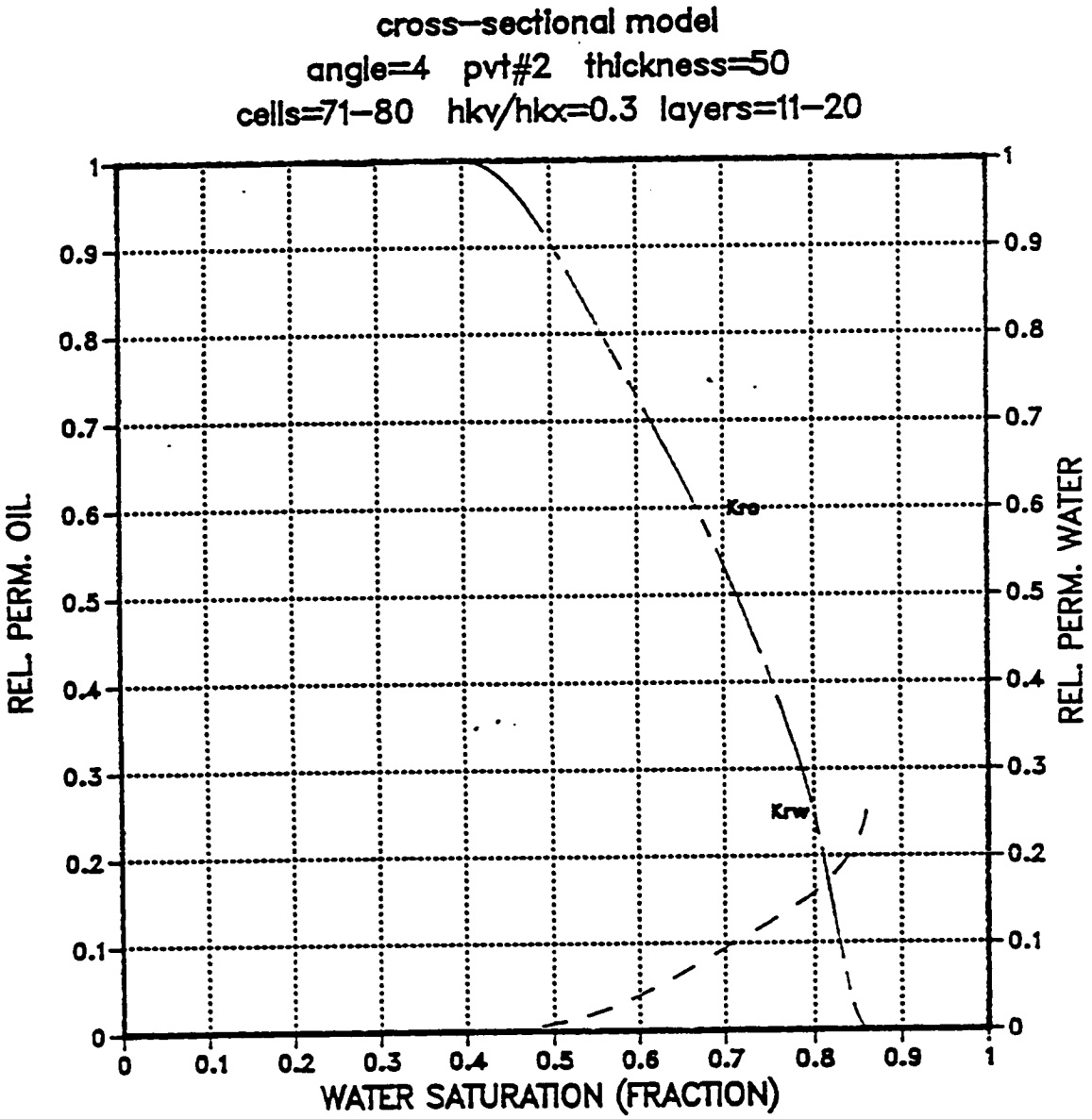
cross-sectional model
angle=4 pvt#2 thickness=50
cells=71-80 hkv/hkx=0.3 layers=11-20
REL. PERM. OIL
REL. PERM. WATER
WATER SATURATION (FRACTION)
Kro
Krw
0
0.1
0.2
0.3
0.4
0.5
0.6
0.7
0.8
0.9
1

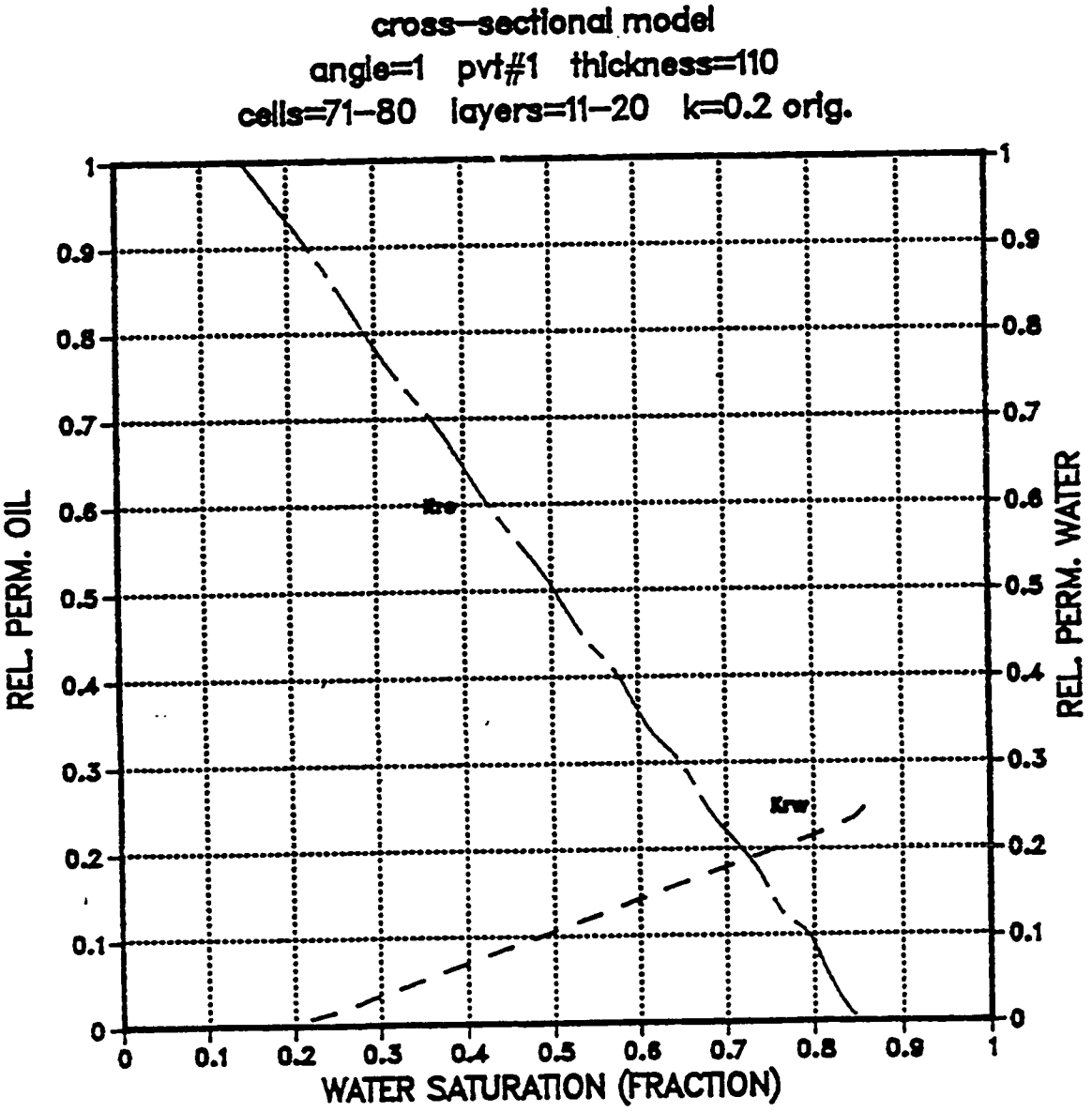
cross-sectional model
angle=1 pvt#1 thickness=110
cells=71-80 layers=11-20 k=0.2 orig.
REL. PERM. OIL
REL. PERM. WATER
WATER SATURATION (FRACTION)
Kro
Krw
0
0.1
0.2
0.3
0.4
0.5
0.6
0.7
0.8
0.9
1

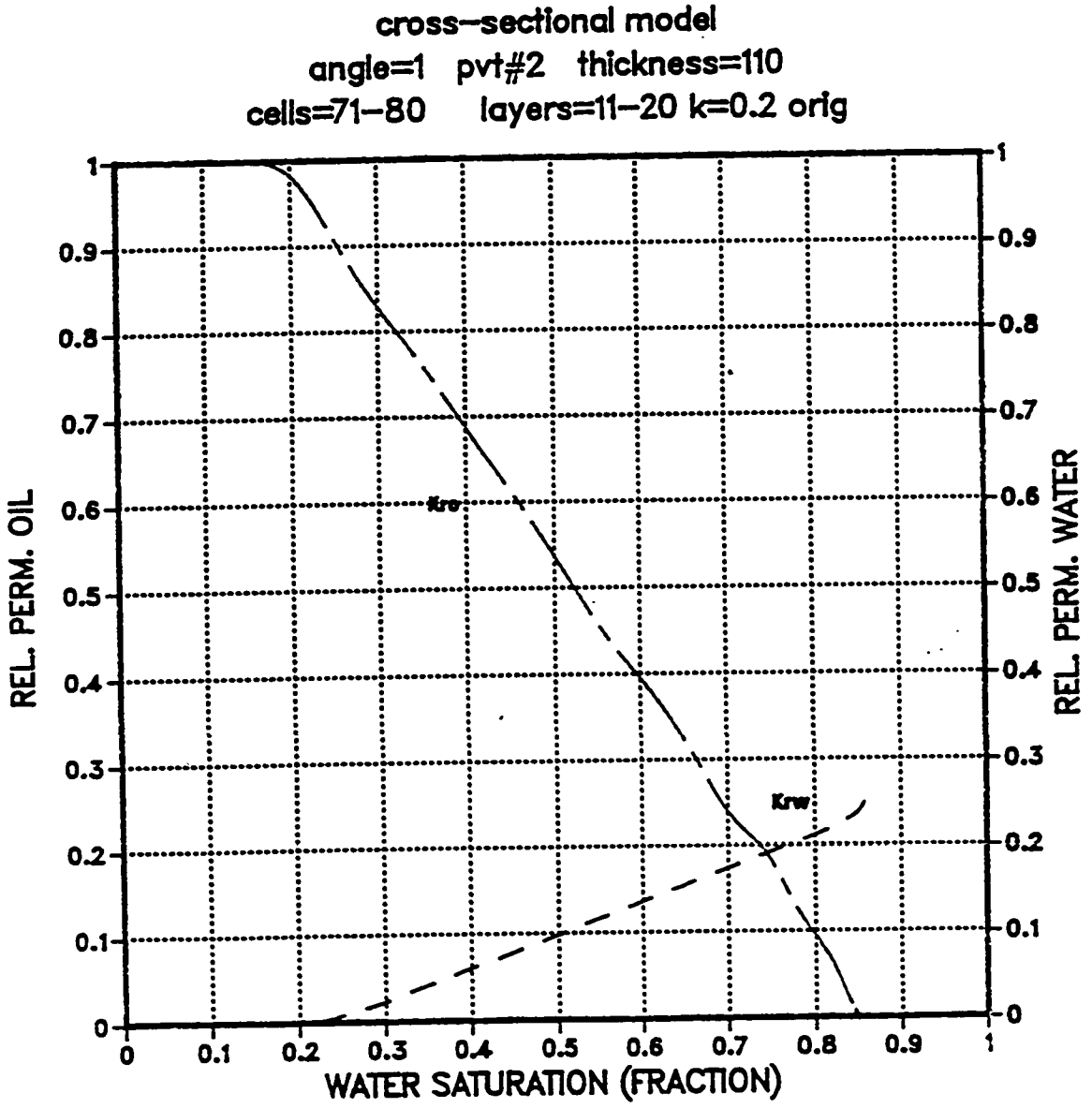
cross-sectional model
angle=1 pvt#2 thickness=110
cells=71-80 layers=11-20 k=0.2 orig
REL. PERM. OIL
REL. PERM. WATER
WATER SATURATION (FRACTION)
Kro
Krw
0
0.1
0.2
0.3
0.4
0.5
0.6
0.7
0.8
0.9
1

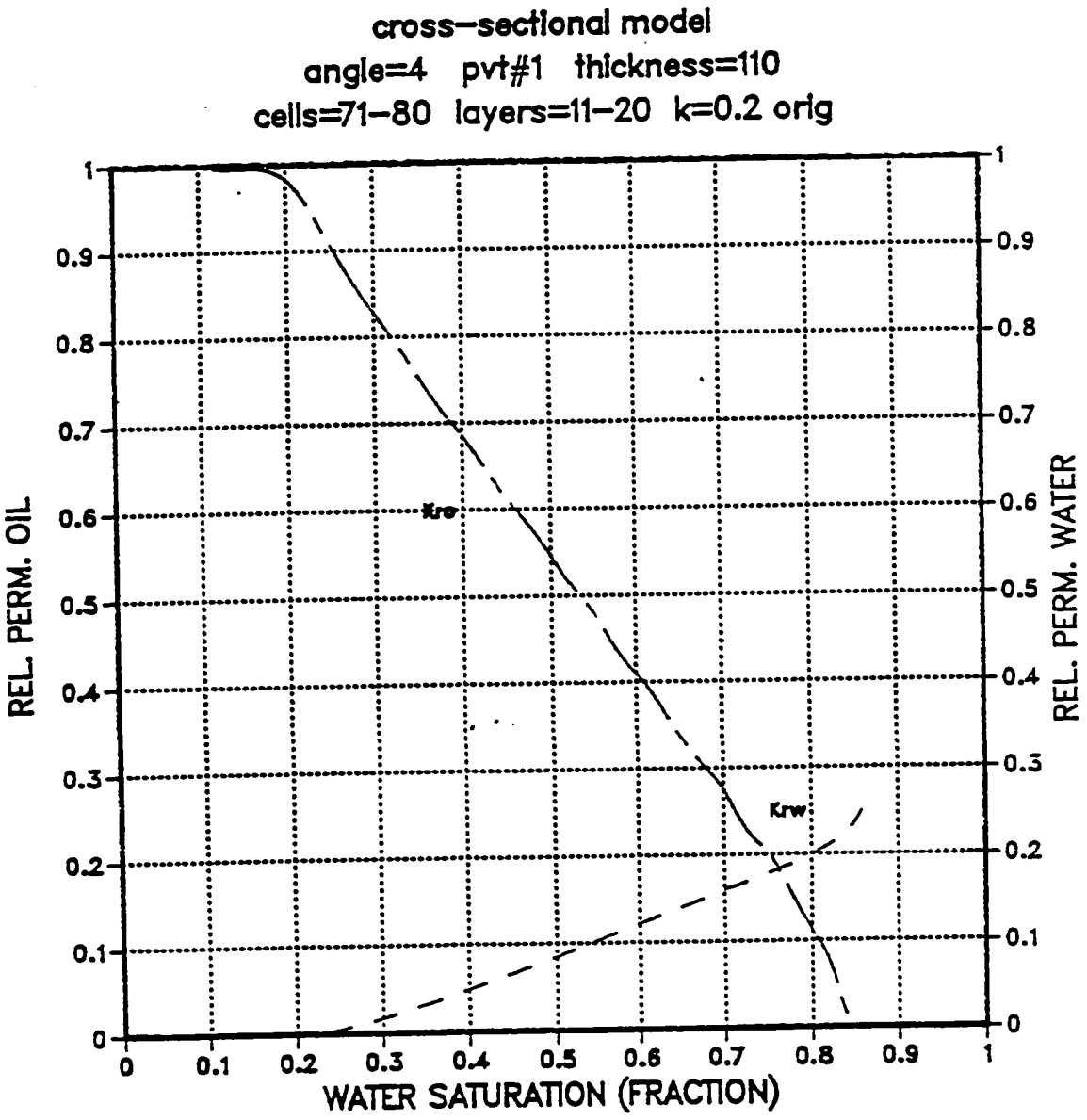
cross-sectional model
angle=4 pvt#1 thickness=110
cells=71-80 layers=11-20 k=0.2 orig
REL. PERM. OIL
REL. PERM. WATER
WATER SATURATION (FRACTION)
Kro
Krw
0
0.1
0.2
0.3
0.4
0.5
0.6
0.7
0.8
0.9
1

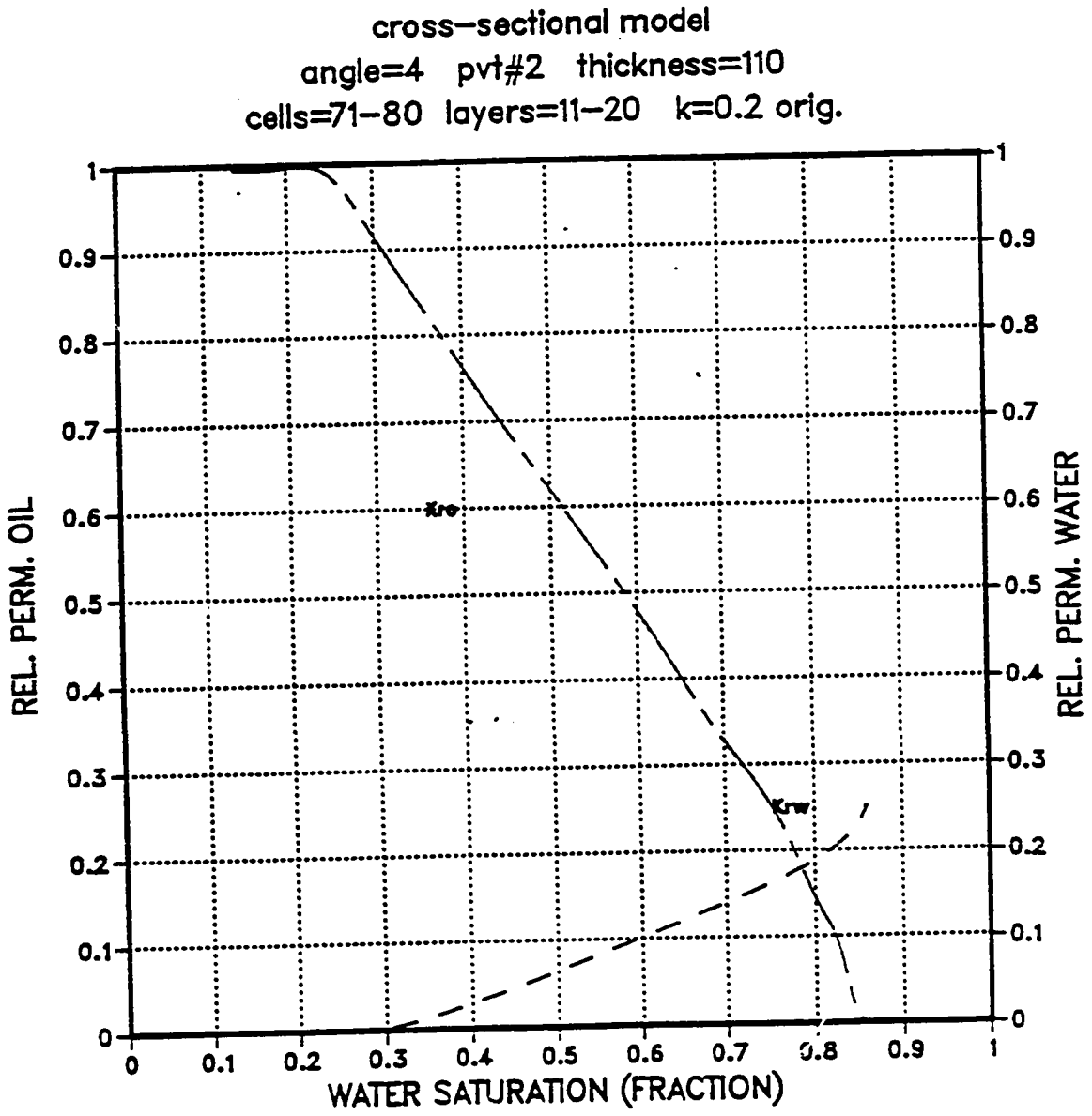
cross-sectional model
angle=4 pvt#2 thickness=110
cells=71-80 layers=11-20 k=0.2 orig.
REL. PERM. OIL
REL. PERM. WATER
WATER SATURATION (FRACTION)
Kro
Krw
0
0.1
0.2
0.3
0.4
0.5
0.6
0.7
0.8
0.9
1

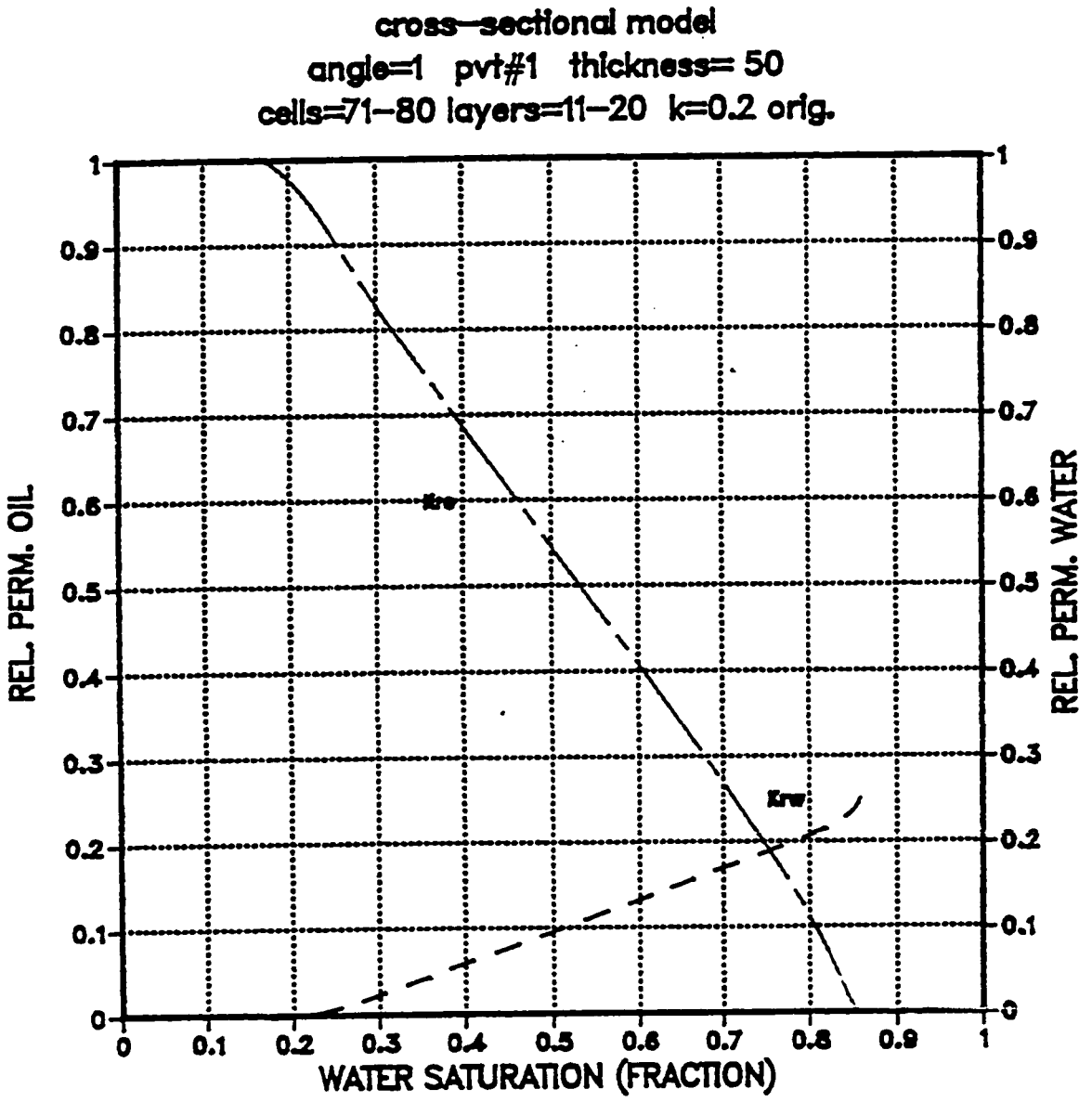
cross-sectional model
angle=1 pvt#1 thickness= 50
cells=71-80 layers=11-20 k=0.2 orig.
REL. PERM. OIL
REL. PERM. WATER
WATER SATURATION (FRACTION)
Kro
Krw
0
0.1
0.2
0.3
0.4
0.5
0.6
0.7
0.8
0.9
1

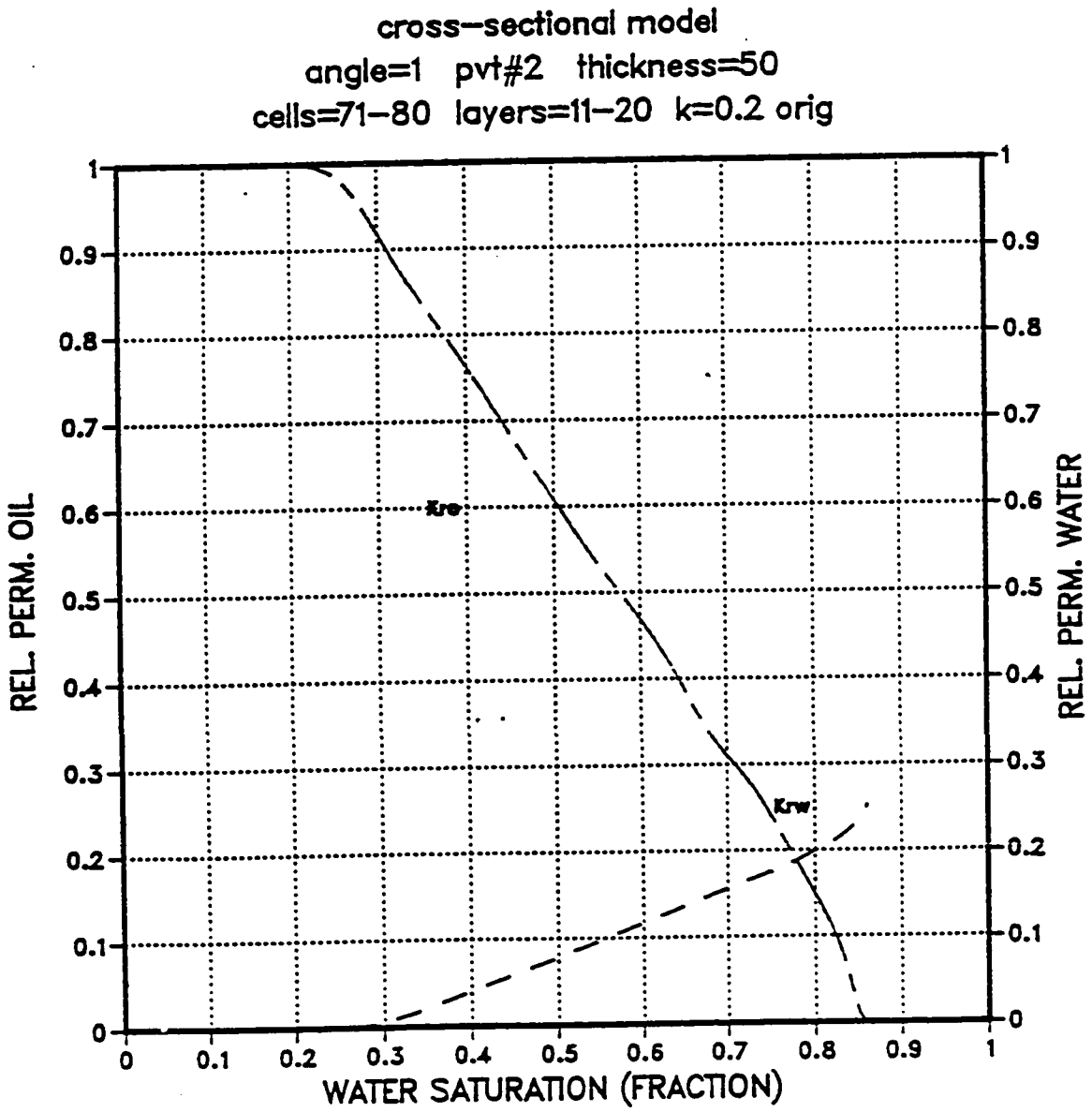
cross-sectional model
angle=1 pvt#2 thickness=50
cells=71-80 layers=11-20 k=0.2 orig
REL. PERM. OIL
REL. PERM. WATER
WATER SATURATION (FRACTION)
Kro
Krw
0
0.1
0.2
0.3
0.4
0.5
0.6
0.7
0.8
0.9
1

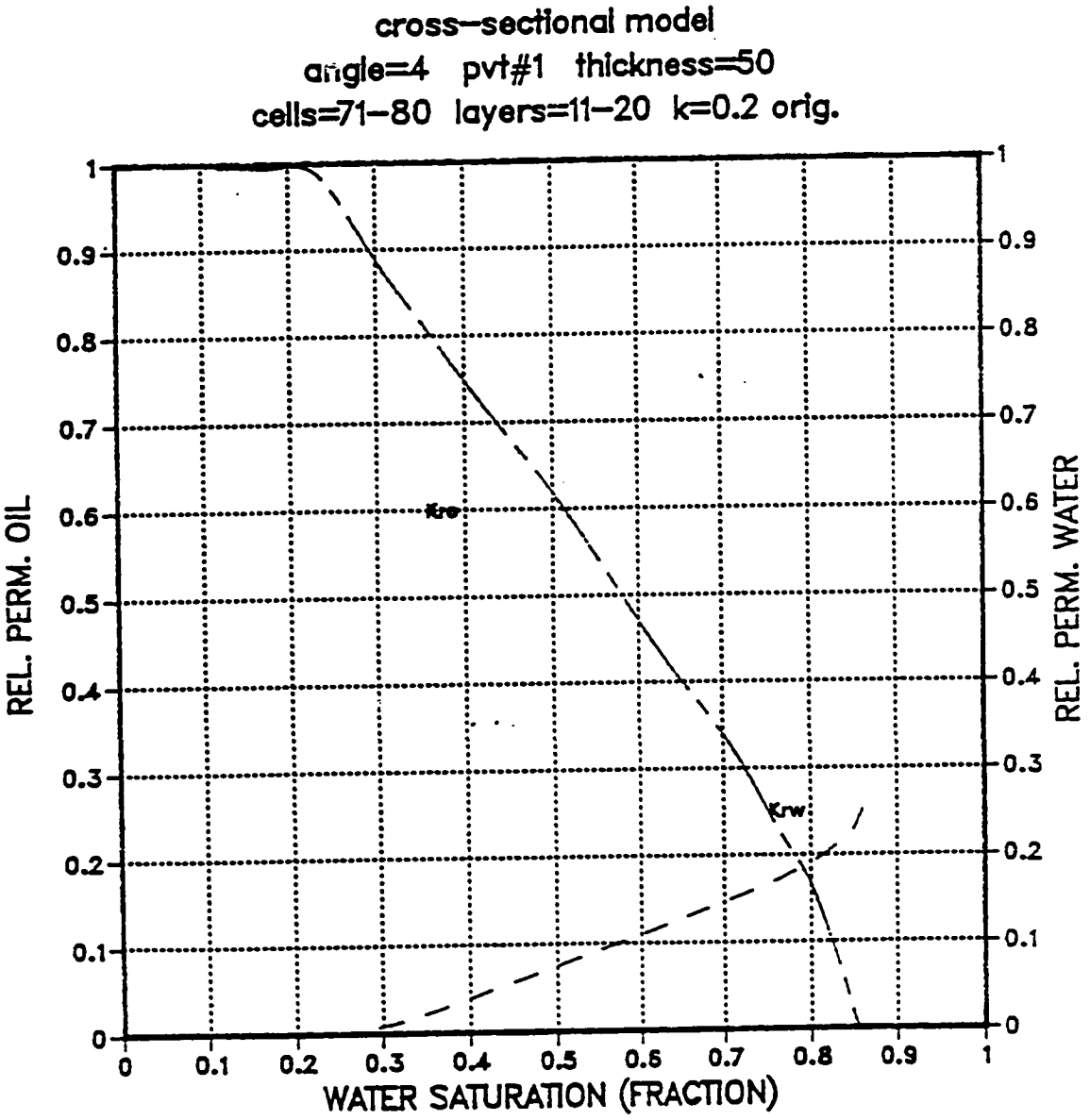
cross-sectional model
angle=4 pvt#1 thickness=50
cells=71-80 layers=11-20 k=0.2 orig.
REL. PERM. OIL
REL. PERM. WATER
WATER SATURATION (FRACTION)
Kro
Krw
0
0.1
0.2
0.3
0.4
0.5
0.6
0.7
0.8
0.9
1

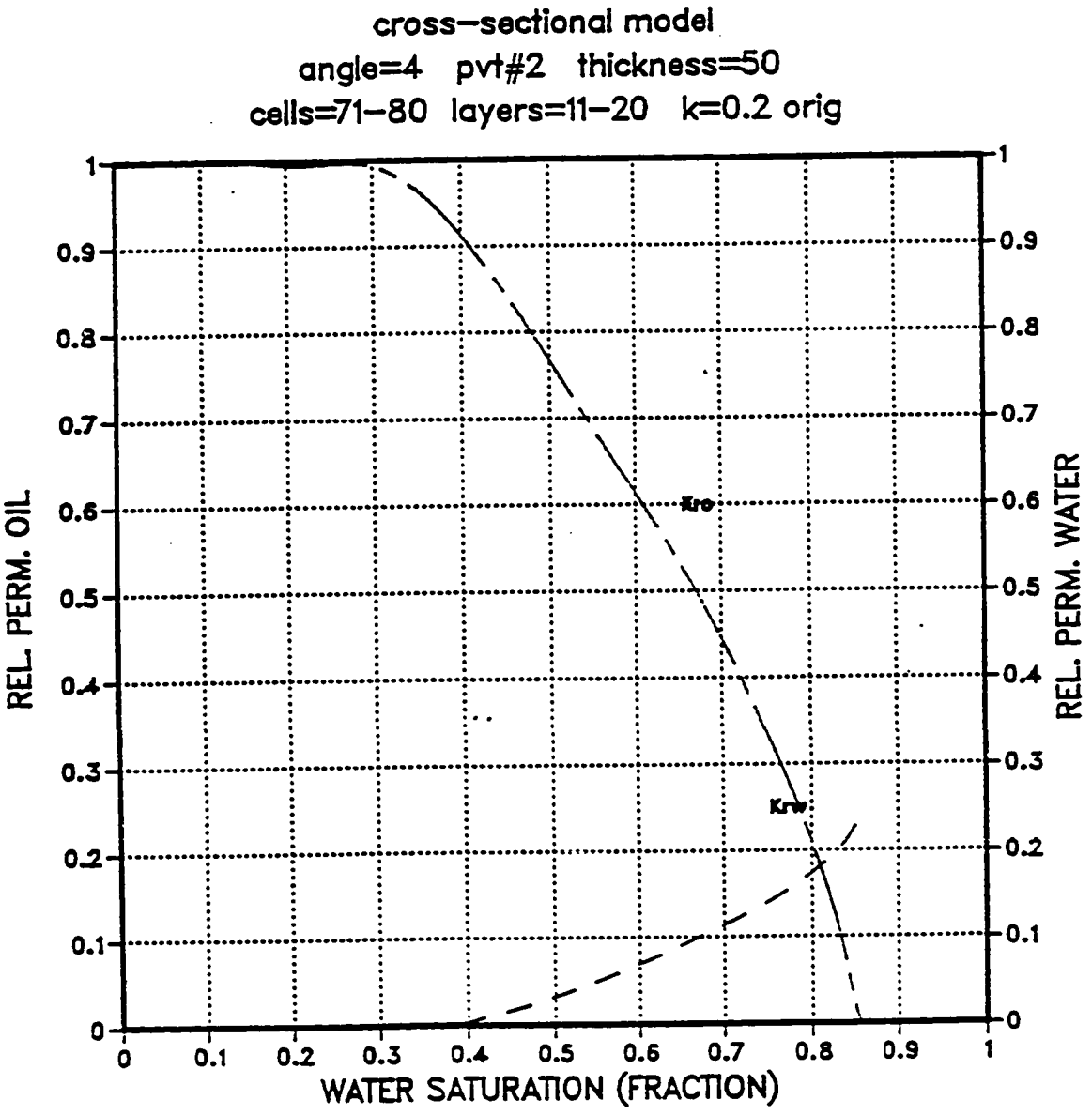
cross-sectional model
angle=4 pvt#2 thickness=50
cells=71-80 layers=11-20 k=0.2 orig
REL. PERM. OIL
REL. PERM. WATER
WATER SATURATION (FRACTION)
Kro
Krw
0
0.1
0.2
0.3
0.4
0.5
0.6
0.7
0.8
0.9
1

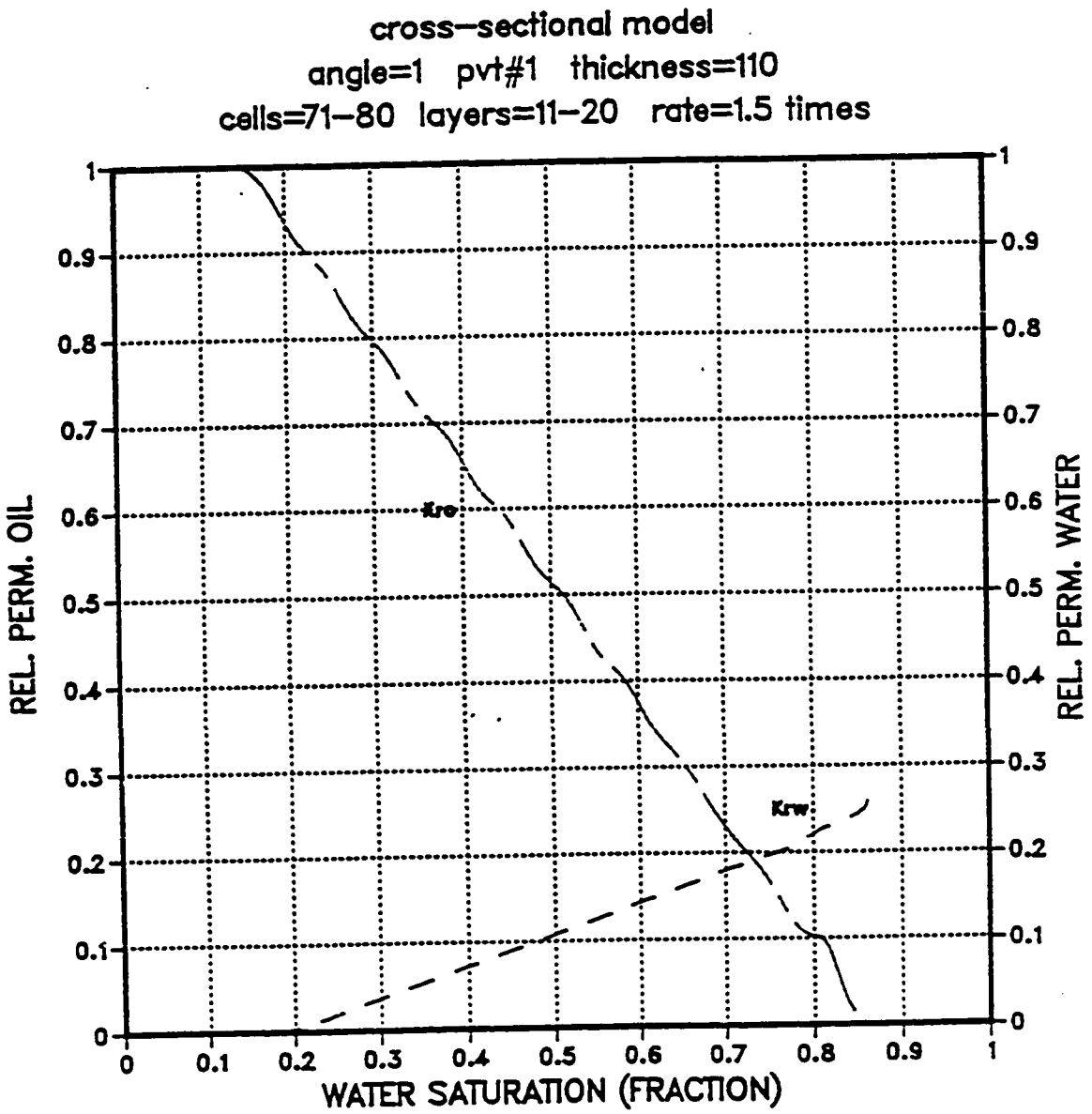
cross-sectional model
angle=1 pvt#1 thickness=110
cells=71-80 layers=11-20 rate=1.5 times
REL. PERM. OIL
REL. PERM. WATER
WATER SATURATION (FRACTION)
Kro
Krw
0
0.1
0.2
0.3
0.4
0.5
0.6
0.7
0.8
0.9
1

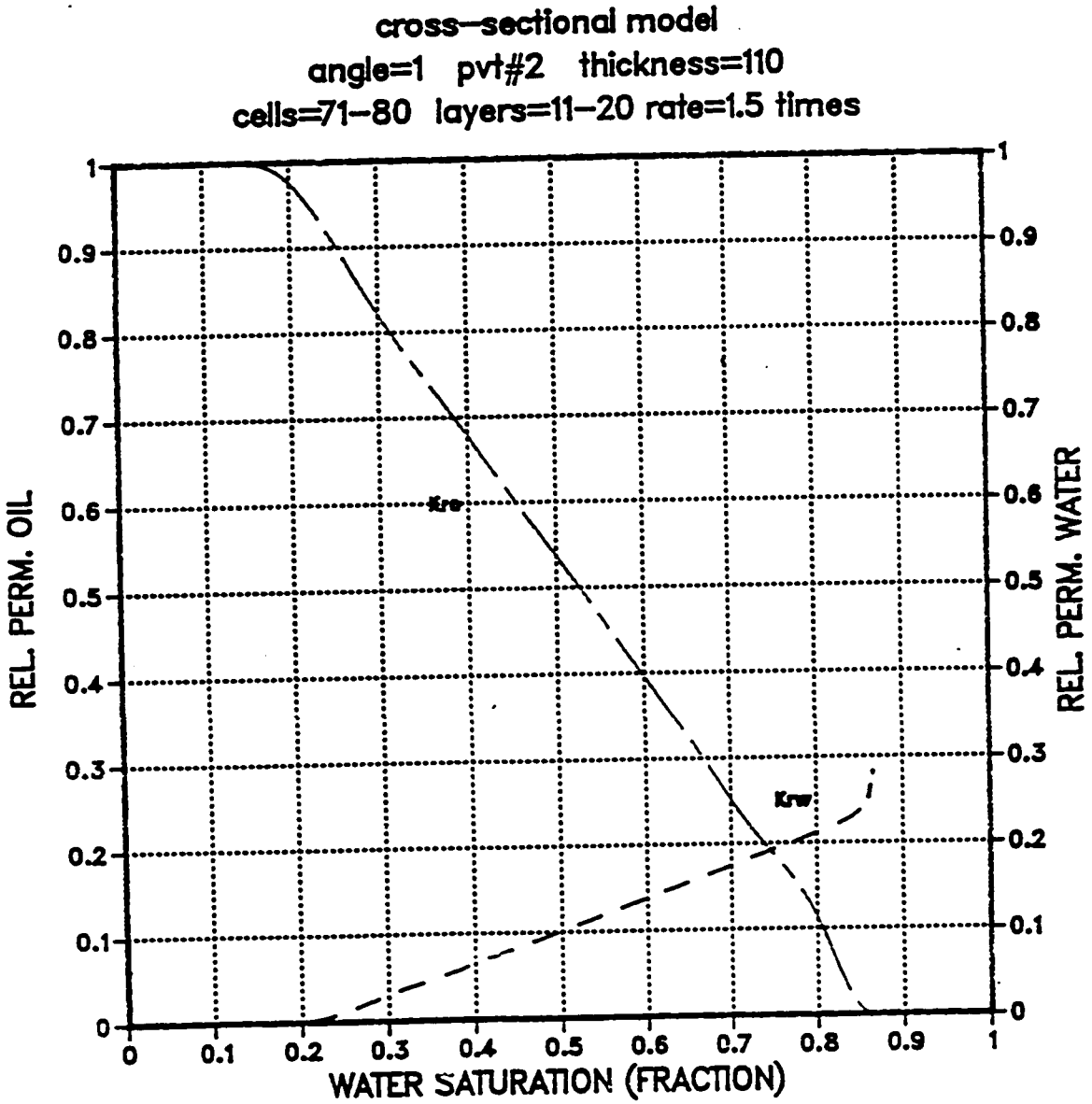
cross-sectional model
angle=1 pvt#2 thickness=110
cells=71-80 layers=11-20 rate=1.5 times
REL. PERM. OIL
REL. PERM. WATER
WATER SATURATION (FRACTION)
Kro
Krw
0
0.1
0.2
0.3
0.4
0.5
0.6
0.7
0.8
0.9
1

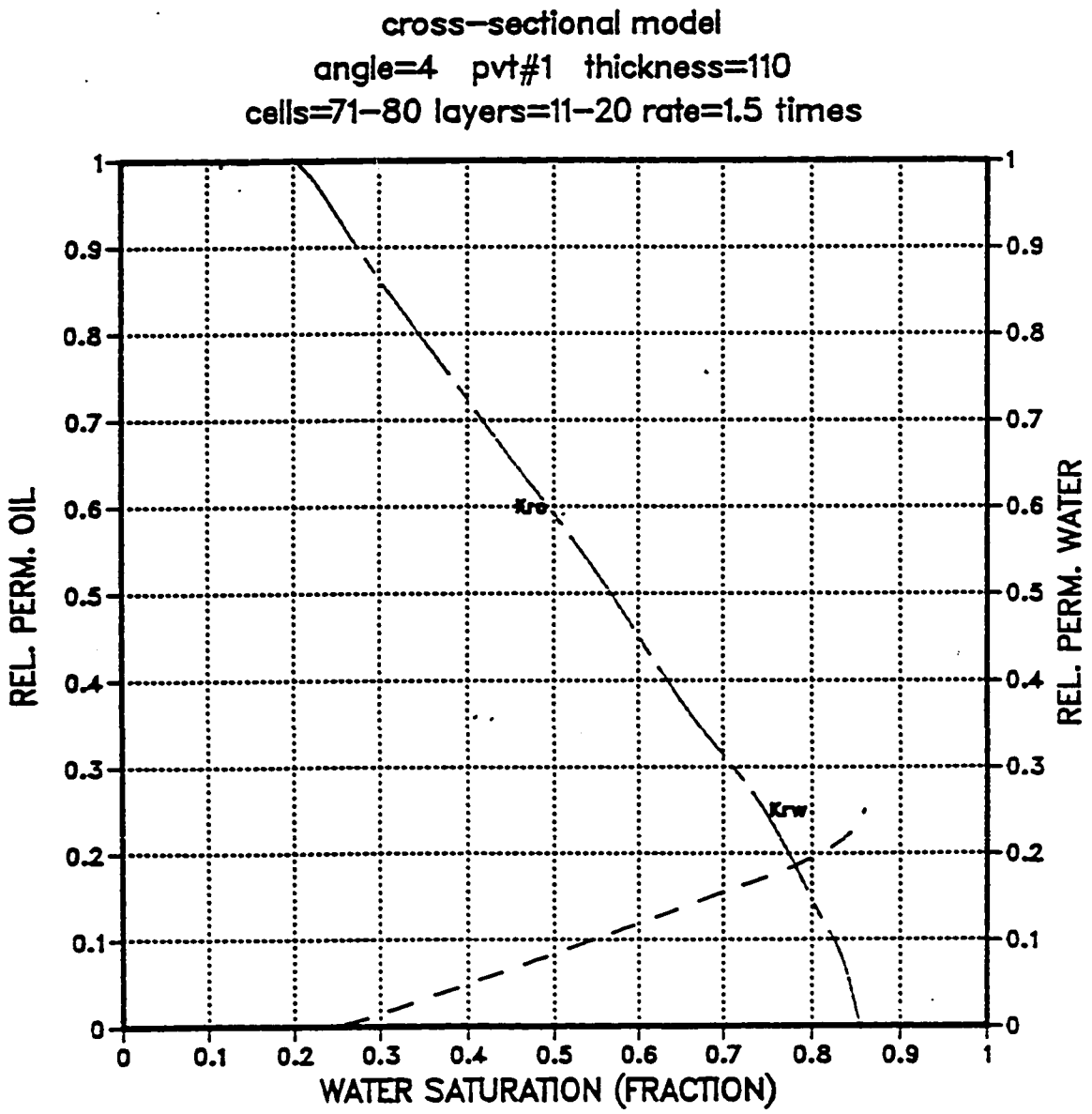
cross-sectional model
angle=4 pvt#1 thickness=110
cells=71-80 layers=11-20 rate=1.5 times
REL. PERM. OIL
REL. PERM. WATER
WATER SATURATION (FRACTION)
Kro
Krw
0
0.1
0.2
0.3
0.4
0.5
0.6
0.7
0.8
0.9
1

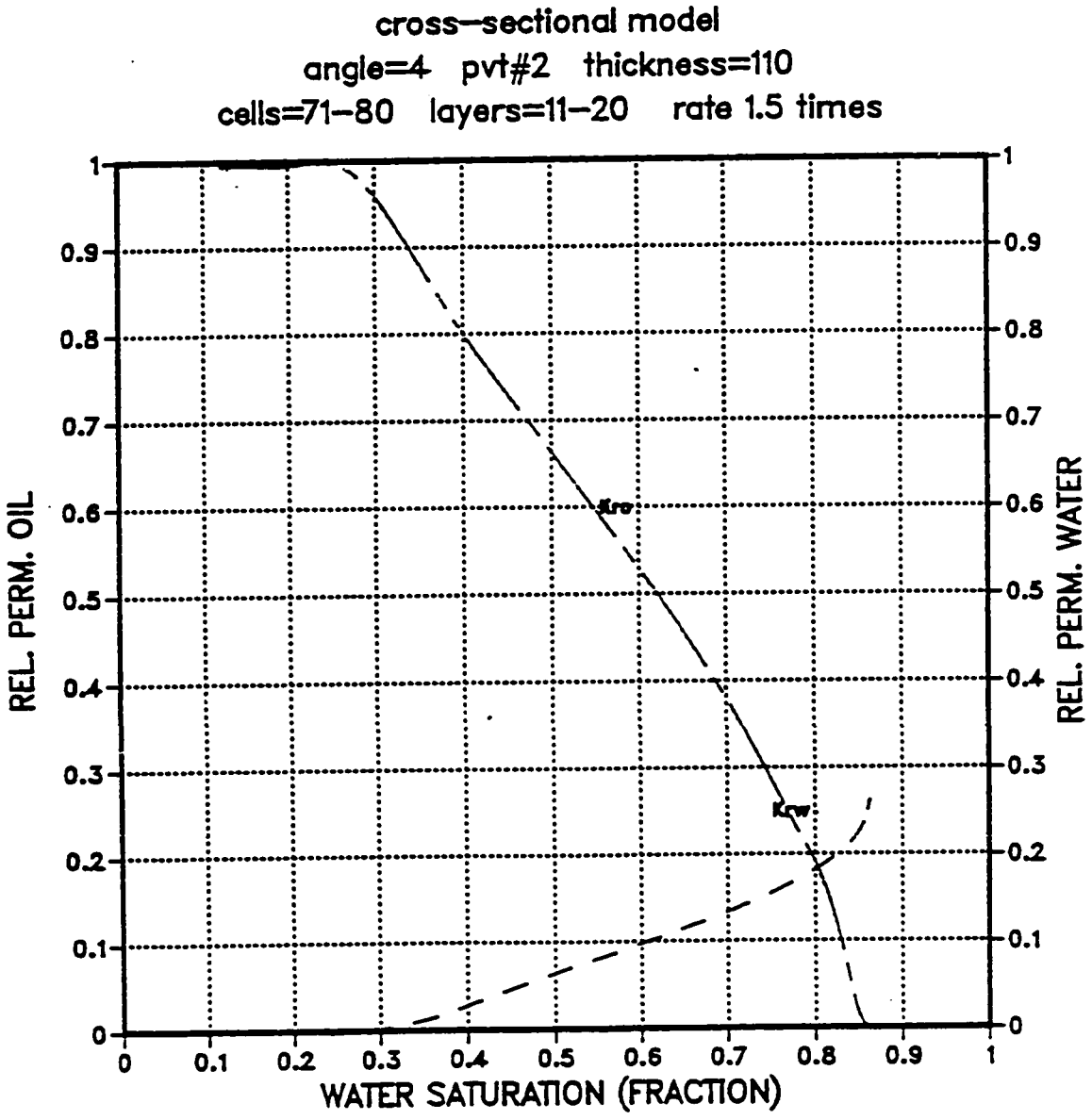
cross-sectional model
angle=4 pvt#2 thickness=110
cells=71-80 layers=11-20 rate 1.5 times
REL. PERM. OIL
REL. PERM. WATER
WATER SATURATION (FRACTION)
Kro
Krw
0
0.1
0.2
0.3
0.4
0.5
0.6
0.7
0.8
0.9
1

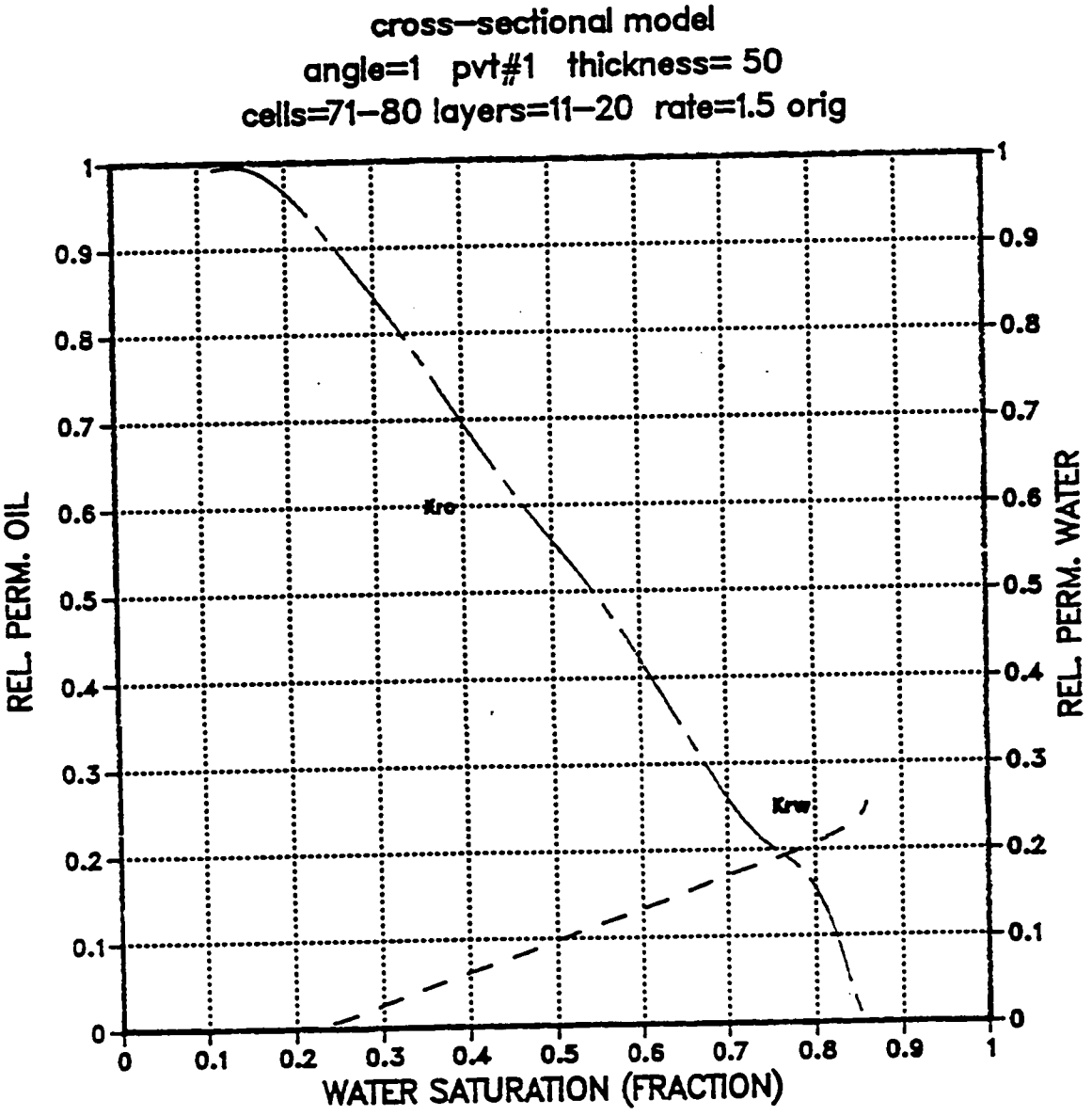
cross–sectional model
angle=1 pvt#1 thickness= 50
cells=71–80 layers=11–20 rate=1.5 orig
REL. PERM. OIL
REL. PERM. WATER
WATER SATURATION (FRACTION)
Kro
Krw
0
0.1
0.2
0.3
0.4
0.5
0.6
0.7
0.8
0.9
1

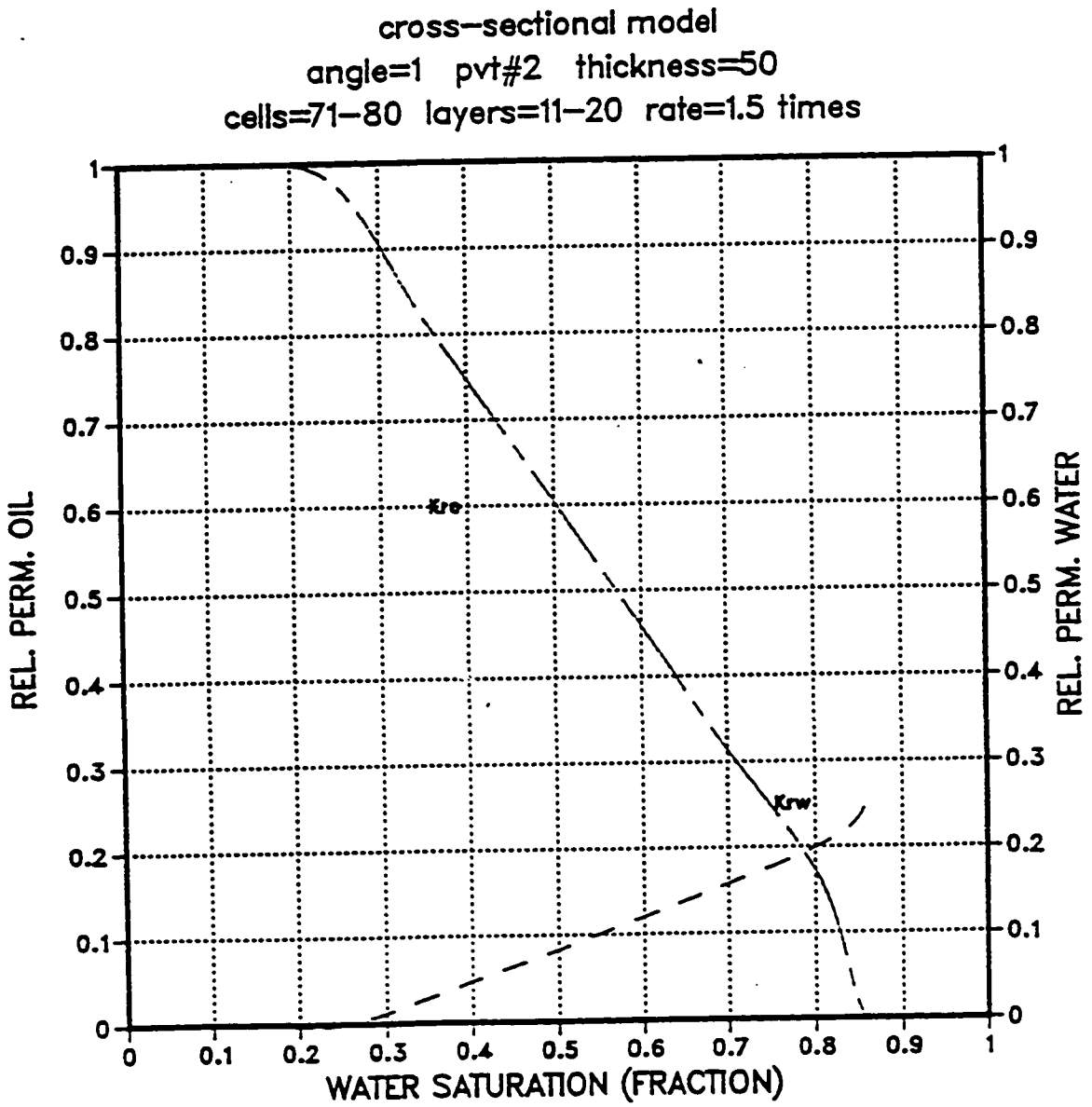
cross-sectional model
angle=1 pvt#2 thickness=50
cells=71-80 layers=11-20 rate=1.5 times
REL. PERM. OIL
REL. PERM. WATER
WATER SATURATION (FRACTION)
Kro
Krw
0
0.1
0.2
0.3
0.4
0.5
0.6
0.7
0.8
0.9
1

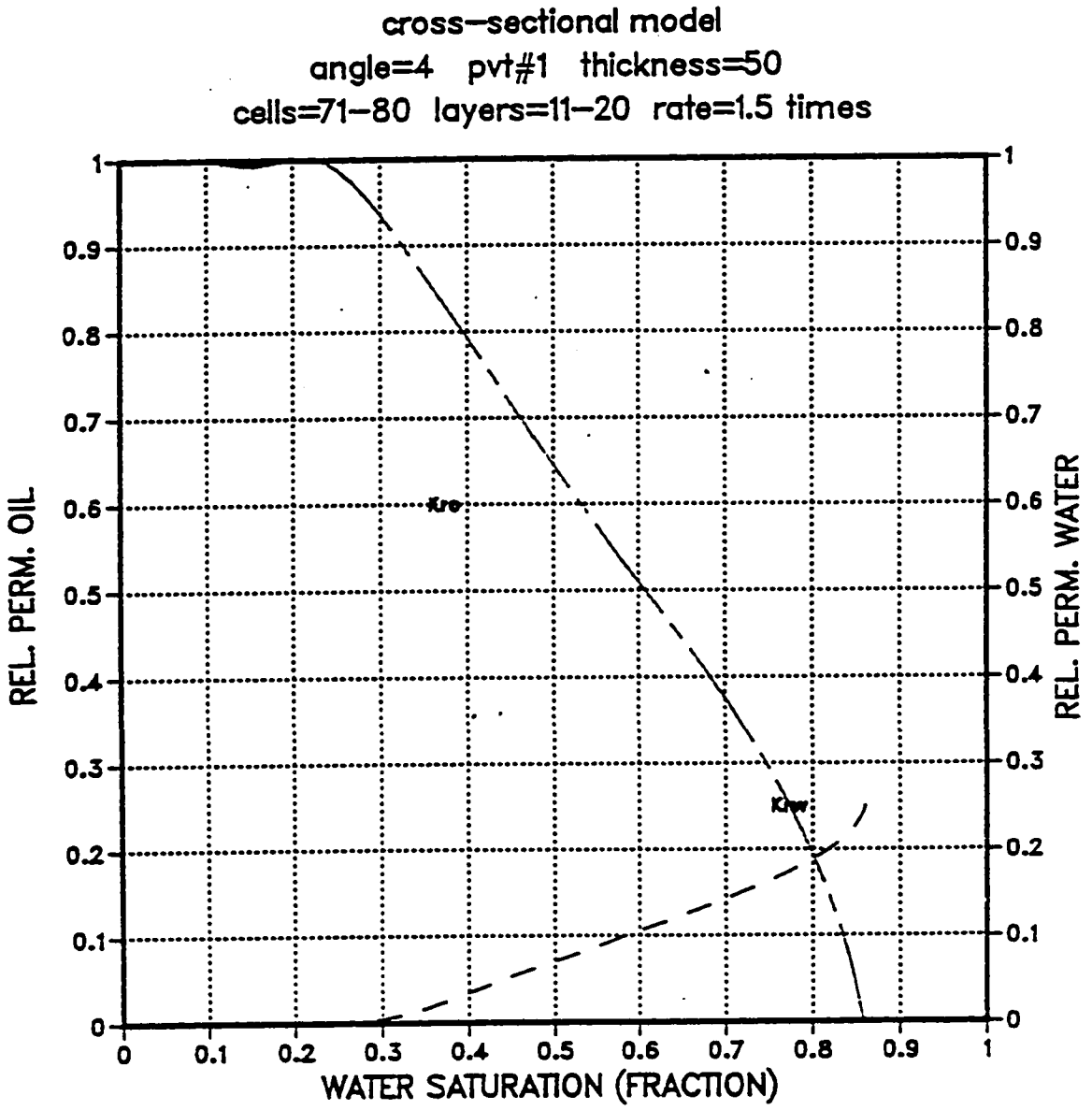
cross-sectional model
angle=4 pvt#1 thickness=50
cells=71-80 layers=11-20 rate=1.5 times
REL. PERM. OIL
REL. PERM. WATER
WATER SATURATION (FRACTION)
Kro
Krw
0
0.1
0.2
0.3
0.4
0.5
0.6
0.7
0.8
0.9
1

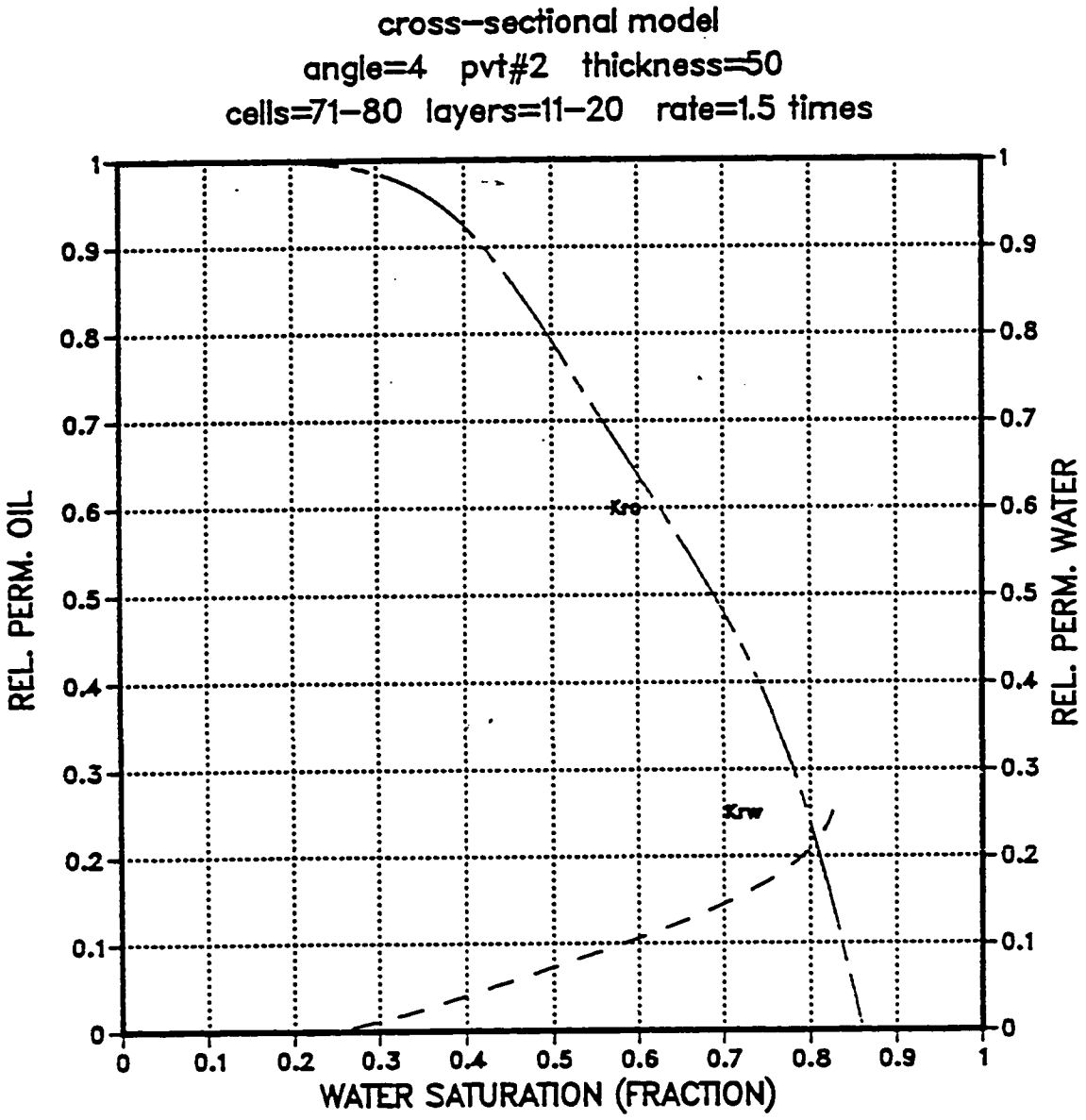
cross-sectional model
angle=4 pvt#2 thickness=50
cells=71-80 layers=11-20 rate=1.5 times
REL. PERM. OIL
REL. PERM. WATER
WATER SATURATION (FRACTION)
Kro
Krw
0
0.1
0.2
0.3
0.4
0.5
0.6
0.7
0.8
0.9
1